OFFICIAL JOURNAL OF THE SCIENTIFIC SOCIETY OF ANATOMISTS, HISTOLOGISTS, EMBRYOLOGISTS AND TOPOGRAPHIC ANATOMISTS OF UKRAINE

DOI: 10.31393
ISSN 1818-1295
eISSN 2616-6194

ВІСНИК МОРФОЛОГІЇ
REPORTS OF MORPHOLOGY

Vol. 24, №4, 2018

Scientific peer-reviewed journal in the fields of normal and pathological anatomy, histology, cytology and embryology, topographical anatomy and operative surgery, biomedical anthropology, ecology, molecular biology, biology of development

Published since 1993
Periodicity: 4 times a year

Vinnytsya • 2018

ВІСНИК МОРФОЛОГІЇ - REPORTS OF MORPHOLOGY

Founded by the "Scientific Society of Anatomists, Histologists, Embryologists, and Topographic Anatomists of Ukraine" and National Pyrogov Memorial Medical University, Vinnytsya in 1993

Certificate of state registration КВ №9310 from 02.11.2004

Professional scientific publication of Ukraine in the field of medical sciences (approved by the order of the Ministry of Education and Science of Ukraine No. 528 dated 12.05.2015, annex 10); professional scientific publication of Ukraine in the field of biological sciences by specialty groups 14.01.00-14.03.00 (approved by the order of the Ministry of Education and Science of Ukraine No. 747 dated 13.07.2015, annex 17)

Approved by the Academic Council of National Pyrogov Memorial Medical University, Vinnytsya, protocol №5 from 27.12.2018

Indexation: CrossRef, elibrary.ru, Google Schoolar Metrics, National Library of Ukraine Vernadsky

Address editors and publisher:
Pyrogov Str. 56,
Vinnytsya, Ukraine - 21018
Tel.: +38 (0432) 553959
E-mail: nila@vnmu.edu.ua

Computer page-proofs - Klopotovska L.O.
Translator - Gunas V.I.
Technical support - Levenchuk S.S., Lunik A.Yu.
Scientific editing - editorship

The site of the magazine - https://morphology-journal.com

CONTENT

Sahan N.T. Morphofunctional changes of structural components of masticatory muscles of mature animals in mercazolilum-induced hypothyroidism **5**

Dmitriev M.O., Gunas I.V., Gnenna V.O., Smolko N.M. Determination of individual linear and angular characteristics of the position of upper central incisors in Ukrainian young men and women with orthognathic bite **15**

Kramar S.B., Volkov K.S., Nebesna Z.M. Morphometric studies of the damaged skin area after experimental thermal trauma and during correction with cryo-lyophilized xenograft skin substrate **22**

Chernysh A.V., Hasiuk P.A., Yasko V.V., Smolko D.G. Regression models of individual cephalometric indicators used in the method of E.P. Harvold **29**

Monastyrskyi V.M. Organometric parameters of the remaining kidney after removal of the contralateral in immature rats **35**

Gunas V.I., Mishalov V.D., Serebrennikova O.A., Klimas L.A. General phenotypological picture of the finger dermatoglyphics of Ukrainian men: the contribution of individual regions **41**

Podolyuk M.V. Comparative anatomy of the uterine tube of human and laboratory white rat females **47**

Volkov K.S., Muha S.Yu. Electron microscopic changes of the testis germinal epithelium after an experimental thermal trauma in the application of cryo-lyophilized xenograft skin substrate **53**

Rekun T.O., Vernygorodskyi S.V., Kyselova T.M., Tataryna O.V., Cherepakha O.L. The role of the transcription factor Sox2 and cytokeratins in the formation and development of the gastroesophageal junction epithelial cell differon **58**

Turchyna N.S., Savosko S.I., Ribalko S.L., Starosila D.B., Kolisnik D.I. Pathological changes on basis of ischemia with associated virus infection in mice brain **66**

DOI: 10.31393/morphology-journal-2018-24(4)-01 Reports of Morphology, Vol. 24, №4, Pages 5-14

ISSN 1818-1295 eISSN 2616-6194

REPORTS OF MORPHOLOGY

Official Journal of the Scientific Society of Anatomists, Histologists, Embryologists and Topographic Anatomists of Ukraine

journal homepage: https://morphology-journal.com

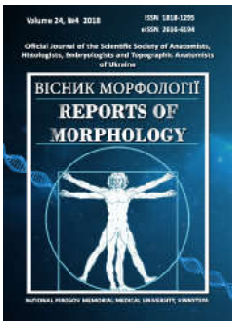

Morphofunctional changes of structural components of masticatory muscles of mature animals in mercazolilum-induced hypothyroidism

Sahan N.T.

Ivano-Frankivsk National Medical University, Ivano-Frankivsk, Ukraine

ARTICLE INFO

Received: 20 September, 2018

Accepted: 15 October, 2018

UDC: 616.742+616-092.9+616.441-008.64

CORRESPONDING AUTHOR

e-mail: antimis2012@gmail.com

Sahan N.T.

The damage of the muscular system is one of the frequent complications in thyroid diseases, but today there is no unanimous view on the morphofunctional changes in masticatory muscules in hypothyroidism. The purpose of this study was to determine the peculiarities of the structural organization of the masseter and lateral pterygoid muscles of mature rats in various stages of experimentally modeled hypothyroidism. The study was performed on the masticatory muscles of mature male rats during the 14th, 21th, 28th days of the development of mercazolilum-induced hypothyroidism. The following research methods were used: injection method of study of the circulatory bed of the masticatory muscles; histological examination of blood vessels and tissue elements of the masticatory muscles; electron microscopic examination; morphometric analysis (mean value of blood vessels' lumen and thickness of their walls; number of capillaries in 1 ?m2 of cross section of muscular fiber; the quantity of the capillaries at one muscular fiber, the percentage of oxidative (OMF), oxidative-glycolytic (OGMF), glycolytic (GMF) muscular fibers, average muscular fiber area, biochemical methods, and statistical analysis was conducted out using the software RV.3.0. The development of hypothyroidism is indicated by the reduction of hormones of the thyroid gland in the blood. During the 14th day of the experiment in the arterial bed in the injection of Parisian blue in the masticatory muscles there is a deformation of the vascular pattern. The number of hemocapillaries decreases. The edema of the cytoplasm of endothelial cells is submicroscopically marked. In muscular fibers, the cross-striation is broken, the area of their cross-section is enlarged, the dilation and vacuolization are observed in the endomysium. A change was determined in the quantitative distribution of all types of fibers (the number of OGMF and OMF decreased, and the amount of GMF increased). At the ultramicroscopic level, there were observed pronounced changes in all types of muscular fibers, especially in the GMF and OMF of the masseter muscle. On the 21st day, a significant deformation of the vascular pattern was observed, with a decrease of the arterial lumen and an increase of the vein lumen. The number of hemocapillaries continues to decrease. Ultra-structurally, in the endothelial cells of the hemocapillaries of the masticatory muscles, edema changes progress. In muscular fibers there is a loss of cross-striation and observed swelling. There is a tendency to decrease of the number of OGMF and OMF and increase of the amount of GMF. At the ultramicroscopic level, there are pronounced changes in all types of fibers, especially in the masseter muscle. During the 28th day of mercazolilum-induced hypothyroidism changes in the vessels and muscle fibers are progressing. Described morphological changes are associated with the dynamics of the trace substances' composition. Thus, in mercazolilum-induced hypothyroidism in the masticatory muscles there are edematous changes both in the vascular bed and in muscular fibers. Moreover, the changes are deepened depending on the duration of the experiment.

Keywords: *hypothyroidism, muscular fiber, ontogenesis, hemomicrocirculatory bed.*

Introduction

The study of the morphology of masticatory muscles was performed for a long time by many native and foreign scholars [8, 16, 17, 21, 22, 23, 29]. However, there is no clear and unanimous point of view of the morphology of

these muscles. The study of masticatory muscles under the influence of various factors, including the changes of the thyroid status are of particular relevance. Damage of the muscular system is one of the most frequent complications in diseases of the thyroid gland. An overview of scientific literature showed that 5% of all myopathies are associated with pathology of the thyroid gland [9, 14, 15, 20, 24, 29, 30]. Deficiency of thyroid hormones results in a violation of the expression of the heavy chain myosin genome, redistribution of its isoforms, inhibition of protein synthesis and, consequently, muscular growth. Besides, in the deficiency of hormones of the thyroid gland, the mobilization of free fatty acids from adipose tissue is disturbed, which leads to the insufficient lipid delivery to the skeletal muscles and is a possible cause of muscular weakness and reduced ability to work [1, 6, 31].

Taking into account the topicality of this issue and the constant increase and spread of morbidity (in Ukraine, as of January 1, 2012, there were registered 90.884 thousand patients with hypothyroidism (in 1999 - 53 thousand); the incidence rate in 2011 was 22.1 per 100.000), the study of the morphofunctional state of masticatory muscles in hypothyroidism requires further study.

Thus, the *aim* of our study is to establish the peculiarities of the structural organization of the masseter and lateral pterygoid muscles of the mature rats at various stages of experimentally modeled hypothyroidism.

Materials and methods

The material for the study was masseter and lateral pterygoid muscles of the 48 white outbred mature male rats. The material was taken in clearly defined symmetrical places of the masseter and lateral pterygoid muscles during the 14th, 21th, 28th days of experimentally modeled hypothyroidism. Animals were divided into groups: group I - intact (12 animals), which were kept under normal conditions of vivarium using natural for rodent feeding; group II - under the conditions of mercazolilum-induced hypothyroidism (36 animals).

Maintenance of animals, their nutrition and manipulations with them were performed in compliance with ethical and legislative norms and requirements during the implementation of scientific and morphological studies, in accordance with the provisions of the "European Convention for the Protection of Vertebrate Animals used for the experiments and other scientific purposes" (Strasbourg, 1986), Appendix 4 to the "Rules for the performance of the works using experimental animals", approved by the Order of the Ministry of Health of Ukraine №755 of 12.08.1997, the Helsinki Declaration of the World Medical Association (2000), "On Measures as to Further Improvement of the Organization of Forms of Work with the Use of Experimental Animals" and the provisions of the "General Principles of Animal Experiments" taken by the First National Congress on Bioethics (Kyiv, 2001); in accordance with the Law of Ukraine №3447-IV "On the Protection of Animals from Cruel Treatment" of 21.02.2006 (Expert Opinion of the Bioethics Commission of Ivano-Frankivsk National Medical University, Protocol №104/18 dated October 25, 2018).

Euthanasia of animals was performed by intraperitoneal administration of sodium thiopental (2% solution of sodium thiopental in a dose of 25 mg/kg).

The following research methods were used: modeling of mercazolilum-induced hypothyroidism [19, 7]; injection method of study of the circulatory bed of the masticatory muscles ("Parisian blue"); histological examination of blood vessels and tissue elements of the masticatory muscles (coloring with hematoxylin and eosin, fuchsin according to Hart, trichrome staining according to Masson, hematoxylin-main fuchsin-picric acid according to Van Gieson; the histochemical method of masticatory muscles studying (succinate dehydrogenase (SDG) according to M. Nachlas method); electron microscopic examination; morphometric analysis (mean value of blood vessels' lumen and thickness of their walls; number of capillaries in 1 μm^2 of cross section of muscular fiber; the quantity of the capillaries at one muscular fiber, the percentage of oxidative (OMF), oxidative-glycolytic (OGMF), glycolytic (GMF) muscular fibers, average muscular fiber area, biochemical methods, and statistical analysis.

Variational-statistical processing was carried out using the software RV.3.0. The data of the descriptive statistics is given as M ± m (selective average ± standard deviation).

Results

Thyroid homeostasis in the dynamics of the induced hypothyroidism during the 14th day was: T_3 - 2.68 ± 0.23 nM/l ($p<0.01$), T_4 - 26.86 ± 2.80 ($p<0.01$) nM/l. During the 21st day: TSH - 0.08 ± 0.01 uIU/mL ($p<0.01$), T_3 - 2.56 ± 0.26 nM/l ($p<0.01$), T_4 - 19.89 ± 2.00 ($p<0.01$) nM/l. During the 28th day of induced hypothyroidism: TSH - 0.07 ± 0.01 uIU/mL ($p<0.01$), T_3 - 2.61 ± 0.25 nM/l ($p<0.01$), T_4 - 24.41 ± 3.00 ($p<0.01$) nM/l.

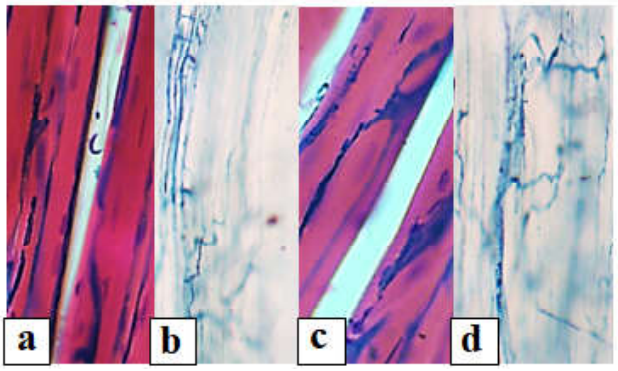

Fig. 1. Unevenness and mosaicity of the vascular pattern of the masseter (a, b) and lateral pterygoid (c, d) muscles of mature rats during the 14th day of mercazolilum-induced hypothyroidism. Staining: a, c - injection with Parisian blue with additional coloring of hematoxylin and eosin; b, d - injection with Parisian blue. Microphotograph. ocular lens x10, field lens x20.

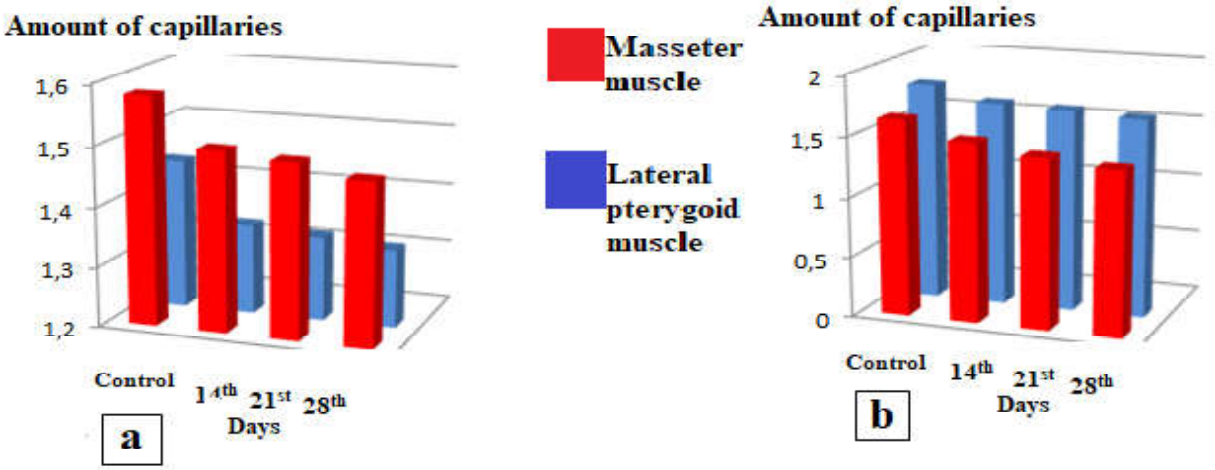

Fig. 2. Reduction of the number of hemocapillaries in 1 μm^2 (a) and the amount of hemocapillaries pertaining to one muscular fiber (b) in the masticatory muscles of mature animals at various stages of the development of mercazolilum-induced hypothyroidism.

During the 14th day of the experiment in the arterial bed of the mature rats in the injection of Parisian blue both in the masseter and lateral pterygoid muscles, a change of the vascular pattern (Fig. 1) is observed. The number of hemocapillaries decreases in comparison with the norm (Fig. 2).

In a submicroscopic study, there is observed the edema of the endothelial cells of the cytoplasm, which leads to the narrowing of the lumen and, subsequently, to the formation of erythrocytic sludges (Fig. 3). Hemocapillaries are surrounded by an electron-transparent basic substance.

In muscular fibers, cross-striation is much disordered. The nuclei of muscular fibers are enlarged and slightly lumenized. There is an expansion and vacuolization of endomysium between muscular fibers. Visually the perimysium is thickened and loose.

In the study of SDG activity, we have determined a change in the quantitative distribution of all types of fibers (the number of OGMF and OMF decreased and the amount of GMF increased (Fig. 4)). In addition, muscular fibers have been altered and deformed. SDG was unevenly distributed.

Morphometric study reveals a certain increase in the cross-sectional area of all types of fibers in comparison with the norm (Fig. 5). At the ultramicroscopic level, the pronounced changes were observed in all types of muscular fibers, especially in the GMF and OMF of the masseter muscle. A focal loss of cross-striation was noted, since isotropic disks (strip I) and anisotropic disks (strip A), Z-lines are deformed and disorganized. Mitochondria are enlarged, have a bright matrix and ruined crests (Fig. 6).

During the 21st day of the mercazolilum-induced hypothyroidism, there were determined a significant uneven filling of the vessels of the masseter and lateral pterygoid muscles with the injectable mass, resulting in the vascular pattern being deformed and mosaic (Fig. 7).

During histological examination, unevenness and deformation of vascular lumen are observed. The arterial

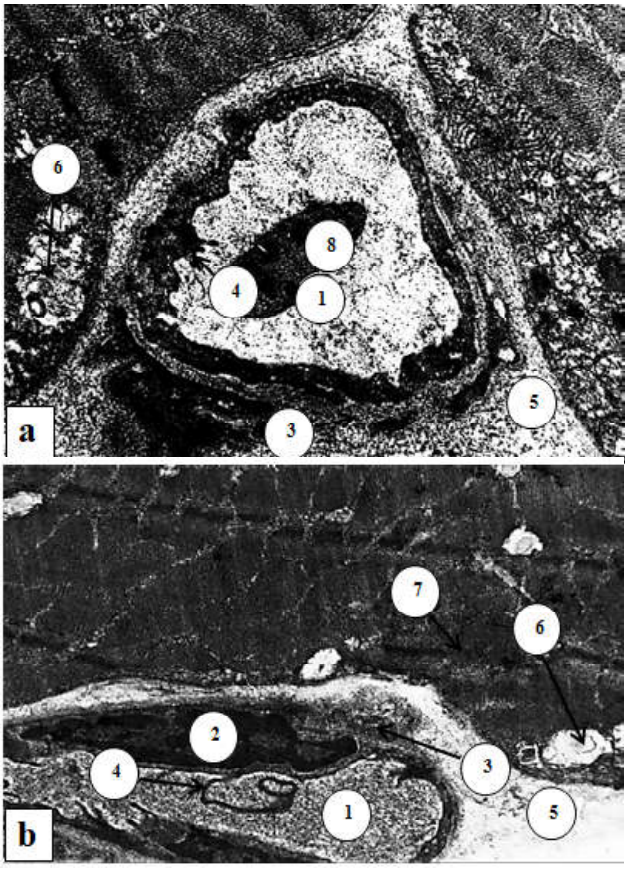

Fig. 3. The ultrastructural organization of the masseter (a) and lateral pterygoid (b) muscles of the mature rat during the 14th day of the development of mercazolilum-induced hypothyroidism. Electronic Microphotograph. 1 - deformed lumen of the hemocapillary, 2 - nucleus of the endothelial cell hemocapillary with marginally located heterochromatin and invaginations of the nuclear membrane, 3 - delaminatability of the basal membrane of the endothelial cell hemocapillary, 4 - cytoplasmic excrescences into the hemocapillary lumen, 5 - dilated and vacuolated perivascular space, 6 - destroyed mitochondria, 7 - violation of cross-striation, 8 - platelet. Magnification: x8000.

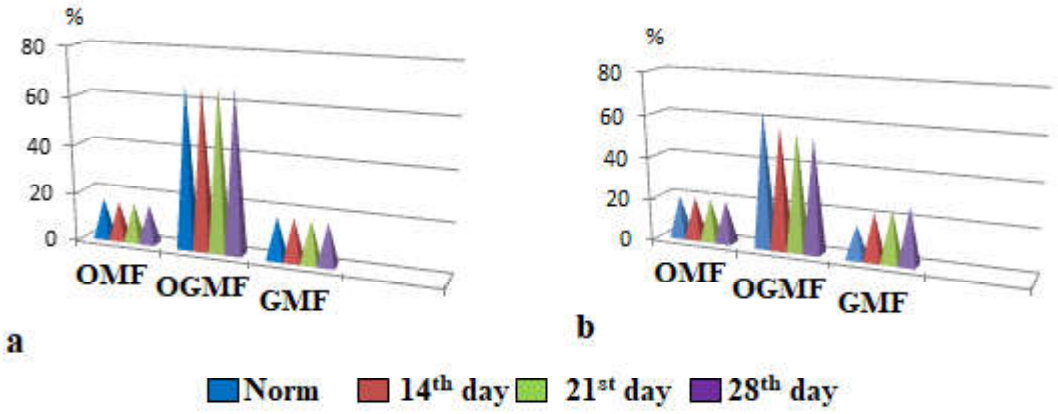

Fig. 4. Change of the quantitative composition of muscular fibers in the masseter (a) and lateral pterygoid (b) muscles of mature animals in different periods of experimental hypothyroidism.

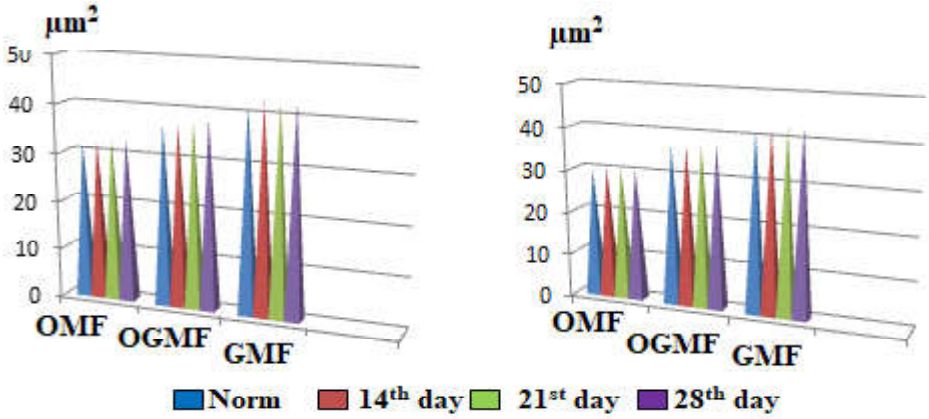

Fig. 5. Change of the cross-sectional area of muscular fibers in the masseter (a) and lateral pterygoid (b) muscles of mature animals at different terms of experimental hypothyroidism.

lumen decreases, compared with control, the venous lumen increases. The number of hemocapillaries in 1 μm^2 of the cross-section of muscular fibers continues to decrease. One muscular fiber also has a smaller amount of hemocapillaries, compared with the norm. Ultrastructurally it is found that there are edematous changes in endothelial cells of hemocapillaries of masticatory muscles. One can observe cytoplasmic excrescences into the lumen of the hemocapillary, indicating the development of hypoxia and disorder of the transcapillary exchange.

In muscular fibers there is a loss of cross-striation, edema of their nuclei, dilation, rupture and edematous changes of endomysium and perimysium with the formation of vacuoles (Fig. 8). During the morphometric study, an increase of the cross-sectional area of all types of fibers is observed (see Fig. 5). During the study of SDG-activity, there was determined some redistribution in the number of different types of muscular fibers, as well as their edematous changes and deformity (see Fig. 4).

At the ultramicroscopic level in the mature animals, there were marked changes in all types of fibers, especially in the masseter muscle, which were characterized by the loss of cross-striation, the destruction of isotropic (strip I) and anisotropic (strip A) discs, Z-lines. The nuclei in every muscular fiber are large, of lowered electron density, and their membrane forms profound invaginations. Mitochondria are of a sack-shaped form, have a bright matrix and destroyed crests (Fig. 9).

During the 28th day of mercazolilum-induced hypothyroidism in the arterial bed of the masseter and lateral pterygoid muscles of mature animals, one can observe the disorders and deformation of the vascular pattern, as a result of which it looks multiglomerular. In the injection with Parisian blue, the areas which are well and poorly filled with staining, are alternating (Fig. 10).

Among the intramuscular small arteries and arterioles one can find the closed ones, in which the paint does not fall. Morphometric study shows a significant narrowing of the arteries and thickening of the arterial wall, as well as the enlargement of the lumen and thinness of the venous wall, compared with the control. Significantly decreases the number of hemocapillaries in 1 μm^2 of the transverse section of muscular fiber (see Fig. 2).

During the ultramicroscopic examination of endothelial cells, an increase of edematous changes is observed. In muscular fibers, there was observed light-optically cross-

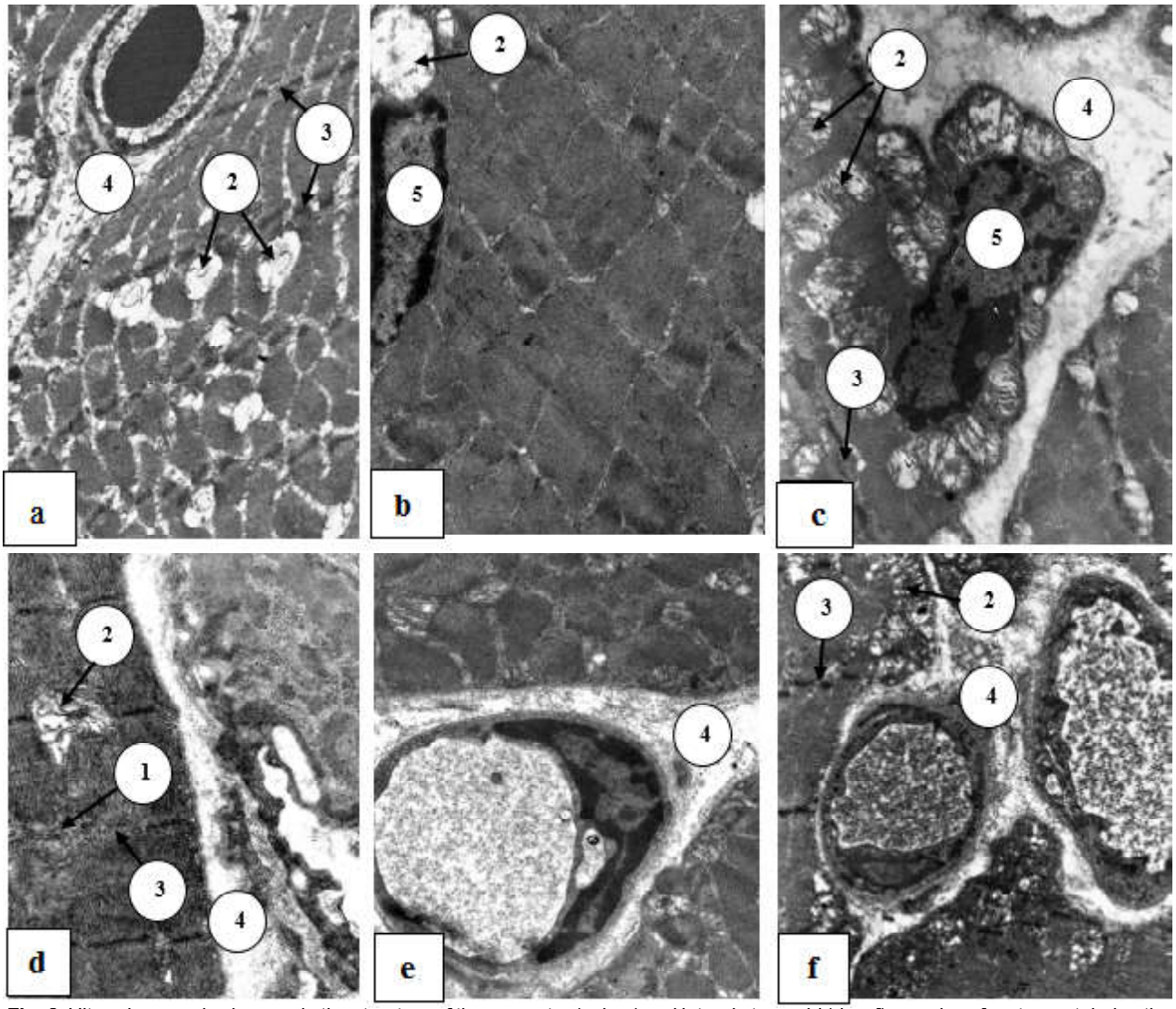

Fig. 6. Ultramicroscopic changes in the structure of the masseter (a, b, c) and lateral pterygoid (d, e, f) muscles of mature rat during the 14th day of the mercazolilum-induced hypothyroidism. Electronic Microphotography. 1 - loss of cross-striation of muscular fiber, 2 - expanded and destroyed mitochondria, 3 expanded and destroyed Z-line, 4 - swollen endomysium, 5 - nucleus of the muscular fiber. Magnification: a - x4800; b, e - x8000; c, f - x6400, d - x12000.

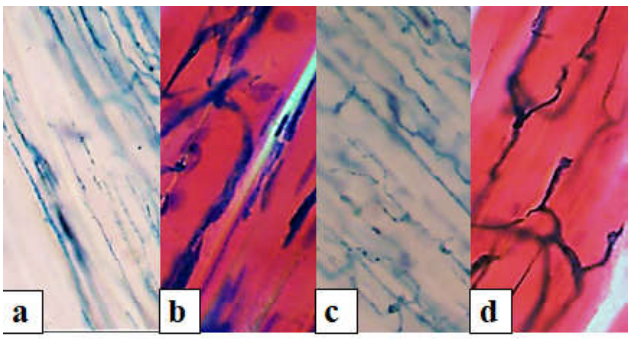

Fig. 7. Angioarchitectonics of the masseter (a, b) and lateral pterygoid (c, d) muscles of mature rats during the 21st day of mercazolilum-induced hypothyroidism. Staining: a, c - injection with Parisian blue; b, d - injection with Parisian blue with additional coloration of hematoxylin and eosin. Microphotograph. Ocular lens x10, field lens x20.

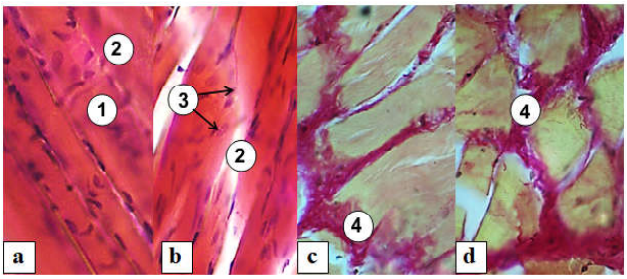

Fig. 8. Histostructure of the masseter (a) and lateral pterygoid (b) muscles of mature rats during the 21st day of experimental hypothyroidism. Staining: a, b - hematoxylin and eosin; c, d - hematoxylin-main fuchsin-picric acid according to Van Gieson. Microphotograph. 1 - loss of cross-striation of muscular fibers, 2 - edema of muscular fibers, 3 - nuclei of muscular fibers, 4 - dilation and edema of the intermuscular layers. Magnification: ocular lens x10, field lens x40.

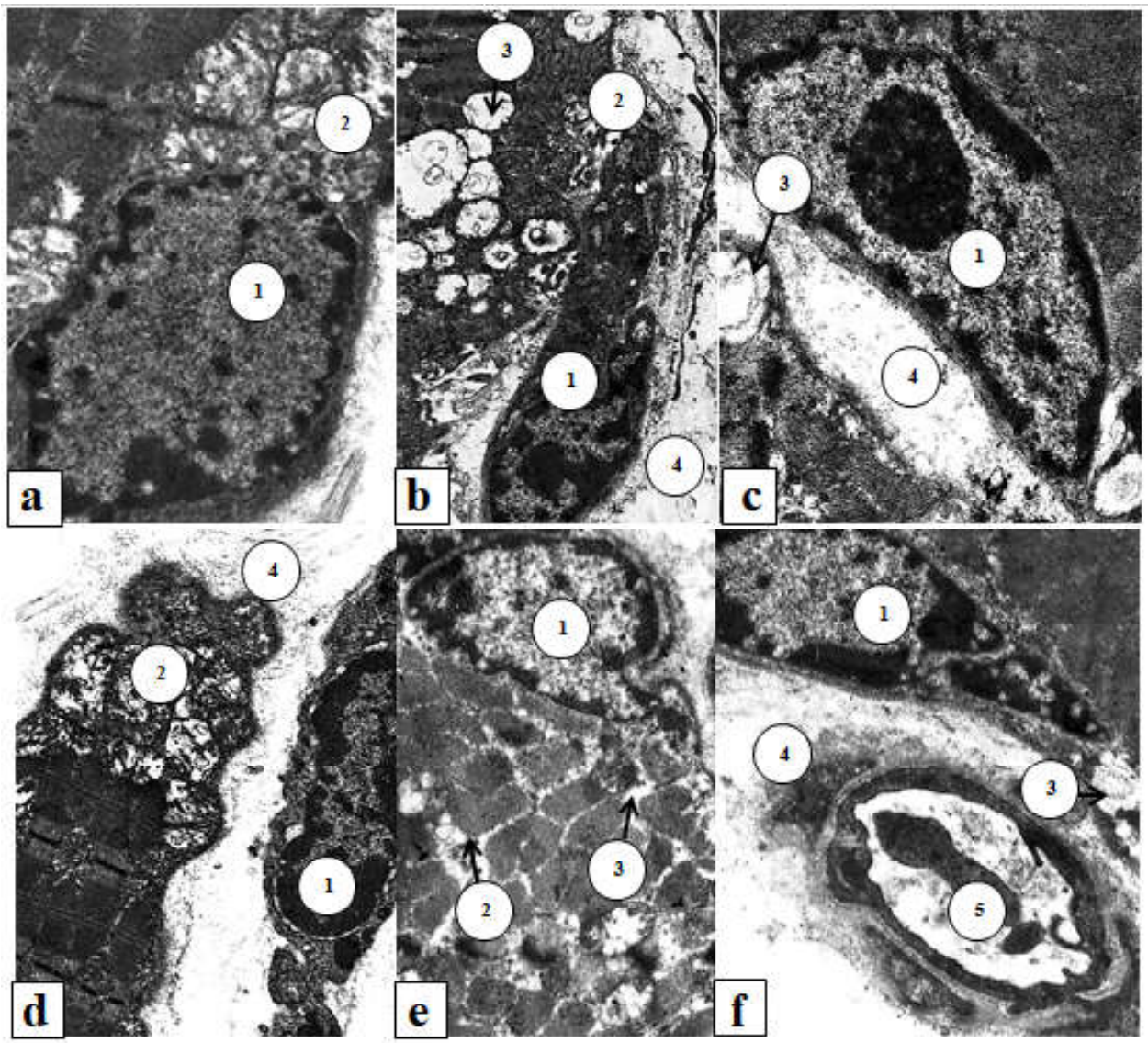

Fig. 9. Sub-microscopic changes in the structure of the masseter (a, b, c) and lateral pterygoid (d, e, f) muscles of mature rat during the 21st day of mercazolilum-induced hypothyroidism. Electronic Microphotograph. 1 - nucleus of the muscular fiber with marginally placed heterochromatin, 2 - expanded and destroyed mitochondria, 3 - vacuolization of muscular fibers, 4 - swollen and disorganized connective tissue elements, 5 - hemocapillary. Magnification: a, c - x8000; b, e, f - 6400; d - x9600.

striation loss, their vacuolization, dilation and vacuolization of endomysium and perimysium with the formation of vacuoles. In the morphometric study, an increase of the cross-sectional area of all types of fibers compared with the norm is noted (see Fig. 5).

In the study of SDG-activity, we have found that the number of OGMF and OMF decreases with the simultaneous increase of the amount of GMF (see Fig, 4). In this case, the fibers appear enlarged and deformed, the enzyme accumulates unevenly. At the ultramicroscopic level, marked edematous changes and destruction of structures, especially mitochondria, were observed in all types of fibers (Fig. 11).

Thus, in mercazolilum-induced hypothyroidism, in muscular fibers there are significant edematous changes both in the histological and ultrastructural levels. In the morphometric study, an increase of the diameter of all types of fibers was determined. Patients mostly suffer from GMF. Swelling and vacuolation of the connective tissue of the endomysium and perimysium are also noted. Moreover, the changes are deepened depending on the duration of the experiment. During study of the succinate dehydrogenase activity of muscular fibers, we've determined that there is a redistribution in the amount of muscular fibers. There is a tendency to decrease of OGMF and a significant increase of GMF.

Such morphological changes are associated with the dynamics of the microelement composition. Thus, the content of Ca, P, Mg, during the 14th day of the experiment was 1.94 ± 0.19 mM/l ($p<0.01$); 29.97 ± 3.07 mM/l ($p<0.01$),

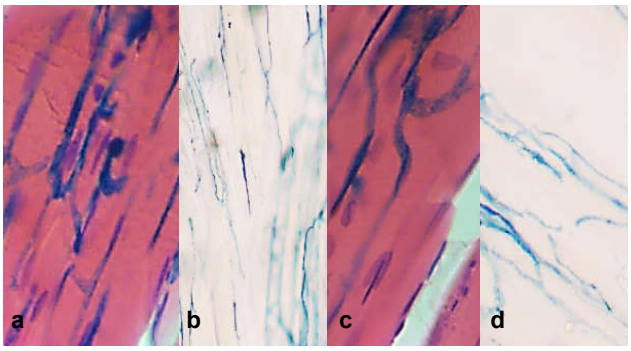

Fig. 10. Desolation and mosaicity of the vascular pattern of the masseter (a, b) and lateral pterygoid (c, d) muscles of mature rats during the 28th day of mercazolilum-induced hypothyroidism. Staining: a, c - injection with Parisian blue with the addition of hematoxylin and eosin; b, d - injection with Parisian blue. Microphotograph. Magnification: ocular lens x10, field lens x20.

1.42 ± 0.17 mM/l (p<0.01) respectively. During the 21st day - 1.82 ± 0.19 mM/l (p<0.01); 1.39 ± 0.18 mM/l (p<0.01); during the 28th day - 1.75 ± 0.16 mM/l (p<0.01); 22.70 ± 2.49 mM/l l (p<0.01), 1.37 ± 0.18 mM/l (p<001), respectively.

Discussion

In hypothyroidism in the vascular bed of masticatory muscles during the 14th day there are significant changes. Our results are consistent with studies of the vascular bed in hypothyroidism [2, 3], where it was found that in patients with hypothyroidism there are sharply expressed violations in the system of terminal blood flow with the predominance of intravascular and vascular changes in the form of foci of microcongestion due to the increased blood viscosity, hematocrit, perivascular hemorrhages, perivascular edema, tortuosity of microvessels of all links of the microcirculatory bed, and "sludge" - a phenomenon in the capillaries. Further during the 21st and 28th day of the mercazolilum-induced hypothyroidism we observe the deepening of changes in the circulatory bed, which corresponds to studies [28], in which morphological changes in the circulatory bed of experimental animals become more significant, with the prolongation of experiment time.

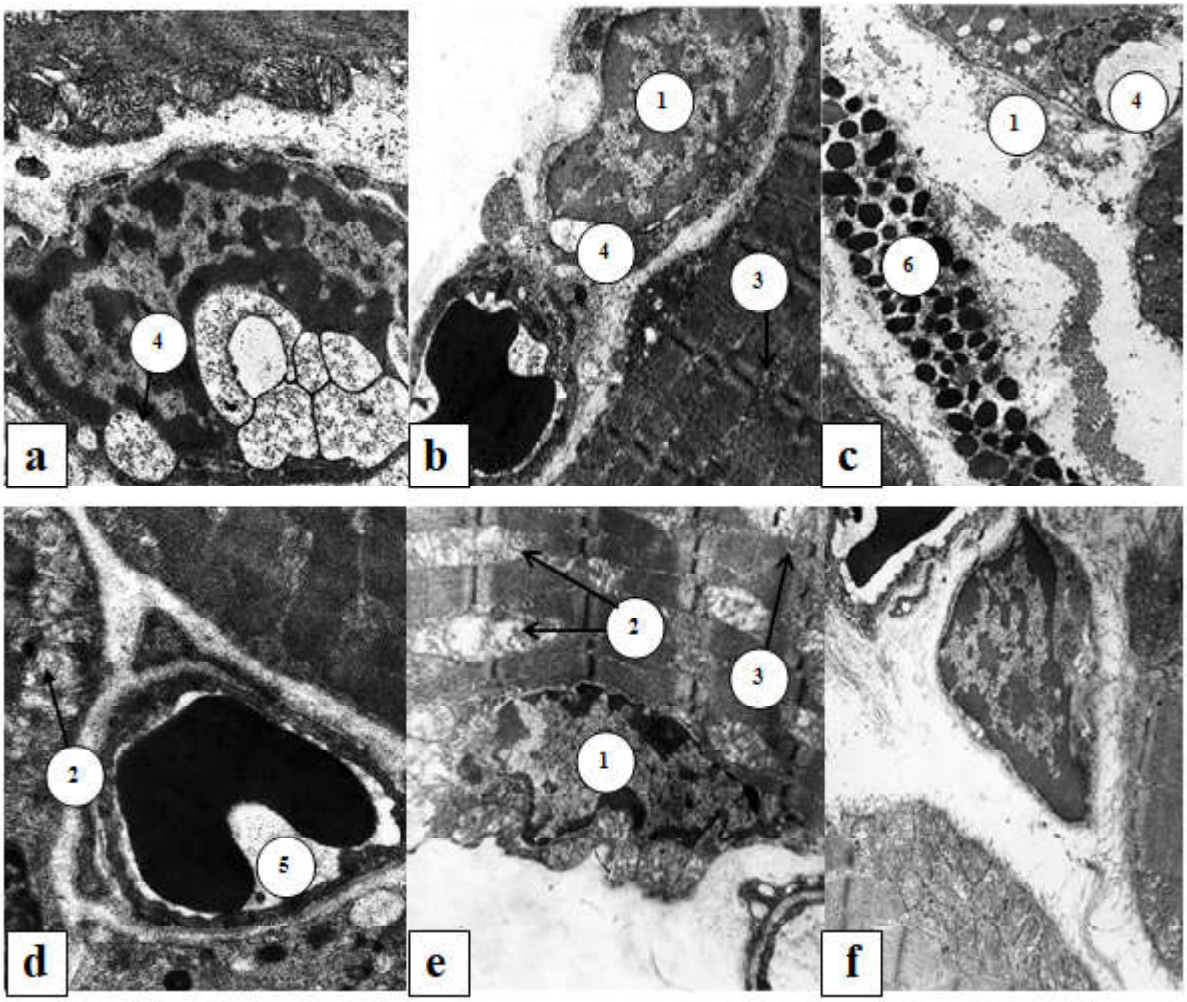

Fig. 11. Submicroscopic organization of the masseter muscle of mature rat during the 28th day of mercazolilum-induced hypothyroidism. Electronic Microphotography. 1 - nucleus of muscular fiber; 2 - mitochondria with uncomplemented crests, 3 - disorganized striation, 4 - vacuoles, 5 - hemocapillary, 6 - mastocyte. Magnification: a - x9600; b, c, d, e, f - x8000.

Multiple studies are devoted to the study of the causes of changes in the vascular bed in hypothyroidism. Thyroid hormones have been found to induce 3-hydroxy-3-methylglutaryl-coenzyme-A-reductase, which is the first step in the synthesis of cholesterol. Triiodothyronine also regulates the activity of receptors of low density lipoprotein, controlling the activity of their responsible genes and protects them from oxidation [11]. T_3 regulates the activity of cholesterol-7α-hydroxylase - key enzyme in the synthesis of bile acids, which in hypothyroidism conditions slows down the cholesterol, contributing to its increase in blood [25, 26]. It has been found that in hypothyroidism the concentration and activity of HDLLp-PLA2, which is associated with the anti-atherogenic effect of low density lipoprotein, decreases. Thus, in hypothyroidism, the level of cholesterol increases and there is a dyslipidemia that has an atherogenic nature and increases the risk of atherosclerosis [12, 10]. Perhaps, the development of atherosclerosis leads to further vascular damage.

Also, the disorders in the vascular bed of masticatory muscles in hypothyroidism could be attributed to the development of endothelial dysfunction and violation of relaxation of smooth muscular cells in vessels, which leads to an increase in peripheral vascular resistance. Some studies have described thickening of the intima-media complex in people with hypothyroidism [16].

In the study of muscular fibers during the 14th, 21st and especially 28th days of experimental mercazolilum-induced hypothyroidism, one can note the increasing edematous changes in all types of muscular fibers, and especially in glycolytic ones, which confirms the opinion that the severity of morphological changes in somatic muscles depends on the duration of hypothyroidism, not on the severity and depth of the process [28]. Our studies are consistent with others, which determined that fast muscular fibers are much more likely to be damaged than slow ones [27]. They believe, that this is due to the thinner Z- and M-discs. Biochemically, it was found that in the case of muscular damage, the concentration of "fast" myosin in the blood is twice that of "slow" one, which indicates more violations of the structure of the corresponding muscular fibers [13]. Significant edema can be observed in the connective tissue components of the endo- and perimysium, the diffuse accumulation of glycoproteins, which is the determining factor of exudation. Initial manifestations of experimental hypothyroidism were detected during the 14th day, the full picture - during the 28th, and during the 60th day - the day when in studied structure the severe structural changes with necrosis were determined. The acuteness of inflammation was characterized by inflammatory polymorphic cellular infiltrate with a high content of neutrophilic granulocytes, as well as an exudative component that occurs as a result of accumulation in glycoproteins tissues. At the same time, chromotropic substances are released from the bonds with proteins and are accumulated mainly in the intermediate substance, followed by the replacement of collagenous fibers with mucus-shaped masses. Infiltrate accumulates in large quantities in the intermediate substance, as a result there is a compression of cells, dystrophy, necrobiosis, necrosis and atrophy.

The cross-sectional area in all types of muscular fibers increases. These changes are described as "pseudo-hypertrophy" in Kocher-Debre-Semelaigne syndrome in hypothyroidism in children. It is accompanied by an increase of muscular fibers, but not of the increase of muscular strength, but rather a decrease of muscular strength and the development of muscular hypotonia [5]. Reduction of the muscular power of skeletal muscles in hypothyroidism may be due to the unconventional effects of T_4 at the structural and functional characteristics of the membranes, including the membrane of the sarcoplasmic reticulum. In this case, both lipid and protein component of the "liquid" bilayer is changing. This reduces the activity of Ca^{2+}ATPase and decreases the rate of absorption of calcium ions [18]. Changes of muscles in hypothyroid myopathy are characterized by their increase and induration. Patients often complain of muscular soreness in the palpation and movements. The slowing down of the contraction and relaxation of the muscles is characteristic for pseudomyotonic syndrome, which is not accompanied by a violation of electrical conductivity [4].

The performed morphofunctional research is the theoretical basis for the development and pathogenetic substantiation of measures aimed at correction and prevention of the development of iodine deficiency disorders, which, in turn, will lead to the prevention and reduction of the level of morbidity, its complications, disability and mortality caused by them.

Conclusions

In mercazolilum-induced hypothyroidism in the masticatory muscles there are edematous changes both in the vascular bed and in muscular fibers. Patients suffer mostly from GMF. Swelling and vacuolation of the connective tissue of the endomysium and perimysium are also observed, which is confirmed by both histological and submicroscopic studies. Moreover, the changes are deepened depending on the duration of the experiment.

References

[1] Alexander, E. K., Pearce, E. N., Brent, G. A., Brown, R. S., Chen, H., Dosiou, C., … Sullivan, S. (2017). Guidelines of the American Thyroid Association for the Diagnosis and Management of Thyroid Disease During Pregnancy and the Postpartum. *Thyroid,* 27(3), 315-389. doi: 10.1089/thy.2016.0457.

[2] Arslanbekova, A. Ch., Abusuyev, S. A., & Magomedov, M. A. (2007). Morphofunctional analysis of microcirculation after complex treatment using interval hypoxytherapy 17of primary hypothyroidism. *Morfologicheskiye vedomosti,* 3(4), 85-87.

[3] Arslanbekova, A. Ch., Abusuyev, S. A., & Magomedov, M. A. (2007). The state of microcirculatory hemodynamics after complex treatment using interval hypoxytherapy of primary

hypothyroidism. *Ural Medical Journal,* 12(40), 53.
[4] Bodnar, P. M. (2010). *Endocrinology.* Vinnitsa: Nova knyha.
[5] Bogova, E. Ya., & Shyriaeva, T. Yu. (2017). Pseudohypertrophic myopathy in hypothyroidism in a child (Kocher-Debre-Semelaigne syndrome). *Problemy endokrinologii,* 63(2), 121-123. doi: 10.14341/probl2017632121-123.
[6] B?lling, T., Geisenheiser, A., Pape, H., Martini, C., R?be, C., Timmermann, B. … Willich, N. (2011). Hypothyroidism after Head-and-Neck Radiotherapy in Children and Adolescents: Preliminary Results of the "Registry for the Evaluation of Side Effects after Radiotherapy in Childhood and Adolescence" (RiSK). *International Journal of Radiation Oncology Biology Physics,* 81(5), 787-791. doi: 10.1016/j.ijrobp.2010.10.037.
[7] Charnosh, S. M. (2007). The comparative characteristic of three experimental models of hypothyroidism. *Visnyk naukovykh doslidzhen,* 2, 113-115.
[8] Ciavarella, D. (2014). Influence of vision on masticatory muscles function: surface electromyographice valuation. Annalidi Stomatologia, 2, 61-65.
[9] Dayan, C. M., & Panicker, V. (2013). Thyroid hormones association with depression. *Eur. Thyroid. J.,* 2, 168-179. doi: 10.1159/000353777.
[10] Didushko, O. M. (2014). Age-specific peculiarities of lipid metabolism in patients with manifested hypothyroidism. *Archive of clinical medicine*, 20(1), 21-23.
[11] Faure, P., Oziol, L., Artur, Y., & Chomard, P. (2004). Thyroid hormone (T3) and its acetic derivative (TA3) protect low-density lipoproteins from oxidation by different mechanisms. *Biochimie,* 86, 411-418. doi: 10.1016/j.biochi.2004.04.009.
[12] Goncharov, O. A. (2011). Lipid-lowering and pleiotropic effects of atorvastatin in women with autoimmune thyroiditis. *Liky Ukrayiny,* 6, 96-98.
[13] Guerrero, M., Rialp, J., & Urbano, D. (2008). The Impact of Desirability and Feasibility on Entrepreneurial Intentions: A Structural Equation Model. *International Entrepreneurship Management Journal,* 4, 35-40. doi: 10.1007/s11365-006-0032-x.
[14] Jiskra, J. (2001). Changes in muscle tissue in hypothyroidism. *Vnitr. Lek.,* 47(9), 609-612.
[15] Kerimov, E. E. (2009). The metabolic and structural changes in periodontal tissue in patients with hypothyroidism. *Georgian Med. News,* 177, 23-27.
[16] Kim, S. K., Kim, S. H., & Park, K. S. (2009). Regression of the increased common carotid artery-intima media thickness in subclinical hypothyroidism after thyroid hormone replacement. *Endocr. J.*, 56(6), 753-758.
[17] Konnov, V. V., Lepilin, A. V., Bagarjan, E. A., & Arushanjan, A. R. (2011). *Funkcionalnoe sostojanie zhevatelnyh myshc u pacientov s perelomami nizhnej cheljusti po dannym elektromiografii.* Abstracts are presented in materials XV Mezhdunar. nauch. konf. "Zdorovesemi - XXI vek", Torremolinos (pp. 11-13). Torremolinos, Ispanija: Perm': OT i DO.
[18] Kotelnikov, A. I., Tatiyanenko, L. V., Vystorop, I. V., Dobrokhotova, O. V., & Pikhtelev, I. Yu. (2016). The effect of cyclic hydroxamic acids on the activity of Ca^{2+}ATPase of the sarcoplasmic reticulum and cyclic guanosine monophosphate phosphodiesterase. *Rossiyskiy bioterapevticheskiy zhurnal,* 3, 23-27.
[19] Kulimbetov, M. T., Rashitov, M. M., & Saatov, T. S. (2009). Simulation of experimental hypothyroidism due to natural chronic iodine deficiency in the diet. *International Endocrinological Journal,* 2(20), 22-27.
[20] McCarthy, H. D. (2013). Skeletal muscle mass reference curves for children and adolescents. Pediatr. Obes., 18, 45-58. doi: 10.1111/j.2047-6310.2013.00168.x.
[21] McNeil, C. J. (2013). Testing the excitability of human motoneurons. *Front. Hum. Neurosci.,* 7, 1-9. doi: 10.3389/fnhum.2013.00152
[22] Mi, Y. F., Li, X. Y., Tang, L. J. Lu, X. C., Fu, Z. Q., & Ye, W. H. (2009). Improvement in cardiac function after sarcoplasmic reticulum Ca^{2+}-ATPase gene transfer in a beagle heart failure model. *Chin. Med. J.* (Engl), 122(12), 1423-1428.
[23] Obata, H. (2014). Modulation between bilateral legs and within unilateral muscle synergists of postural muscle activity changes with development and aging. *Exp. Brain. Res.,* 232(1), 1-11. doi: 10.1007/s00221-013-3702-2.
[24] Onigata, K. (2014). Thyroid hormone and skeletal metabolism. *Clin. Calcium,* 24(6), 821-827. doi: CliCa1406821827.
[25] Rush, J. M., Danzi, S., & Klein, I. (2006). Role of thyroid disease in the development of statin-induced myopathy. *Endocrinologist.,* 16, 279-285. Doi: 10.1097/01.ten.0000240960.40281.2b
[26] Salman, R. (2008). The influence of age on the relationship between subclinical hypothyroidism and ischemic heart disease: a metaanalisis. *J. Clin. Endocrinol. Metabol.,* 93(8), 59-67. doi: 10.1210/jc.2008-0167.
[27] Samsonova, L. N., & Kasatkina, E. P. (2007). Standards for the level of thyroid-stimulating hormone in the blood: modern state of the problem. *Endocrinology problems*, 539(6), 40-43.
[28] Sorokina, N. D., Gioeva, Yu. A., Selitsky, G. V., & Markovtseva, M. A. (2016). Neurophysiological aspects of the study of functional disorders in the maxillofacial area. *Rossiyskiy meditsinskiy zhurnal,* 22(2), 98-104.
[29] Strongin, L. G., Nekrasova, T. A., Ledentsova, O. W., Kasakova L. V., & Lukushkina, A. Y. (2012). *Dyslipidemia and endothelial dysfunction in patients with the mildest hypothyroidism: relationship to TSH values and levothyroxine treatment.* Abstracts are presented in book of Abstracts 36-th annual meeting of the European Thyroid Association (ETA), Pisa (p. 80). Pisa: [2012].
[30] Tambovseva, R. V. (2010). *Growth and development of skeletal muscles boys.* Int. Abstracts are presented in materials symposium "Biological Motility from Fundamental Achievements to Nanotechnologies", Pushchino (pp. 276-278). Pushchino: [w.p.].
[31] Zahid, T. M., Wang, B. Y., & Cohen, R. E. (2011). The effects of thyroid hormone abnormalities on periodontal disease status. *J. Int. Acad. Periodontol.,* 13(3), 80-85.

МОРФОФУНКЦІОНАЛЬНІ ЗМІНИ СТРУКТУРНИХ КОМПОНЕНТІВ ЖУВАЛЬНИХ М'ЯЗІВ СТАТЕВОЗРІЛИХ ТВАРИН ПРИ МЕРКАЗОЛІЛІНДУКОВАНОМУ ГІПОТИРЕОЗІ

Саган Н.Т.

Ураження м'язової системи є одним з частих ускладнень при захворюваннях щитоподібної залози, однак на сьогодні немає одностайного погляду на морфофункціональні зміни жувальних м'язів при гіпотиреозі. Метою даного дослідження було встановити особливості структурної організації власне жувального та бічного крилоподібного м'язів статевозрілих щурів на різних етапах експериментально змодельованого гіпотиреозу. Дослідження виконували на жувальних м'язах статевозрілих щурів-самців на 14, 21, 28 добу розвитку мерказоліліндукованого гіпотиреозу. Використовували наступні методи дослідження:

ін'єкційний метод дослідження кровоносного русла жувальних м'язів; гістологічне дослідження кровоносних судин та тканинних елементів жувальних м'язів; електронно-мікроскопічне дослідження; морфометричний аналіз: середнє значення просвіту кровоносних судин та товщина їх стінки, кількість капілярів в 1 мкм^2 поперечного перерізу м'язового волокна, кількість капілярів, які припадають на одне м'язове волокно, процентне співвідношення окисних м'язових волокон (ОМВ), окисно-гліколітичних (ОГМВ), гліколітичних (ГМВ), середня площа м'язового волокна; біохімічні методи; статистичний аналіз проводили за допомогою програмного забезпечення RV.3.0. Про розвиток гіпотиреозу свідчить зменшення гормонів щитоподібної залози в крові. На 14 добу експерименту в артеріальному руслі при ін'єкції паризькою синьою у жувальних м'язах відмічається деформація судинного рисунка. Кількість гемокапілярів зменшується. Субмікроскопічно відмічається набряк цитоплазми ендотеліоцитів. У м'язових волокнах поперечна посмугованість порушена, збільшувалась площа їх поперечного перерізу, в ендомізії спостерігається розширення та вакуолізація. Було встановлено зміну в кількісному розподілі всіх типів волокон (зменшувалася кількість ОГМВ і ОМВ та збільшувалася кількість ГМВ). На ультрамікроскопічному рівні спостерігалися виражені зміни в усіх типах м'язових волокон, особливо в ГМВ та ОМВ власне жувального м'яза. На 21 добу встановлено значну деформацію судинного рисунку зі зменшенням просвіту артерій та збільшенням просвіту вен. Продовжує зменшуватися кількість гемокапілярів. Ультраструктурно в ендотеліоцитах гемокапілярів жувальних м'язів прогресують набрякові зміни. У м'язових волокнах спостерігається втрата поперечної посмугованості та їх набряк. Зберігається тенденція до зменшення кількості ОГМВ і ОМВ та збільшення кількості ГМВ. На ультрамікроскопічному рівні виражені зміни в усіх типах волокон, особливо у власне жувальному м'язі. На 28 добу мерказоліліндукованого гіпотиреозу зміни в судинному руслі та у м'язових волокнах прогресують. Описані морфологічні зміни асоціюють із динамікою мікроелементного складу. Таким чином, при мерказоліліндукованому гіпотиреозі у жувальних м'язах спостерігаються набрякові зміни як в судинному руслі так і в м'язових волокнах. Причому зміни поглиблюються в залежності від терміну експерименту.
Ключові слова: *гіпотиреоз, м'язове волокно, онтогенез, гемомікроциркуляторне русло.*

МОРФОФУНКЦИОНАЛЬНЫЕ ИЗМЕНЕНИЯ СТРУКТУРНЫХ КОМПОНЕНТОВ ЖЕВАТЕЛЬНЫХ МЫШЦ ПОЛОВОЗРЕЛЫХ ЖИВОТНЫХ ПРИ МЕРКАЗОЛИЛИНДУЦИРОВАННОМ ГИПОТИРЕОЗЕ

Саган Н.Т.

Поражения мышечной системы являются одним из частых осложнений при заболеваниях щитовидной железы, однако сегодня нет единодушного взгляда на морфофункциональные изменения жевательных мышц при гипотиреозе. Целью данного исследования было установить особенности структурной организации собственно жевательной и боковой крыловидной мышцы половозрелых крыс на разных этапах экспериментально смоделированного гипотиреоза. Исследование выполняли на жевательных мышцах половозрелых крыс-самцов на 14, 21, 28 сутки развития мерказолилиндуцированного гипотиреоза. Использовали следующие методы исследования: инъекционный метод исследования кровеносного русла жевательных мышц; гистологическое исследование кровеносных сосудов и тканевых элементов жевательных мышц; электронно-микроскопическое исследование; морфометрический анализ: среднее значение просвета кровеносных сосудов и толщина их стенки, количество капилляров в 1 мкм^2 поперечного сечения мышечного волокна, количество капилляров, приходящихся на одно мышечное волокно, процентное соотношение окислительных мышечных волокон (ОМВ), окислительно-гликолитических (ОГМВ) и гликолитических (ГМВ), средний размер мышечного волокна; биохимические методы; статистический анализ проводили с помощью программного обеспечения RV.3.0. О развитии гипотиреоза свидетельствует уменьшение гормонов щитовидной железы в крови. На 14 сутки эксперимента в артериальном русле при инъекции парижской синей в жевательных мышцах отмечается деформация сосудистого рисунка. Количество гемокапилляров уменьшается. Субмикроскопически отмечается отек цитоплазмы эндотелиоцитов. В мышечных волокнах поперечная исчерченность нарушена, увеличивалась площадь их поперечного сечения, наблюдается расширение и вакуолизация эндомизия. Было установлено изменение в количественном распределении всех типов волокон (уменьшалось количество ОГМВ и ОМВ и увеличивалось количество ГМВ). На ультрамикроскопическом уровне наблюдались выраженные изменения во всех типах мышечных волокон, особенно в собственно жевательной мышце. На 28 сутки мерказолилиндуцированного гипотиреоза изменения в сосудистом русле и в мышечных волокнах прогрессируют. Описанные морфологические изменения ассоциируют с динамикой микроэлементного состава. Таким образом, при мерказолилиндуцированом гипотиреозе в жевательных мышцах наблюдаются отечные изменения как в сосудистом русле, так и в мышечных волокнах. Причем изменения усугубляются в зависимости от срока эксперимента.
Ключевые слова: *гипотиреоз, мышечное волокно, онтогенез, гемомикроциркуляторное русло.*

DOI: 10.31393/morphology-journal-2018-24(4)-02 Reports of Morphology, Vol. 24, №4, Pages 15-21

ISSN 1818-1295 eISSN 2616-6194

REPORTS OF MORPHOLOGY

Official Journal of the Scientific Society of Anatomists, Histologists, Embryologists and Topographic Anatomists of Ukraine

journal homepage: https://morphology-journal.com

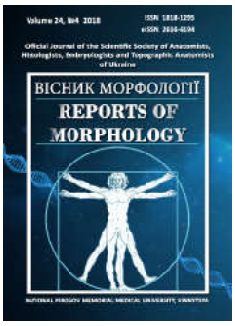

Determination of individual linear and angular characteristics of the position of upper central incisors in Ukrainian young men and women with orthognathic bite

Dmitriev M.O., Gunas I.V., Gnenna V.O., Smolko N.M.

National Pirogov Memorial Medical University, Vinnytsya, Ukraine

ARTICLE INFO

Received: 28 September, 2018

Accepted: 17 October, 2018

UDC: 616.716.8-071-084:613.956: 617.52: 616.34.25-007.481-7

CORRESPONDING AUTHOR

e-mail: dmitriyevnik@gmail.com

Dmitriev M.O.

Taking into account the importance of determining the teleroentgenographic indicators of the spatial position of central incisors, arises a scientific and clinical interest in conducting such studies. The purpose of the study is to develop mathematical models of individual characteristics of the position of upper central incisors in young men and women of Ukraine with orthognathic bite by studying the cephalometric indices and conducting direct stepwise regression analysis. With the help of Veraviewepocs 3D device, Morita (Japan) 38 young men (aged 17 to 21 years) and 55 young women (aged 16 to 20 years) with occlusion close to orthognathic bite and balanced faces received side teleroentgenograms. Cephalometric analysis was performed using OnyxCeph^{3}™ software. Cephalometric points and measurements were performed according to the recommendations of A.M. Schwarz, J. McNamara, W.B. Downs, R.A. Holdway, P.F. Schmuth, C.C. Steiner and C.H. Tweed. In the licensed statistical package "Statistica 6.0", using the direct stepwise regression analysis, the following teleroentgenographic characteristics of the position of the upper central incisors were performed: distance 1u_APog, distance 1u_Avert, distance 1u_NA, angle Max1_NA, angle Max1_SN and angle Max1_SpP. In young men and women with occlusion close to orthognathic bite and balanced face, reliable regression models of individual teleroentgenographic characteristics of the position of upper central incisors with a determination coefficient of greater than 0.50 have been developed, depending on the peculiarities of the metric characteristics of the craniofacial complex: in young men of 6 possible models, have been constructed 5 with coefficients of determination R^2 from 0.672 to 0.928, and for young women - all 6 possible models with determination coefficient R^2 from 0.508 to 0.663. In the analysis of models with a determination coefficient higher than 0.50, it was found that in young men most often the regression equations include - the angle AB_NPOG (12.0%); distance COND_GN, inclination angle I, MAX maxillary length, Se_N distance, Nap angle, NBa-PtGn angle, SND angle and Wits indicator (by 8.0%). In young women most often models include - the angle AB_NPOG and the Wits indicator (by 15.4%); angle N_POG (11.5%); the angle Gl'SnPog' and the distance LPALAT (by 7.7%).

Keywords: *upper central incisors position, cephalometry, regression analysis, young men and women, orthognathic bite.*

Introduction

One of the most common reasons for appeals to an orthodontist doctor is to improve your smile and not only change the color of the teeth but also position of the frontal group of teeth. After all, in a society successful, prospective, position in society is often associated with beauty and a beautiful smile [36].

The rapid development of computed technology and the use of digital tools offers a new perspective for daily clinical activity. They allow the physician to visualize the ultimate goal of treatment, taking into account the basic laws of aesthetics and harmony, as well as the patient's own wishes, creating an effective communication tool between the dentist and the patient.

When assessing the smile and facial expression in a

non-stressed condition, which is usually evaluated in three projections [30], the physician pays attention to the shape, size and position of the front teeth. The use of digital smile design tools - DSD (digital smile design) [16, 25, 29, 31, 38] helps to determine if there is a need to change the shape and size of the teeth themselves by direct or indirect restorations. But if you need to change your face profile, you often need orthodontic treatment. After all, orthodontists, having the ability to change the position of the frontal group of teeth, can also significantly affect the patient's profile. Many studies are devoted to this issue and changes that occur with the face during and after orthodontic treatment are described and continue to be studied by many authors [4, 15, 23, 37, 45, 46].

But the doctor who plans to change the person's face needs to have a clear idea not only about the average standard values of the corresponding facial and dental indices, but also to take into account the ethnic peculiarities of the perception of the true meaning of "beauty" [42], face type [32], and also taking into account aesthetic preference of the patient when creating an individual treatment plan [5, 7].

Taking into account the importance of determining the teleroentgenographic indices of the spatial position of central incisors and the diversity of the proposed methods [14, 28, 40, 43], as well as the lack of the possibility of identifying the individual normal values of these indicators, there is a scientific and clinical interest in conducting research on these issues. And the use of modern mathematical techniques allows us to develop tools for determining the individual normal values of the position of central incisors, taking into account their ethnic [24, 27], sexual, age [26] and anatomical [6] features of man.

The purpose of the study is to develop mathematical models of individual characteristics of the position of upper central incisors in young men and women of Ukraine with orthognathic bite by studying the cephalometric indices and conducting direct stepwise regression analysis.

Materials and methods

With the help of Veraviewepocs 3D device, Morita (Japan) in 38 young men (17 to 21 years of age) and 55 young women (aged 16 to 20 years) with occlusion close to the orthognathic bite and balanced face received side teleroentgenograms. Cephalometric analysis was performed using OnyxCeph^{3}™ software. Cephalometric points and measurements were performed according to the recommendations of A.M. Schwarz, J. McNamara, W.B. Downs, R.A. Holdway, P.F. Schmuth, C.C. Steiner and C.H. Tweed [14, 20, 21, 28, 33, 40, 41, 43]. The analysis of teleroentgenograms and the results of their researches for Ukrainian young men and women is described in detail and set out in a number of articles [8-11, 18, 19, 44].

We, in accordance with the above-mentioned methods, simulated the following teleroentgenographic characteristics of the position of the upper central incisors (Fig. 1): **APOG_1U** (distance 1u_APog) - the distance from the point Is1u (*the incisal edge of the upper central incisor*) to the line A-Pog; **AVERT_1U** (distance 1u_Avert) is the distance from the point of Is1u (*the incisal edge of the upper central incisor*) to the perpendicular to the Frankfurt plane (Po-Or) through the point A (if the distance located medially, that is, the incisal edge of the incisor is in the front with respect to the line position, then the indicator takes a positive value, and if the distance is distal, that is, the incisal edge of the incisor is in the posterior with respect to the line position, then the figure takes a negative value); **NA_1U** (distance 1u_NA) - distance from the point Ls1u to the line N-A (*defines the anterior-posterior arrangement of the crown part of the upper central incisor to the line N-A*); **MAX1_NA** (angle Max1_NA) - is formed by the lines Ap1u-Is1u (*inclination of the central axis of the upper central incisor*) and N-A; **MAX1_SN** (angle Max1_SN) - formed by the lines Ap1u-Is1u (*inclination of the central axis of the upper central incisor*) and S-N; **MAX1_SPP** (angle Max1_SpP) - is formed by lines Ap1u-Is1u (*inclination of the central axis of the upper central incisor*) and ANS-PNS (*palatal plane SpP*).

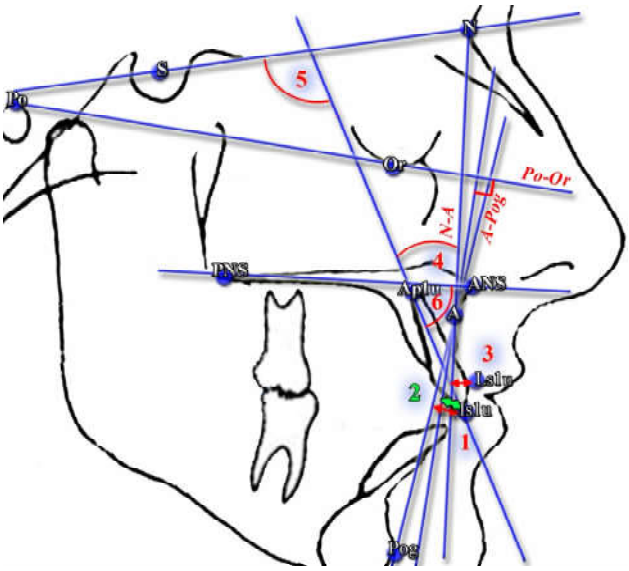

Fig. 1. Teleroentgenographic linear and angular characteristics of the position of upper central incisors. 1 - APOG_1U (distance 1u_APog); 2 - AVERT_1U (distance 1u_Avert); 3 - NA_1U (distance 1u_NA); 4 - MAX1_NA (angle Max1_NA); 5 - MAX1_SN (angle Max1_SN); 6 - MAX1_SPP (angle Max1_SpP).

Construction of models of linear and angular characteristics of the position of upper central incisors, depending on the peculiarities of the metric parameters of the skull, is carried out in the statistical package "Statistica 6.0" using straight-line regression analysis.

Results

As a result of modeling teleroentgenographic characteristics of the position of upper central incisors in young men and women with occlusion close to orthognathic bite and balanced faces, depending on the metric parameters of the skull, we have constructed linear equations for the

following indices.

For young men:

AVERT_1U = -22.96 + 0.271 x AB_NPOG + 0.222 x I + 0.278 x PN_A + 0.177 x NBA_PTGN - 0.317 x MAX + 0.073 x COND_GN (R^2=0.748; $F_{(6.30)}$=14.85; p<0.001; Error of estimate=1.077),

NA_1U = -18.55 + 0.265 x AB_NPOG + 0.137 x LPALAT + 0.166 x N_SE - 0.369 x MAX + 0.149 x I + 0.117 x NBA_PTGN (R^2=0.729; $F_{(6.30)}$=13.48; p<0.001; Error of estimate=0.943),

MAX1_NA = 14.28 - 0.774 x NAPOG + 0.172 x S_L (R^2=0.672; $F_{(2.33)}$=33.73; p<0.001; Error of estimate=3.241),

MAX1_SN = -73.09 + 1.863 x SND + 1.992 x AB_NPOG + 1.611 x WITS + 0.502 x NAPOG + 0.224 x NSBA + 0.209 x N_SE (R^2=0.929; $F_{(6.29)}$=62.98; p<0.001; Error of estimate=2.218),

MAX1_SPP = 164.0 + 0.550 x SND - 1.165 x MM + 1.411 x WITS + 0.113 x COND_GN + 0.184 x ML_NSL (R^2=0.819; $F_{(5.30)}$=27.24; p<0.001; Error of estimate=2.612).

The regression model of the distance of 1u_APog in young men with orthognathic bite has a determination coefficient of less than 0.5 (R2 = 0.483) and therefore has no practical significance for orthodontists.

For young women:

APOG_1U = -2.900 + 0.376 x N_POG_ + 0.128 x AFH - 0.152 x GL_SNPOG - 0.028 x GL_SN_S (R^2=0.508; $F_{(4.49)}$=12.66; p<0.001; Error of estimate=1.323),

AVERT_1U = -30.08 + 0.264 x P_OR_N + 0.342 x AB_NPOG + 0.283 x N_POG_ + 0.085 x COND_GN - 0.092 x GL_SNPOG (R^2=0.663; $F_{(5.48)}$=18.87; p<0.001; Error of estimate=1.244),

NA_1U = 0.248 + 0.505 x AB_NPOG + 0.165 x N_POG_ + 0.198 x MAX_MAND + 0.212 x WITS (R^2=0.662; $F_{(4.49)}$=24.01; p<0.001; Error of estimate=1.056),

MAX1_NA = 36.62 + 1.258 x AB_NPOG - 1.301 x SN_GOGN + 1.017 x ML_NSL + 0.591 x WITS (R^2=0.561; $F_{(4.46)}$=14.67; p<0.001; Error of estimate=3.710),

MAX1_SN = -36.70 + 1.806 x SND + 0.832 x AB_NPOG + 1.010 x WITS + 0.423 x LPALAT - 0.297 x S_L (R^2=0.649; $F_{(5.45)}$=16.65; p<0.001; Error of estimate=3.553),

MAX1_SPP = 210,9 - 1,211 x MM + 0,628 x ANB + 0,698 x WITS + 0,349 x LPALAT (R^2=0,575; $F_{(4,46)}$=15,54; p<0,001; Error of estimate=3,817).

In these models: R^2 - coefficient of determination; $F_{(!,!!)}$=!!,!! - critical $_{(!,!!)}$ and got (!!,!!) value of Fisher's criterion; St. Error of estimate - standard error of the standardized regression coefficient; AB_NPOG - angle formed by lines A-B and N-Pog (defines the position of the plane AB in relation to the N-pog); AFH (distance AFH or front height of the face) - distance from the point Me to the line ANS-PNS; ANB (angle ANB) - is formed by lines A-N and N-B (indicates an angular interstitial relation in the anterior-posterior direction; angle ANB is considered positive if point A is in front of NB; if the lines NA and NB overlap, then the ANB angle is 0°; if point A is behind the NB line, then the angle is considered negative); COND_GN (effective length of mandible, or distance COND_GN) - distance from the point Cond to the point Gn; GL_SN_S (index Gl'_Sn_Sn_Gn' or facial vertical index) - distance ratio of Gl'-Sn and Sn-Gn' (defines vertical relationships in the face profile); GL_SNPOG (angle Gl'SnPog' or indicator of convexity of the soft tissue profile) - formed by lines Gl'-Sn and Sn-Pog'; I (angle I, inclination angle) - angle formed by line ANS-PNS and Pn (nasal perpendicular, perpendicular to the line from the point N' to the line Se-N), angle of inclination of the upper jaw (spinal plane) to the nasal perpendicular; LPALAT (the value of the base of the upper jaw, CT-indicator) - distance between points ANS and PNS; MAX (length of the upper jaw) - distance from the constructive point apMax to the point PNS; MAX_MAND (maxillo-mandibular difference) - difference between distances Cond-A and Cond-Gn; ML_NSL (angle ML_NSL, or angle SN_GoMe) - is formed by lines tGo-Me and S-N (angle of inclination of the mandibular plane to the base of the skull); MM (maxillo-mandibular angle) - is formed by lines A-B and ANS-PNS (defines the angle below which the upper jaw is located in relation to the lower jaw in the jet plane); N_POG_ (angle N'Hold_Pog'_Hline) - angle between lines Ls-Pog' (H line, Holdway line) and N'Hold-Pog'; N_SE (distance Se_N or the length of the front of the skull base by Steiner) - distance from the point Se to the point N; NAPOG (angle of the skeletal face obliquity, or angle NaPog) - formed by lines N-A and A-Pog; NBA_PTGN (angle NBa-PtGn or the angle of the front axle) - formed by lines N-Ba and Pt-Gn (determines the direction of development of the mandible); NSBA (angle NSBA) - formed by lines S-N (the front part of the skull base) and S-Ba; P_OR_N (soft tissue angle, or angle P_Or_N'Hold_Pog') - formed by lines Po-Or and N'Hold-Pog'; PN_A (distance PN_A) - distance from the point A to the point PNm (perpendicular line from the point N to the line Po-Or). If the point A is distal from the nasal perpendicular, then the indicator takes a negative value, and if the medial than a positive value; S_L (distance S_L or the front length of the skull base by Steiner) - from the point S to a constructive point L, which is formed at the intersection of the perpendicular carried out from the point Pog to the line Se-N; SN_GOGN (angle SN_GoGn) - is formed by lines Go-Gn and S-N (angle of inclination (MpSt) mandibular plane by Steiner, to the base of the skull); SND (angle SND) - formed by lines S-N and N-D (indicates the anterior-posterior location of the symphysis (D - the center of the symphysis ossification) of the lower jaw to the base of the skull); WITS (indicator Wits) - distance between constructive points AOclP and BOclP - projections of the corresponding points A and B on the line apOcP-

ppOcP (OcPSt, closing plane by Steiner), indicates a linear interjaw ratio in the anterior-posterior direction (if the projection of point A lies ahead of the projection of point B then the indicator takes a positive value; if the projection of point A lies behind the projection of point B then the indicator takes a negative value).

Discussion

To evaluate the position of the frontal group of teeth, several methods can be used by orthodontists. The most ancient method is to measure the inclination of the crown part on the gypsum diagnostic models with the help of a protractor (tooth inclination protractor) TIP [17] - rather cheap and simple method whose significance is significantly different from the teleroentgenographic data and allows only to assess the position of the vestibular-oral and mesiodistal inclinations relative to the occlusion plane, the definition of which is often complicated especially in persons with pronounced closure curves. The most promising and informative method is to use a dental computed tomography, which allows three-dimensional reproductions of bone tissues to be obtained and it is enough to accurately measure linear and angular parameters [2, 13]. Despite the gradual decrease in the price of equipment, an increase in the size of the matrix and an increase in the detail of the image, the method is not yet included in the protocol of orthodontic patient research. It should also be noted that at present, normative bases concerning three-dimensional characteristics of the tooth-jaw system are not presented.

The most accessible and used method is teleroentgenographic research that allows you to determine the position of the central axis of central incisors in relation to different anatomical structures. Different researchers have proposed different methods of determination, each of which has its drawbacks and advantages. So Stainer S. [43] used the angle S-N-A and determined the angular positions of the central axis of the upper central incisor to the lines of this angle, as well as the distance of the vestibular surface of the latter to the line N-A. Downs W. [14] used a inter-incisor angle and a line connecting the upper and lower jaws A-Pog to determine the position of the upper central incisors. Mc Namara [28] determined the distance of the vestibular surface of the central incisor to the perpendicular in relation to the Frankfurt horizontal, conducted through the point A. G. Schmuth [40] used the angle value to the palatal plane ANS-PNS and the angle and distance to the line N-A.

The mathematical analysis of the metric characteristics of the craniofacial complex allows us to create a valuable diagnostic tool for modeling the individual tooth-jaw norm of the patient, identifying the actual pathological abnormalities and methods of treatment [20, 33]. Mathematically analyzed data of cephalometric studies allow to study evolutionary changes, genetic interconnection of ethnic groups, and to establish the influence of different morphological structures on the formation of craniofacial structures [1, 22]. Many studies point to the presence of various dependencies found by regression and correlation analyzes between different anatomical head structures and tooth-jaw system parameters [3, 34, 35, 39].

For Ukrainian young men and women with orthognathic bite we developed reliable regression models of individual teleroentgenographic characteristics of the position of upper central incisors with a determination coefficient greater than 0.50, depending on the peculiarities of the metric characteristics of the craniofacial complex. It was established that in young men from 6 possible models, 5 were constructed with determination coefficient R^2 from 0.672 to 0.928, and in young women - all 6 possible models with determination coefficient R^2 from 0.508 to 0.663.

In the analysis of models with a determination coefficient higher than 0.50, it was found that in young men most often the regression equations include - the angle AB_NPOG (12.0%); distance COND_GN, inclination angle I, MAX maxillary length, Se_N distance, Nap angle, NBa-PtGn angle, SND angle and Wits indicator (by 8.0%). In young women, most often the regression equations include - the angle AB_NPOG and the Wits indicator (by 15.4%); angle N_POG (11.5%); angle Gl'SnPog' and the distance LPALAT (by 7.7%).

In the previous study [12], in the simulation of individual teleroentgenographic characteristics of position of the lower central incisors in young women with orthognathic bite of 7 possible regression models was constructed with 5 with a determination coefficient from 0.694 to 0.849, the most frequent (from 7.7 to 11.5%) included were the angle ANB, facial vertical index, lower face height ANS_ME, NBA_PTGN face angle and distance S_E. In young women, all 7 possible models with a determination coefficient from 0.595 to 0.794 (which is also lower than in the models of the position of the upper central incisors) were constructed, which most often (from 5.6 to 16.7%) included the angle N_POG, the Wits indicator, the inclinational angle I, and the H angle, the angle of the MM and the angle of NBa-PtGn (by 5.6%)

The models we have developed will allow orthodontists to more correctly and effectively change the position of the frontal group of teeth and achieve in the treatment maximum physiological and aesthetic results.

Conclusions

In young men of 6 possible models idividual teleroentgenographic characteristics of the position of upper central incisors, have been constructed 5 with coefficients of determination from 0.672 to 0.928, and for young women - all 6 possible models with determination coefficient from 0.508 to 0.663. In young men most often the regression equations include - the angle AB_NPOG (12.0%); distance COND_GN, inclination angle I, MAX maxillary length, Se_N distance, NaPog angle, NBa-PtGn angle, SND angle and Wits indicator (by 8.0%); and in young women - the angle AB_NPOG and the Wits indicator (by 15.4%); angle N_POG (11.5%); the angle Gl'SnPog' and the distance LPALAT (by 7.7%).

References

[1] Akgul, A. A., & Toygar, T. U. (2002). Natural craniofacial changes in the third dec-ade of life: a longitudinal study. *Am. J. Orthod. Dentofacial Orthop.*, 122(5), 512-522. doi: 10.1067/mod.2002.128861

[2] Berco, M., Rigali, P. H., Miner, R. M., DeLuca, S., Anderson, N. K., & Will, L. A. (2009). Accuracy and reliability of linear cephalometric measurements from cone-beam computed tomography scans of a dry human skull. *Am. J. Orthod. Dentofacial Orthop.,* 136(1), 17-18. doi: 10.1016/j.ajodo.2008.08.021

[3] Bingmer, M., Ozcan, V., Jo, J. M., Lee, K. J., Baik, H. S., & Sneider, G. (2010). A new concept for the cephalometric evaluation of craniofacial pattern (multiharmony). *Eur. J. Orthod.,* 32(6), 645-654. doi: 10.1093/ejo/cjp152

[4] Bowman, S. J., & Johnston, L. E. Jr. (2000). The esthetic impact of extraction and nonextraction treatments on Caucasian patients. *Angle Orthod.,* 70(1), 3-10. doi: 10.1043/0003-3219(2000)070<0003:TEIOEA>2.0.CO;2

[5] Bronfman, C. N., Janson, G., Pinzan, A., & Rocha, T. L. (2015). Cephalometric norms and esthetic profile preference for the Japanese: a systematic review. *Dental Press Journal of Orthodontics,* 20(6), 43-51. doi: 10.1590/2177-6709.20.6.043-051.oar

[6] Dallel, I., Khemiri, M., Fathallah, S., Ben Rejeb, S., Tobji, S., & Ben Amor, A. (2015). Incisor repositioning: a new approach in orthodontics. *Orthod. Fr.*, 86(4), 327-338. doi: 10.1051/orthodfr/2015031

[7] de Oliveira, M. D. V., da Silveira, B. L., Mattos, C. T., & Marquezan, M. (2015). Facial profile esthetic preferences: perception in two Brazilian states. *Dental Press J. Orthod.*, 20(3), 88-95. doi: 10.1590/2176-9451.20.3.088-095.oar

[8] Dmitriev, M. O. (2016). Definition of normative cephalometric parameters by Steiner method for Ukrainian young men and women. *World of Medicine and Biology*, 3(57), 28-32.

[9] Dmitriev, M. O. (2017). Identification of normative cephalometric parameters based on G. Schmuth method for young male and female Ukrainians. *Reports of Morphology,* 23(2), 288-292.

[10] Dmitriev, M. O. (2018). Determination of standard cephalometric parameters using the Downs method for Ukrainian adolescents. *Reports of Morphology*, 24(2), 22-26. doi: 10.31393/morphology-journal-2018-24(2)-03

[11] Dmitriev, M. O., Chugu, T. V., Gerasymchuk, V. V., & Cherkasova, O. V. (2017). Determination of craniometric and gnatometric indicators by A. M. Schvartz metod for Ukrainian boys and girls. *Biomedical and Biosocial Anthropology,* 29, 53-58.

[12] Dmitriev, M. O., Gunas, I. V., Dzevulska, I. V., & Glushak, A. A. (2018). Determination of individual cephalometric characteristics of the lower central incisors position in Ukrainian young men and women with orthognathic bite. *Reports of Morphology*, 24(3), 19-25. doi: 10.31393/morphology-journal-2018-24(3)-03

[13] Dmitriev, N. A., Marchenko, A. V., Filimonov, V. Yu., & Yasko, V. V. (2015). The study of the correctness of the metric studies of three-dimensional anatomical bone objects obtained using a cone-beam computer tomograph Morita Veraviewepocs 3D. *Reports of Morphology,* 21(2), 374-379.

[14] Downs, W. B. (1956). Analysis of the dentofacial profile. *Angle Orthodontist,* 26, 191-212.

[15] Erdinc, A. E., Nanda, R. S., & Dandajena, T. C. (2007). Profile changes of patients treated with and without premolar extractions. *Am. J. Orthod. Dentofacial Orthop.*, 132(3), 324-331. doi: 10.1016/j.ajodo.2005.08.045

[16] Garcia, P. P., da Costa, R. G., Calgaro, M., Ritter, A. V., Correr, G. M., da Cunha, L. F., & Gonzaga, C. C. (2018). Digital smile design and mock-up technique for esthetic treatment planning with porcelain laminate veneers. *J. Conserv. Dent.,* 21(4), 455-458. doi: 10.4103/JCD.JCD_172_18

[17] Ghahferokhi, A. E., Elias, L., Jonsson, S., Rolfe, B., & Richmond, S. (2002). Critical assessment of a device to measure incisor crown inclination. *American Journal of Orthodontics and Dentofacial Orthopedics,* 121(2), 185-191. PMID: 11840133

[18] Gunas, I. V., Dmitriev, M. O., Tikholaz, V. O., Shinkaruk-Dykovytska, M. M., Pastukhova, V. A., Melnik, M. P., & Rudiy, Yu. I. (2018). Determination of normal cephalometric parameters by J. McNamara method for Ukrainian boys and girls. *World of Medicine and Biology,* 1(63), 19-22. doi: 10.26724/2079-8334-2018-1-63-19-22

[19] Gunas, I. V., Dmitriev, M. O., Prokopenko, S. V., Shinkaruk-Dykovytska, M. M., & Yeroshenko, G. A. (2017). Determination regulatory cephalometric options by the method of Tweed International Foundation for Ukrainian boys and girls. *World of Medicine and Biology,* 4(62), 27-31. doi: 10.26724/2079-8334-2017-4-62-27-31

[20] Hammond, P., Hutton, T., Maheswaran, S., & Modgil, S. (2003). Computational models of oral and craniofacial development, growth, and repair. *Adv. Dent. Res.,* 17, 61-64. doi: 10.1177/154407370301700114

[21] Holdaway, R. A. (1984). A soft-tissue cephalometric analysis and its use in orthodontic treatment planning. Part II. *Am. J. Orthod.,* 85, 279-293. doi: https://doi.org/10.1016/0002-9416(84)90185-4

[22] Kjellberg, H., Beiring, M., & Albertsson Wikland, K. (2000). Craniofacial morphology, dental occlusion, tooth eruption, and dental maturity in boys of short stature with or without growth hormone deficiency. *Eur. J. Oral. Sci.,* 108(5), 359-367. PMID: 11037751

[23] Kocadereli, I. (2002). Changes in soft tissue profile after orthodontic treatment with and without extractions. *Am. J. Orthod. Dentofacial. Orthod.,* 122(1), 67-72. PMID: 12142899

[24] Kumari, L., & Das, A. (2017). Determination of Tweed's cephalometric norms in Bengali population. *Eur. J. Dent.,* 11(3), 305-310. doi: 10.4103/ejd.ejd_274_16

[25] Lin, W. S., Zandinejad, A., Metz, M. J., Harris, B. T., & Morton, D. (2015). Predictable restorative work flow for computer-aided design/computer-aided manufacture-fabricated ceramic veneers utilizing a virtual smile design principle. *Oper. Dent.,* 40(4), 357-363. doi: 10.2341/13-295-S

[26] Linjawi, A. I. (2016). Age- and gender-related incisor changes in different vertical craniofacial relationships. *J. Orthod. Sci.,* 5(4), 132-137. doi: 10.4103/2278-0203.192116

[27] Lombardo, L., Perri, A., Arreghini, A., Latini, M., & Siciliani, G. (2015). Three-dimensional assessment of teeth first-, second- and third-order position in Caucasian and African subjects with ideal occlusion. *Prog. Orthod.,* 16, 1-11. doi: 10.1186/s40510-015-0086-9

[28] McNamara, J. A. Jr. (1984). A method of cephalometric evaluation. *Am. J. Orthod.*, 86(6), 449-469. PMID: 6594933

[29] Meereis, C. T., de Souza, G. B., Albino, L. G., Ogliari, F. A., Piva, E., & Lima, G. S. (2016). Digital smile design for computer-assisted esthetic rehabilitation: Two-year follow-up. *Oper. Dent.,* 41(1), 13-22. doi: 10.2341/14-350-S

[30] Meneghini, F., & Biondi, P. (2012). *Clinical facial analysis.*

Elements, principles, and techniques (2nd ed.). Berlin: Springer-Verlag Berlin Heidelberg.

[31] Miranda, M. E., Olivieri, K. A., Rigolin, F. J., & de Vasconcellos, A. A. (2016). Esthetic challenges in rehabilitating the anterior maxilla: A Case report. *Oper. Dent.*, 41(1), 2-7. doi: 10.2341/14-269-S

[32] Mohammed, S. A., Nissan, L. M. K., Ahmed, H. M. A., & Nahidh, M. (2018). Sagittal Lips' Positions in Different Facial Types. *J. Res. Med. Dent. Sci.,* 6(1), 16-21. doi: 10.24896/jrmds.2018614

[33] Nakasima, A., Terajima, M., Mori, N., Hoshino, Y., Tokumori, K., Aoki, Y., & Hashimoto, S. (2005). Three-dimensional computer-generated head model reconstructed from cephalograms, facial photographs, and dental cast models. *Am. J. Orthod. Dentofacial. Orthop.*, 127(3), 282-292. doi: 10.1016/j.ajodo.2003.11.030

[34] Perinetti, G., Ceschi, M., Scalia, A., & Contardo, L. (2018). Cephalometric Floating Norms for the B Angle and MMBP-Wits. *BioMed Research International,* 2018, Article ID 8740731, 6. doi: https://doi.org/10.1155/2018/8740731

[35] Perinetti, G., Cordella, C., Pellegrini, F., & Esposito, P. (2008). The prevalence of malocclusal traits and their correlations in mixed dentition children: results from the Italian OHSAR Survey. *Oral Health & Preventive Dentistry*, 6(2), 119-129. PMID: 18637389

[36] Profit, R. W., Fields, H. W., & Sarver, D. M. (trans. from the English; Ed. L.S. Persina) (2006). *Modern Orthodontics.* M.: MEDpress-inform. ISBN 978-5-00030-448-8

[37] Rathod, A. B., Araujo, E., Vaden, J. L., Behrents, R. G., & Oliver, D. R. (2015). Extraction vs no treatment: Long-term facial profile changes. *Am. J. Orthod. Dentofacial Orthop.,* 147(5), 596-603. doi: 10.1016/j.ajodo.2015.01.018.

[38] Reshad, M., Cascione, D., & Magne, P. (2008). Diagnostic mock-ups as an objective tool for predictable outcomes with porcelain laminate veneers in esthetically demanding patients: A clinical report. *J. Prosthet. Dent.,* 99(5), 333-339. doi: 10.1016/S0022-3913(08)00056-5

[39] Scala, A., Auconi, P., Scazzocchio, M., Caldarelli, G., McNamara, J. A., & Franchi, L. (2014). Complex networks for data-driven medicine: the case of Class III dentoskeletal disharmony. *New Journal of Physics.*, 16(11), 1-17. doi: 10.1088/1367-2630/16/11/115017

[40] Schmuth, G. P. F. (1971). Methodische Schwierigkeiten bei der Anwendung der Röntgenkephalometrie in der Kieferorthopädie. *Fortschritte der Kieferorthopädie,* 32(2), 317-325.

[41] Schwarz, A. M. (1960). *Röntgenostatics; practical evaluation of the tele-X-ray-photo.* Publisher: Brooklyn, N.Y.: Leo L. Bruder.

[42] Shindoi, J. M., Matsumoto, Y., Sato, Y., Ono, T., & Harada, K. (2013). Soft tissue cephalometric norms for orthognathic and cosmetic surgery. *J. Oral. Maxillofac. Surg.*, 71(1), 24-30. doi: 10.1016/j.joms.2012.08.015

[43] Steiner, C. C. (1959). Cephalometrics in clinical practice. *Angle Orthod.*, 29, 8-29.

[44] Tweed, C. H. (1954). The Frankfort-Mandibular Incisor Angle (FMIA) in Orthodontic Diagnosis, Treatment Planning and Prognosis. *Angle Orthod.,* 3, 121-169.

[45] Wholley, C. J., & Woods, M. G. (2003). The effects of commonly prescribed premolar extraction sequences on the curvature of the upper and lower lips. *Angle Orthod.,* 73(4), 386-395. doi: 10.1043/0003-3219(2003)073<0386:TEOCPP>2.0.CO;2

[46] Zierhut, E. C., Joondeph, D. R., Artun, J., & Little, R. M. (2000). Long term profile changes associated with successfully treated extraction and nonextraction Class II, Division I malocclusions. *Angle Orthod.*, 70(3), 208-219. doi: 10.1043/0003-3219(2000)070<0208:LTPCAW>2.0.CO;2

ВИЗНАЧЕННЯ ІНДИВІДУАЛЬНИХ ЛІНІЙНИХ ТА КУТОВИХ ХАРАКТЕРИСТИК ПОЛОЖЕННЯ ВЕРХНІХ ПРИСЕРЕДНІХ РІЗЦІВ В УКРАЇНСЬКИХ ЮНАКІВ І ДІВЧАТ З ОРТОГНАТИЧНИМ ПРИКУСОМ

Дмітрієв М.О., Гунас І.В., Гненна В.О., Смолко Н.М.

Враховуючи важливість визначення телерентгенографічних показників просторового положення присередніх різців виникає наукова та клінічна зацікавленість у проведенні подібних досліджень. Мета дослідження - шляхом вивчення цефалометричних показників і проведення прямого покрокового регресійного аналізу розробити у юнаків та дівчат України з ортогнатичним прикусом математичні моделі індивідуальних характеристик положення верхніх присередніх різців. За допомогою пристрою Veraviewepocs 3D, Morita (Япония) у 38 юнаків (віком від 17 до 21 року) та 55 дівчат (віком від 16 до 20 років) з оклюзією, наближеною до ортогнатичного прикусу, та збалансованими обличчями були отримані бокові телерентгенограми. Цефалометричний аналіз проводили за допомогою програмного забезпечення OnyxCeph³™. Цефалометричні точки та вимірювання проводили згідно рекомендацій A.M. Schwarz, J. McNamara, W.B. Downs, R.A. Holdway, P.F. Schmuth, C.C. Steiner та C.H. Tweed. У ліцензійному статистичному пакеті "Statistica 6.0" з використанням прямого покрокового регресійного аналізу проведено моделювання наступних телерентгенографічних характеристик положення верхніх присередніх різців: відстані 1u_APog, відстані 1u_Avert, відстані 1u_NA, кута Max1_NA, кута Max1_SN і кута Max1_SpP. В юнаків і дівчат із оклюзією, наближеною до ортогнатичного прикусу, та збалансованим обличчям розроблені достовірні регресійні моделі індивідуальних телерентгенографічних характеристик положення верхніх присередніх різців з коефіцієнтом детермінації більшим 0,50 в залежності від особливостей метричних характеристик краніофаціального комплексу: в юнаків із 6 можливих моделей побудовано 5 з коефіцієнтом детермінації R^2 від 0,672 до 0,928, а у дівчат - усі 6 можливих моделей з коефіцієнтом детермінації R2 від 0,508 до 0,663. При аналізі моделей з коефіцієнтом детермінації більшим 0,50 встановлено, що в юнаків найбільш часто до регресійних рівнянь входять - кут AB_NPOG (12,0%); відстань COND_GN, інклінаційний кут I, довжина верхньої щелепи MAX, відстань Se_N, кут NaPog, кут NBa-PtGn, кут SND та показник Wits (по 8,0%). У дівчат найбільш часто до моделей входять - кут AB_NPOG і показник Wits (по 15,4%); кут N_POG (11,5%); кут Gl'SnPog' і відстань LPALAT (по 7,7%).

Ключові слова: *положення верхніх присередніх різців, цефалометрія, регресійний аналіз, юнаки та дівчата, ортогнатичний прикус.*

ОПРЕДЕЛЕНИЕ ИНДИВИДУАЛЬНЫХ ЛИНЕЙНЫХ И УГЛОВЫХ ХАРАКТЕРИСТИК ПОЛОЖЕНИЯ ВЕРХНИХ ЦЕНТРАЛЬНЫХ РЕЗЦОВ У УКРАИНСКИХ ЮНОШЕЙ И ДЕВУШЕК С ОРТОГНАТИЧЕСКИМ ПРИКУСОМ

Дмитриев Н.А., Гунас И.В., Гненная В.О., Смолко Н.Н.

Учитывая важность определения телерентгенографических показателей пространственного положения медиальных резцов возникает научная и клиническая заинтересованность в проведении подобных исследований. Цель исследования -

путем изучения цефалометрических показателей и проведения прямого пошагового регрессионного анализа разработать у юношей и девушек Украины с ортогнатическим прикусом математические модели индивидуальных характеристик положения верхних медиальных резцов. С помощью устройства Veraviewepocs 3D, Morita (Япония) у 38 юношей (в возрасте от 17 до 21 года) и 55 девочек (в возрасте от 16 до 20 лет) с окклюзией, приближенной к ортогнатическому прикусу, и сбалансированными лицами были получены боковые телерентгенограммы. Цефалометрический анализ проводили с помощью программы OnyxCeph³™. Цефалометрические точки и измерения проводили согласно рекомендациям A.M. Schwarz, J. McNamara, W.B. Downs, R.A. Holdway, P.F. Schmuth, C.C. Steiner и C.H. Tweed. В лицензионном статистическом пакете "Statistica 6.0" с использованием прямого пошагового регрессионного анализа проведено моделирование следующих телерентгенографических характеристик положения верхних медиальных резцов: расстояния 1u_APog, расстояния 1u_Avert, расстояния 1u_NA, угла Max1_NA, угла Max1_SN и угла Max1_SpP. У юношей и девушек с окклюзией, приближенной к ортогнатическому прикусу, и сбалансированным лицом разработаны достоверные регрессионные модели индивидуальных телерентгенографических характеристик положения верхних медиальных резцов с коэффициентом детерминации большим, чем 0,50 в зависимости от особенностей метрических характеристик краниофациального комплекса: у юношей из 6 возможных моделей построено 5 с коэффициентом детерминации R^2 от 0,672 до 0,928, а у девушек - все 6 возможных моделей с коэффициентом детерминации R^2 от 0,508 до 0,663. При анализе моделей с коэффициентом детерминации большим 0,50 установлено, что у юношей наиболее часто к регрессионным уравнениям входят - угол AB_NPOG (12,0%); расстояние COND_GN, инклинационный угол I, длина верхней челюсти MAX, расстояние Se_N, угол NaPog, угол NBa-PtGn, угол SND и показатель Wits (по 8,0%). У девушек наиболее часто к моделям входят - угол AB_NPOG и показатель Wits (по 15,4%); угол N_POG (11,5%); угол Gl'SnPog "и расстояние LPALAT (по 7,7%).

Ключевые слова: *положение верхних центральных резцов, цефалометрия, регрессионный анализ, юноши и девушки, ортогнатический прикус.*

DOI: 10.31393/morphology-journal-2018-24(4)-03 Reports of Morphology, Vol. 24, №4, Pages 22-28

ISSN 1818-1295 eISSN 2616-6194

REPORTS OF MORPHOLOGY

Official Journal of the Scientific Society of Anatomists, Histologists, Embryologists and Topographic Anatomists of Ukraine

journal homepage: https://morphology-journal.com

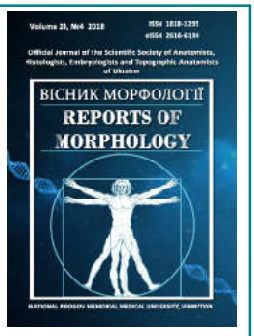

Morphometric studies of the damaged skin area after experimental thermal trauma and during correction with cryo-lyophilized xenograft skin substrate

Kramar S.B., Volkov K.S., Nebesna Z.M.
Ivan Horbachevsky Ternopil State Medical University, Ternopil, Ukraine

ARTICLE INFO
Received: 3 October, 2018
Accepted: 2 November, 2018

UDC: 616.5-001.17-085.324:599.731.1-035.51-076.4]-092.9

CORRESPONDING AUTHOR
e-mail: kramar.solomija@gmail.com
Kramar S.B.

According to WHO, burns rank third place among other injuries, and in some countries, the second, after traffic injuries. One of the promising tools for treating burn wounds is the use of lyophilized xenograft skin substrate. The purpose of this work was to determine the morphometric parameters of the affected by burns area of the skin in the dynamics after an experimental thermal trauma and in the case of correction by crushed lyophilized xenograft skin substrate. Burning of third degree on the shaved skin of the back of the guinea pig was applied to the vapor under general anesthetic. Morphometrically, at 7, 14, and 21 days of the experiment, the thickness of the epidermis (thin skin without a layer of scales), the number of fibroblast cells per unit area, the outer and inner diameter of the capillaries were determined in the boundary and central areas of the wound. Morphometric studies were carried out using programs VideoTest-5.0, KAAPA Image Base and Microsoft Excel on a personal computer. Statistical processing of the obtained quantitative data was carried out using methods of variation statistics with the determination of the mean arithmetic and its error (M±m), Student's criterion (t) and reliability index (p). Differences are considered valid at $p \leq 0.05$. It has been established that already in the 7 day of the experiment, under conditions of wound closure by xenograft skin substrate marked a significant thickening of the epidermis on the periphery of the wound appear. Activation of the process of boundary epithelization contributes to the renewal of components of the microcirculatory bed, the formation of granulation tissue. It was found that on the 14 day of application of the corrective factor in the peripheral zone of the wound, the number of cells of the fibroblast row and the mean value of the thickness of the epidermis reach their peak value, significantly ($p<0.001$) exceeding such indices of animals in intact group and group of animals without correction. The morphometric parameters of capillaries in this period of the experiment indicate a good development of the microcirculation, which improves regional epithelization. On the 21 day of the experiment, under the condition of correction, the border between the regional and central parts of the wound is almost lost. Thus, the results of morphometric studies indicate that the use of cryo-lyophilized xenograft skin substrate after a thermal trauma of the skin contributes to the healing of the wound defect with the formation of connective tissue of the dermis, angiogenesis, and complete epithelization of the surface of the affected epidermis layer.

Keywords: *skin, thermal trauma, cryoliophilized xenodermal substrate, morphometric studies.*

Introduction

Burns are one of the widespread skin damages. The urgency of the problem of thermal damages is determined by the relatively high frequency of their occurrence in everyday life and in the workplace, the severity of the burn disease, the complexity and duration of treatment of such patients, high disability and mortality. In Ukraine, this figure is about 100,000 patients annually [4, 8, 11].

The term recovery of the burned skin determines the course of burn disease, the formation of complications, the cosmetic effect. It is known that deep and large thermal

burns are not limited only to local damages of tissues, but also cause significant violations of all systems and organs, metabolic processes in the body [1, 2, 4, 6]. The primary link in the pathogenesis of burn disease is the destruction of the skin, significant hemodynamic disorders and violation of neuroendocrine regulation [6, 12, 14].

In the case of wounds occurrence, the main task is to eliminate the defect in order to restore the integrity of tissues, through reparative regeneration [5]. In recent years, one of the new directions in the treatment of wound process is the creation and application of biologically active covers that can release biologically active substances that affect the reparative processes [5, 10, 18, 21].

A number of scientific studies have shown [4, 8, 11, 19] that the use of lyophilized xenograft skin is promising in the treatment of the burned organism, but studies on the use of its crushed substrate, after the early necrectomy of the affected areas, are still insufficient. It is established that it possesses high sorption-antitoxic, metabolic, plastic and oxidative-reduction potentials, and is available as a tablet formulation containing biologically active compounds rich in amino acids and trace elements [9]. However, the morphological features of healing of thermal wounds during its use remain little studied.

Taking into account the above, the *purpose* of this work was to establish the morphometric parameters of the affected by burns area of the skin in the dynamics after an experimental thermal trauma and under conditions of correction by crushed lyophilized xenograft skin substrate.

Materials and methods

Experimental studies were performed on 42 sexually mature guinea pigs. In conducting research, the international rules and principles of the "European Convention for the Protection of Vertebrate Animals used for Experiments and for Other Scientific Purposes" (Strasbourg, 1986) and "General Ethical Principles of Animal Experiments" (Kyiv, 2001) have been respected.

Experimental animals were divided into three groups: intact guinea pigs; animals with severe thermal trauma; animals with burn injury, which, after the early necrectomy of damaged tissues, were covered with crushed cryo-lyophilized xenograft skin substrate.

The burning of the third degree on the shaved surface of the skin of the animal's back was applied by water vapor at a temperature of 96-97°C for 60 seconds under general anesthetic. The size of the damages was 18-20% of the body surface.

To investigate the features of morphometric changes in the skin after burn injury, the animals were decapitated using a guillotine under general, etheric anesthesia at 7, 14 and 21 days of the experiment, which corresponds to the stages of early and late toxemia and septicotoxemia of the burn disease [4]. Animals of the third experimental group after a thermal trauma after 1 day of the experiment performed an early necrectomy of damaged tissue followed by wound closure by the cryo-lyophilized xenograft skin substrate. Therefore, the removal of animals from the experiment and the study of the morphometric state of the skin in the central and marginal areas of the wound was carried out at 7, 14 and 21 days after burning.

The material was collected for microscopic studies in accordance with the generally accepted method [7, 16]. Sections of the skin from the central and marginal part of the wound were fixed in 10% formalin solution. Dehydration of the material was carried out in alcohols of increasing concentration in a machine for histological processing of tissues AT-4, poured in paraffin blocks. The received on the snuff-microtome MS-2 sections of 5-6 microns thickness were stained with hematoxylin and eosin.

Morphometric studies were performed using a system of visual analysis of histological preparations. The images were taken to a computer monitor using microscope MICROmed SEO SASAN with Vision CCD Camera. Morphometric studies were carried out using programs VideoTest-5.0, KAAPA Image Base and Microsoft Excel on a personal computer. The research was carried out at definite dates of the experiment on preparations painted with hematoxylin and eosin. Morphometrically in the boundary and central areas of the wound, the thickness of the epidermis (thin skin without a layer of scales), the number of fibroblast cells per unit area, the outer and inner diameter of the capillaries were determined.

The number of fibroblast cells per unit area was determined by the formula:

$$N_f=\Sigma_f/S_d,$$

where N_f - number of fibroblasts per unit area (1 mm^2), Σ_f - total number of fibroblasts, S_d - area of the dermis.

Statistical processing of the obtained quantitative data was carried out using methods of variation statistics with the determination of the mean arithmetic and its error (M±m), Student's criterion (t) and reliability index (p). Differences are considered valid at $p\leq0.05$.

Results

The healing of a wound defect after a thermal injury to the skin is accompanied by compensatory restoration of its undamaged sites, especially the perifocal zone, therefore the morphometric changes of not only the center of the defeat, but also its periphery were investigated.

Table 1 shows the quantitative parameters of the studied parameters in all terms of the experiment.

It has been established that at application of lyophilized xenograft skin substrate on 7 day of the experiment in the marginal zone of the wound marked significant thickening of the epidermis. Morphometrically it was found that the average value of its thickness is (83.23±2.86) μm, which significantly ($p<0.01$) exceeds the data of group II of animals in 1.16 times, and the index of intact group of animals in 1.58 times ($p<0.001$) (see Table 1). The number of cells of the fibroblast row in this zone is significantly growing ($p<0.001$), with an average value of (2107±27) cells/mm^2,

Table 1. Morphometric parameters of the structural components of the skin of animals at different terms after a thermal trauma and under conditions of use of lyophilized xenograft skin substrate.

The terms of the experiment			Parameters (M±m)			
			Thickness of the epidermis, μm	The number of fibroblastic series cells, cells/mm^2	External diameter of hemocapillars, μm	Diameter of hemocapillaries lumen, μm
Intact			52.54±2.03	1432±31	8.022±0.391	6.052±0.373
Burn	7 day	MAW	71.69±2.48 ***	1035±26 ***	11.97±0.31 ***	8.353±0.261 ***
		CAW	-	268.3±18.1 ***	14.46±0.24 ***	11.84±0.16 ***
	14 day	MAW	80.45±3.07 ***	1607±34 ***	10.75±0.34 ***	7.811±0.211 ***
		CAW	18.52±2.33 ***	439.2±21.1 ***	6.163±0.172 ***	5.051±0.140 *
	21 day	MAW	85.38±2.69 ***	1750±34 ***	10.56±0.13 ***	7.833±0.172 ***
		CAW	25.45±2.08 ***	610.2±23.2 ***	6.751±0.132 **	5.011±0.143 *
Correction	7 day	MAW	83.23±2.86 ***/##	2107±27 ***/###	10.84±0.11 ***/##	8.094±0.092 ***
		CAW	-	568.3±31.3 ***/###	11.04±0.16 ***/###	8.564±0.123 ***/###
	14 day	MAW	141.3±4.6 ***/###	3209±48 ***/###	10.65±0.13 ***	7.831±0.151 ***
		CAW	48.74±1.53 ###	1876±37 ***/###	8.322±0.121 ###	6.893±0.114 */###
	21 day	MAW	97.63±1.97 ***/###	2487±33 ***/###	8.931±0.111 */###	7.272±0.142 **/#
		CAW	71.25±2.07 ***/###	1761±19 ***/###	8.542±0.113 ###	6.321±0.093 ###

Notes: * - values that are statistically significantly different from those of an intact group of animals (* - p<0.05; ** - p<0.01; *** - p<0.001); # - values that are statistically significantly different from those of a group of animals with a burn (# - p<0.05; ## - p<0.01; ### - p<0.001); MAW - marginal area of the wound; CAW - central area of the wound.

which is 1.47 and 2.04 times, respectively, exceeds the I and II experimental groups of animals.

The morphometric investigations of the area of the damage in this period of the experiment have established that the average value of the number of cells of the fibroblast row per unit area is (568.3±31.3) cells/mm^2, which is significantly (p<0.001) higher than the group of animals without correction in 2.12 times, but significantly (p<0.001) is less than that data of animals of group I - in 2.52 times (see Table 1). The mean value of the diameter of the blood capillaries in this zone is (11.04±0.16) μm and the average diameter of their lumen is (8.564±0.123) μm, which is significantly (p<0.001) lower than II groups of animals in 1.31 and 1.38 times respectively. However, these indices are significantly higher (p<0.001) in comparison with the intact group of animals, because parameters of not only newly created hemocapillars, but also of stored vasodilated vessels in the central zone of the wound are measured morphometrically.

Morphometrically, it was found that on the 14 day of the experiment, using the corrective factor in the peripheral regions of the wound, the epidermis was thickened, its average value was (141.3±4.6) μm, which significantly (p<0.001) exceeds the intact group of animals and animals with burning injury and without correction is 2.69 and 1.76 times respectively (see Table 1).

In the dermis of the perifocal area there is an intensive increase in the number of cells of the fibroblastic row, whose average value is (3209±48) cells/mm^2 and significantly (p<0.001) exceeds such an indicator of animals of the I and II experimental groups at 2.24 and 2.00 times respectively (see Table 1).

In the peripheral zones, wounds on the 14 day after a thermal trauma under conditions of correction microscopically marked expanded vessels of the microcirculatory bed, the morphometric parameters of which are: the outer diameter - (10.65±0.13) μm, the diameter of the lumen - (7,831±0,151) μm and with a confidence p<0.001 exceed these parameters of animals of the intact group. While in the healing zone of the wound, the average values of the outer and inner diameters of the blood capillaries are respectively (8,322±0,121) μm and (6,893±0,114) μm. At the same time, the average value of the outer diameter does not significantly differ from the indicator of the group of intact animals, and the internal one - exceeds the norm index by 1.14 times (p<0.05) (see Table 1).

Microscopically, during this experiment period, a young granulation tissue that is rich in cells of the fibroblastic series with a mean density of (1876±37) cells/mm^2, which significantly (p<0.001) exceeds such an indicator of groups I and II, is well expressed in the area of burn wound. respectively 1.31 and 4.27 times. At 14 day of the experiment under conditions of crushed cryo-lyophilized xenograft skin substrate, the mean value of the thickness of the epidermal regenerate over the granulation tissue is (48.74±1.53) μm and significantly (p<0.001) exceeds the II experimental group of animals at 2.63 times (see Table 1).

On the 21 day of the application of the corrective factor, it was morphometrically determined that the mean value of

the thickness of the epidermis in the healing area is (71.25±2.07) μm, which is significantly (p<0.001) higher than the values of the I and II experimental groups of animals at 1.36 and 2.80 times respectively. In the perifocal zone of the wound, in comparison with the previous term of the experiment, the thickness of the epidermis from which the epidermal regenerate starts are reduced by 1.45 times, but it remains significantly (p<0.001) greater in 1.86 and 1.14 times than the corresponding indices of the intact group animals and animals with a burn injury and without the use of corrective factors (see Table 1).

According to the results of morphometric studies, the average value of the number of fibroblasts in the border zone of the healing zone is reduced by 1.29 times compared with the previous trial, however, it remains significantly (p<0.001) greater in 1.74 and 1.42 times than for the corresponding values of this parameter of the group intact animals and animals with burn injury and without correction (see Table 1). In the central zone of the wound, the average value of the number of these cells per unit area is (1761±19) cells/mm^2, which significantly (p<0.001) exceeds the indicators of groups I and II in animals at 1.23 and 2.89 times respectively (see Table 1).

At the periphery of the healing area according to the morphometric studies, the average value of the outer diameter of the capillaries is equal to (8,931±0,111) μm, and the inner - (7,272±0,142) μm, which is significantly lower than the animals' of experimental group, respectively, in 1.18 (p<0.001) and 1.07 (p<0.05) times (see Table 1).

In the center of the damaged area at 21 day of application of the corrective factor, there is a presence in the papillary region of the dermis of newly formed hemocapillaries, whose endothelial cells have large nuclei and an enlarged cytoplasmic zone. The average value of the outer diameter of these vessels is (8,542±0,113) μm, and the average value of the diameter of the lumen is (6,321±0,093) μm, which does not significantly differ from the corresponding morphometric indices of animals intact group (see Table 1).

The dynamics of changes in the thickness of the epidermis and the density of fibroblasts per unit area is illustrated in Figures 1 and 2, respectively.

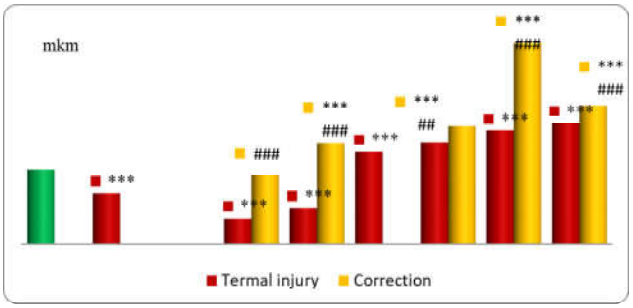

Fig. 1. Dynamics of thickness changes in the epidermis of the marginal and central zones of the animals skin after thermal injury and under correction conditions. * - values that statistically significantly differ from the indicators of the intact group of animals (*** - p<0.01); # - values that statistically significantly differ from the indicators of the group of animals with a burn (## - p<0.01; ### - p<0.001).

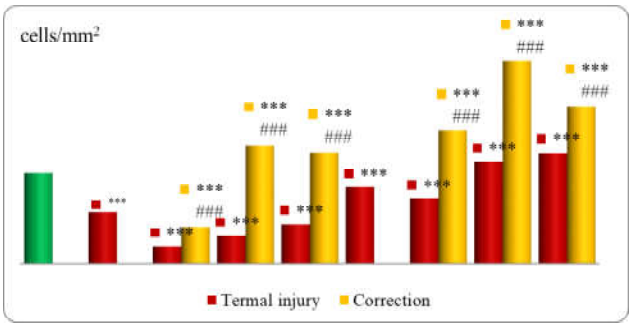

Fig. 2. Dynamics of changes in the number of fibroblasts of the marginal and central zones of the animals skin after thermal injury and under correction conditions. * - values that statistically significantly differ from the indicators of the intact group of animals (*** - p<0.001); # - values that statistically significantly differ from the indicators of the group of animals with a burn (## - p<0.01; ### - p<0.001).

Discussion

Morphometric and quantitative research methods, which give an opportunity to more objectively evaluate the morphofunctional state of histological structures in the normal way, as well as to detect patterns of compensatory, adaptive, destructive and regenerative processes [3], take an important place among morphological investigations.

It is known that healing of the wound defect is accompanied by compensatory reconstruction of the preserved areas of the skin, especially of perifocal zone [6, 13, 20]. However, for today the features of remodeling of structural components of the skin of the marginal region of the wound have not been sufficiently studied, therefore morphometric changes not only of the center of the damage, but also of its periphery were not investigated.

The performed morphometric studies have found that already in the early term of the experiment (7 day), under conditions of wound closure by xenodermal substrate marked a significant thickening of the epidermis on the periphery of the wound due to an increase in the mitotic activity of the cells of the germ layer (see Fig. 1). Activation of the boundary epithelization process promotes the renewal of the components of the microcirculatory bed, the formation of granulation tissue [18, 20].

It is common knowledge that the largest population of cells of the connective tissue base of the skin are fibroblasts that produce, renew the components of the intercellular substance, participate in wound healing, regulate inflammation, differentiate keratinocytes, processes of cellular interactions, and stimulate angiogenesis [15, 21, 23]. Some authors have already established [17, 20, 21, 22, 23] that they are involved in the formation of granulation tissue with a burn injury; migrate to the site of defeat and synthesize the components of the intercellular matrix, which promotes the involvement of macrophages, neutrophils in

the wound process; produce metal proteases, a number of cytokines, growth factors that stimulate other cells prior to migration and proliferation. Therefore, at day 7 of the experiment, under the conditions of correction in the peripheral area of the wound, the number of fibroblasts per unit area increased by 1.47 times compared to the rate of intact animals and by 2.04 times compared with the animals of the second group (see Fig. 2). The established morphometric indices of structural components of the skin indicate the activation of reparative processes already in the early term of the experiment.

According to morphometric studies, at 14 day of application of the corrective factor in the peripheral zone of the wound, the number of cells of the fibroblast number and the mean thickness of the epidermis reach their peak value, significantly ($p<0.001$) exceeding such indices of animals of the intact group and group of animals without correction (see Fig. 1, 2). The morphometric parameters of the capillaries in this period of the experiment indicate good development of the microcirculatory bed, which, in turn, improves regional epithelization (see Table 1) [15, 24].

At the 21 day of the experiment in animals of the third group, the border between the regional and central parts of the wound is almost lost. In the perifocal region of the damage, in comparison with the previous trial, the mean thickness of the epidermis from which the epidermal regenerate starts are reduced by 1.45 times, due to the moderate mitotic activity of the keratinocytes and the healing of the wound defect at that time (see Fig. 1). In the central area, the number of fibroblast cells per unit area is significantly ($p<0.001$) higher than the intact group of animals in 1.23 times and 2.89 times the rate of animals with thermal trauma without correction (see Fig. 2). Morphometric parameters of hemocapillaries are not significantly different from those of intact animals. the amount per unit area is significantly ($p<0.001$) higher than the intact group of animals in 1.23 times and 2.89 times the rate of animals with thermal trauma without correction (see Table 1).

Obtained new scientific results reveal the peculiarities of morphometric changes in the skin during severe thermal trauma and the application of cryo-lyophilized xenograft skin substrate, which is theoretical and practical ground for the development of adequate methods for correction of the effects of thermal trauma.

Conclusions

1. Morphometrically it was found that the application of crushed cryo-lyophilized xenograft skin substrate to the wound that was formed after the necrectomy of the thermally damaged areas already in the early period after burn (7 day) activates regenerative processes. There is a formation of epithelial regenerate in the marginal region of the wound, whose thickness is significantly ($p<0.01$) exceeding the data of the group of animals without correction in 1.16 times, and the data of intact group of animals in 1.58 times ($p<0.001$). In the affected area, granulation tissue is saturated with fibroblasts, the number of which is significantly ($p<0.001$) exceeding the indicator of a group of animals without correction in 2.12 times.

2. In late terms (14, 21 days), the positive effect of using cryo-lyophilized xenograft skin substrate after an experimental thermal trauma is manifested by healing of the wound defect with the formation of connective tissue of the dermis, in which the number of fibroblasts increases and reliably ($p<0.001$) exceeds the indicator of the group of animals without correction in 2.89 times. An active course of angiogenesis and complete epithelization of the surface of the damage with an epidermal layer is set, whose thickness is significantly ($p<0.001$) exceeds the indicator of a group of animals with burn injury without correction in 2.80 times.

References

[1] Adeloye, D., Bowman, K., Chan, K. Y., Patel, S., Campbell, H., & Rudan, I. (2018). Global and regional child deaths due to injuries: an assessment of the evidence. *J. Glob. Health*, 8(2), 021104. doi: 10.7189/jogh.08.021104.

[2] Andrade, P., Kaura, A. S., Bryant, J. R., & Burke, E. (2018). Thermal Burn Injury from a Wedding Ring: An Unusual Case. *J. Am. Coll. Clin. Wound Spec*., 9(1-3), 32-34. doi: 10.1016/j.jccw.2018.06.004

[3] Avtandilov, H. H. (2002). *Basics of quantitative pathological anatomy.* Moskow: Medicine.

[4] Bihuniak, V. V., & Povstianyi, M. Yu. (2004). *Termal injury.* Ternopil: Ukrmedknuha.

[5] Han, C. M., Yu, M. R., & Wang, X. G. (2018). Summary of advances in the research of wound therapy. *Zhonghua Shao Shang Za Zhi.*, 34(12), 864-867. doi: 10.3760/cma.j.issn.1009-2587.2018.12.009.

[6] Hanglin, Ye., & Suvranu, D. (2017). Thermal injury of skin and subcutaneous tissues: A review of experimental approaches and numerical models. *Burns,* 43(5), 909-932. doi:10.1016/j.burns.2016.11.014.

[7] Horalskyi, L. P., Khomych, V. T., & Kononskyi, O. I. (2005). *Fundamentals of histological technology and morphofunctional methods of research in norm and in pathology.* Zhytomyr: Polissia.

[8] Huda, N. V., & Bihuniak A. V. (2007). The usege of lyophilized xenoderm transplantants for the treatment of derma burns in the elderly. *Hospital surgery*, 3, 81-83.

[9] Huda, N. V., & Tsymbaliuk, A. V. (2012). Content of aminoacids and microelements in crioliofilized xenoskin as an indicator of its biological activity. *Medical chemistry*, 14(1), 50, 70-72.

[10] John, P. A., John, S., John, G., Sparrow, E., & Minkowycz, W. J. (2018). Tissue burns due to contact between a skin surface and highly conducting metallic media in the presence of inter-tissue boiling. *Burns*. https://doi.org/10.1016/j.burns.2018.09.010

[11] Kovalchuk, A. O., & Piatkovskyi, T. I. (2010). Dynamical changes of results of experimental burn wounds after early necrectomy using lyophilized xenodermotransplants of secondary cutting. *Reports of scientific researches*, 2, 46-49.

[12] Lee, J. H., Kim, J. W., Lee, J. H., Chung, K. J., Kim, T. G., Kim, Y.

H., & Kim, K. J. (2018). Wound healing effects of paste type acellular dermal matrix subcutaneous injection. *Arch Plast Surg.,* 45(6), 504-511. doi: 10.5999/aps.2018.00948.
[13] Leszczynska, A., Kulkarni, M., Ljubimov, A. V., & Saghizadeh, M. (2018). Exosomes from normal and diabetic human corneolimbal keratocytes differentially regulate migration, proliferation and marker expression of limbal epithelial cells. *Sci. Rep.*, 8(1), 15173. doi: 10.1038/s41598-018-33169-5.
[14] Liu, Y. C., Ang, H. P., Teo, E. P., Lwin, N. C., Yam, G. H., & Mehta, J. S. (2016). Wound healing profiles of hyperopic-small incision lenticule extraction (SMILE). *Sci. Rep.,* 6, 29802. doi: 10.1038/srep29802.
[15] Miadelets, O. D., & Adaskevich, V. P. (2006). *Morphofunctional dermatology.* Moskow: Medlit.
[16] Sarkisov, D. S., & Perova, Yu. L. (1996). *Microscopic technique.* Moskow: Medcine.
[17] Sarrazy, V., Billet, F., Micallef, L., Coulomb, B., & Desmouliere, A. (2011). Mechanisms of pathological scarring: Role of myofibroblasts and current developments. *Wound Repair and Regeneration*, 19 (1), 10-15. doi: 10.1111/j.1524-475X.2011.00708.x.
[18] Smeringaiova, I., Reinstein Merjava, S., Stranak, Z., Studeny, P., Bednar, J., & Jirsova, K. (2018). Endothelial Wound Repair of the Organ-Cultured Porcine Corneas. *Curr. Eye Res.,* 43(7), 856-865. doi: 10.1080/02713683.2018.1458883.
[19] Viter, V. S. (2014). Ultrastructural state of muscular tunic of the heart after experimental thermal injury in applying lyophilized xenografts. Nauka i Studia, 8 (118), 107-111.
[20] Willenborg, S., & Eming, S. A. (2018). Cellular networks in wound healing. *Science,* 362 (6417), 891-892. doi: 10.1126/science.aav5542.
[21] Woodley, D. T. (2017). Distinct Fibroblasts in the Papillary and Reticular Dermis: Implications for Wound Healing. *Dermatol. Clin.,* 35(1), 95-100. doi: 10.1016/j.det.2016.07.004.
[22] Xiao, W., Tang, H., Wu, M., Liao, Y., Li, K., Li, L., & Xu, X. (2017). Ozone oil promotes wound healing by increasing the migration of fibroblasts via PI3K/Akt/mTOR signaling pathway. *Biosci. Rep.,* 37(6). pii: BSR20170658. doi: 10.1042/BSR20170658.
[23] Yoon, D., Yoon, D., Sim, H., Hwang, I., Lee, J. S., & Chun, W. (2018). Accelerated Wound Healing by Fibroblasts Differentiated from Human Embryonic Stem Cell-Derived Mesenchymal Stem Cells in a Pressure Ulcer Animal Model. *Stem Cells Int.,* 30, 4789568 doi: 10.1155/2018/4789568
[24] Zviahintseva, T. V., Hrun, V. V., & Naumova, O. V. (2013). Morphological changes in the skin of guinea pigs after local ultraviolet irradiation with the use of drugs with photoprotective activity. *Medicine today and tomorrow,* 58(1), 59-63.

МОРФОМЕТРИЧНІ ДОСЛІДЖЕННЯ УШКОДЖЕНОЇ ДІЛЯНКИ ШКІРИ ПІСЛЯ ЕКСПЕРИМЕНТАЛЬНОЇ ТЕРМІЧНОЇ ТРАВМИ ТА ЗА УМОВ КОРЕКЦІЇ КРІОЛІОФІЛІЗОВАНИМ КСЕНОДЕРМАЛЬНИМ СУБСТРАТОМ

Крамар С.Б., Волков К.С., Небесна З.М.

За даними ВООЗ опіки посідають третє місце серед інших травм, а в деяких країнах - друге, поступаючись лише транспортному травматизму. Одним із перспективних засобів у лікуванні опікової рани є використання ліофілізованого ксенодермального субстрату. Метою цієї роботи було встановлення морфометричних параметрів ураженої опіком ділянки шкіри в динаміці після експериментальної термічної травми та за умов корекції подрібненим субстратом ліофілізованої ксеношкіри. Опік III ступеня наносили водяною парою під загальним ефірним наркозом на епільовану поверхню шкіри спини морської свинки. Морфометрично на 7, 14 та 21 доби досліду у крайовій та центральній ділянках рани визначали товщину епідермісу (тонкої шкіри без шару рогових лусочок), кількість клітин фібробластичного ряду на одиницю площі, зовнішній та внутрішній діаметри капілярів. Морфометричні дослідження проводили за допомогою програм ВидеоТест-5.0, KAAPA Image Base та Microsoft Excel на персональному комп'ютері. Статистичну обробку отриманих кількісних даних проводили за допомогою методів варіаційної статистики з визначенням середньої арифметичної величини та її похибки (M±m), критерію Стьюдента (t) та показника достовірності (p). Достовірними вважаються відмінності при p≤0,05. Встановлено, що вже на 7 добу досліду в умовах закриття рани ксенодермальним субстратом відмічається суттєве потовщення епідермісу на периферії рани. Активації процесу крайової епітелізації сприяє оновлення компонентів мікроциркуляторного русла, утворення грануляційної тканини. З'ясовано, що на 14 добу застосування коригуючого чинника у периферійній зоні рани кількість клітин фібробластичного ряду та середнє значення товщини епідермісу сягають свого пікового значення, достовірно (p<0,001) перевищуючи такі показники тварин інтактної групи та групи тварин без корекції. Морфометричні параметри капілярів у цей термін досліду свідчать про добру розвиненість мікроциркуляторного русла, що покращує крайову епітелізацію. На 21 добу досліду за умов корекції майже втрачається межа між крайовою та центральними ділянками рани. Таким чином, результати морфометричних досліджень свідчать, що використання кріоліофілізованого ксенодермального субстрату після термічної травми шкіри сприяє загоєнню раневого дефекту з утворенням сполучної тканини дерми, ангіогенезом та повною епітелізацією поверхні ураження епідермальним пластом.

Ключові слова: *шкіра, термічна травма, кріоліофілізований ксенодермальний субстрат, морфометричні дослідження.*

МОРФОМЕТРИЧЕСКИЕ ИССЛЕДОВАНИЯ ПОВРЕЖДЕННОГО УЧАСТКА КОЖИ ПОСЛЕ ЭКСПЕРИМЕНТАЛЬНОЙ ТЕРМИЧЕСКОЙ ТРАВМЫ И ПРИ КОРРЕКЦИИ КРИОЛИОФИЛИЗИРОВАННЫМ КСЕНОДЕРМАЛЬНЫМ СУБСТРАТОМ

Крамар С.Б., Волков К.С., Небесная З.М.

По данным ВОЗ ожоги занимают третье место среди других травм, а в некоторых странах - второе, уступая лишь транспортному травматизму. Одним из перспективных средств в лечении ожоговой раны является использование лиофилизированного ксенодермального субстрата. Целью этой работы было установление морфометрических параметров участка кожи, поврежденного ожогом, в динамике после экспериментальной термической травмы и в условиях коррекции измельченным субстратом лиофилизированной ксенокожи. Ожог III степени на эпилированную поверхность кожи спины морской свинки наносили водяным паром под общим эфирным наркозом. Морфометрически на 7, 14 и 21 сутки опыта в краевом и центральном участках раны определяли толщину эпидермиса (тонкой кожи без слоя роговых чешуек), количество клеток фибробластического ряда на единицу площади, внешний и внутренний диаметры капилляров. Морфометрические исследования проводили с помощью программ ВидеоТест-5.0, Kaape Image Base и Microsoft Excel на персональном

компьютере. Статистическую обработку полученных количественных данных проводили с помощью методов вариационной статистики с определением средней арифметической величины и ее погрешности (M±m), критерия Стьюдента (t) и показателя достоверности (p). Достоверными считаются различия при p≤0,05. Установлено, что уже на 7 сутки опыта в условиях закрытия раны ксенодермальным субстратом отмечается существенное утолщение эпидермиса на периферии раны. Активации процесса краевой эпителизации способствует обновление компонентов микроциркуляторного русла, образование грануляционной ткани. Выяснено, что на 14 сутки применения корректирующего фактора в периферической зоне раны количество клеток фибробластического ряда и среднее значение толщины эпидермиса достигают своего пикового значения, достоверно (p<0,001) превышая такие показатели животных интактной группы и группы животных без коррекции. Морфометрические параметры капилляров в этот срок опыта свидетельствуют о хорошей развитости микроциркуляторного русла, что улучшает краевую эпителизацию. На 21 сутки опыта в условиях коррекции практически стирается грань между краевым и центральным участками раны. Таким образом, результаты морфометрических исследований свидетельствуют, что использование криолиофилизованного ксенодермального субстрата после термической травмы кожи способствует заживлению раневого дефекта с образованием соединительной ткани дермы, ангиогенезом и полной эпителизацией поверхности поражения эпидермальным пластом.

Ключевые слова: *кожа, термическая травма, криолиофилизированный ксенодермальный субстрат, морфометрические исследования.*

DOI: 10.31393/morphology-journal-2018-24(4)-04 Reports of Morphology, Vol. 24, №4, Pages 29-34

ISSN 1818-1295 eISSN 2616-6194

REPORTS OF MORPHOLOGY

Official Journal of the Scientific Society of Anatomists, Histologists, Embryologists and Topographic Anatomists of Ukraine

journal homepage: https://morphology-journal.com

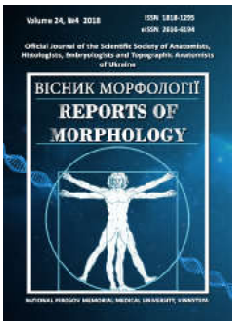

Regression models of individual cephalometric indicators used in the method of E.P. Harvold

Chernysh A.V.[1], Hasiuk P.A.[2], Yasko V.V.[1], Smolko D.G.[1]

[1]National Pirogov Memorial Medical University, Vinnytsya, Ukraine
[2]Ivan Horbachevsky Ternopil State Medical University, Ternopil, Ukraine

ARTICLE INFO
Received: 5 October, 2018
Accepted: 5 November, 2018

UDC: 616-073.75:616.314.26-053.81

CORRESPONDING AUTHOR
e-mail: andre.chernysh@gmail.com
Chernysh A.V.

Many scientific studies have shown the superiority of the Harvold method when performing linear measurements for both the upper and lower jaw. The purpose of the work is to construct and analyze the regression models of teleroentgenographic indices used in the method of E.P. Harvold young men and women with normal occlusion close to orthognathic bite and harmonic face. The analysis of lateral teleroentgenograms of 38 young men (aged from 17 to 21) and 55 young women (aged from 16 to 20 years) with normal occlusion close to orthognathic bite and harmonic face, obtained using the Veraviewepocs 3D device, Morita (Japan), was performed according to the techniques of R.M. Ricketts, C.J. Burstone, E.P. Harvold. In the course of the study, all the indicators of the above methods, were divided into three groups: 1 - metric characteristics of the skull, which usually do not change during surgical and orthodontic treatment; 2 - indicators of the tooth-jaw system that allow people with already formed bone skeleton to change the width, length, angles and position of the bones of the upper and lower jaws; 3 - indicators that characterize the position of each individual tooth relative to each other, to the bony cranial structures and face profile. In the licensed package "Statistica 6.0", regression models were constructed for the following parameters included in the second group, depending on the parameters of the first group: ANS-Cond (maxillary length in the Harvold method described as TM-ANS), Pog-Cond (mandibular length in the E.P. Harvold method is indicated as TM-PGN), Max-Mand - (difference in jaw lengths); as well as the index included in the third group, depending on the indicators of the first and second groups - Ap1uAp1l-DOP (angle Ap1uAp1l-DOP). In the young men, all three possible reliable models of teleroentgenographic parameters were constructed using the E.P. Harvold method, which were included in the second group, depending on the indicators of the first group (R^2 = from 0.616 to 0.940), and in young women only the length of the upper and lower jaws (R^2=0.857 and 0.792). In both young men and women, all models of the second group of models built according to the indicators of the first group included the distance P-PTV. Up to two models for young men and one model for young women included the distance Pt-N. Also, one model for young men and women included the angle of the cranial tilt (POr-NBa). Only young women have models for the front length of the skull base (N-CC). As for young men and women, we also built a reliable model of the third group indicator, depending on the indicators of the first and second groups (the angle Ap1uAp1l-DOP) (respectively, R^2=0.626 and R^2=0.584). And in young men and women, the size of the distance A-B is included to the constructed regression equations. In addition, in young men, the regression equation includes the value of the distance P-PTV; while in young women - the angles of the ANS-Xi-PM, MeGo-NPog and N-CF-A, as well as the difference in jaw lengths Max-Mand.

Keywords: *regression analysis, cephalometry, Harvold analysis, young men and women, orthognathic bite.*

Introduction

One way of forming a correct and beautiful smile is to use a cephalometric analysis, which is the clinical point of applying cephalometry. The basis of this analysis is the determination of the relationship between the dental and

skeletal facial structures, which is possible when performing the X-ray method of investigation, in the majority of cases - lateral teleroentgenograms [4, 17].

During the 19th century, orthodontists offered many techniques, each of which has its own specifics, advantages and disadvantages and, depending on this, has been recognized or practically not used in practice. It should be noted that a significant widely used have cephalometric analysis by McNamara [1, 16], Legan-Burstone [2, 7, 20, 22], Steiner [12], Tweed [5, 18], Ricketts [6], Schwartz [13], Jarabak Bjork [19] and Harvold [15].

In our opinion, the last author and his technique deserves special attention. Thus, Egil Peter Harvold, before becoming a well-known American scientist, worked as an orthodontist in Norway, and defended his doctorate dissertation on anatomy in Oslo in 1954. It was during this period that he began to be interested in the topic of congenital defects of the face (cheiloschisis, etc.), which became the basis of the research topic for the next decades, and already in 1963 he became director of the Center of Cranio-Facial anomalies in San- Francisco In 1974, he first published work, the basis of his own method of cephalometric analysis [15].

The main feature of the Harvold technique was the creation of standards for the length of the upper and lower jaws. Particular attention is drawn to the ratio of the size of the upper and lower jaw. At the same time - the location of teeth for this technique is not important [14].

The method of analysis has not lost its relevance yet and is the subject of many foreign authors' work. Thus, Singh A.K. with co-authors [21] compared the effectiveness of using different methods of cephalometric analysis in order to fix the maxillary-mandibular ratio. The study was attended by 50 people (25 girls and 25 boys) aged 18 to 26 years old, without orthodontic or dental treatment in history with orthognathic facial features. After statistical data processing, it was discovered that the Harvold method is a method of choice if it is impossible to conduct a teleroentgenographic study in the natural state of the head.

Wu B.W., Kaban L.B., and Peacock Z.S. [23] compared the effectiveness of Harvold and Steiner's methods for orthogonathic surgery. A retrospective study was conducted at Massachusetts Hospital between 2012 and 2016 and covered 388 patients, of which 289 were included in the study. The study showed the superiority of the E.P. Harvold method when performing linear measurements for both the upper and lower jaw - they were more likely with clinical assessments.

The *purpose* of the work is to construct and analyze the regression models of teleroentgenographic indices used in the method of E.P. Harvold in young men and women with normal occlusion close to orthognathic bite and harmonic face.

Materials and methods

Primary lateral teleroentgenograms of 38 young men (aged 17-21 years) and 55 young women (aged 16-20 years) with normal occlusion close to orthognathic bite and harmonic face, obtained from the Veraviewepocs 3D device, Morita (Japan), taken from the bank data of research center of National Pirogov Memorial Medical University, Vinnytsya.

The analysis of lateral teleroentgenograms was carried out according to the methods of R.M. Ricketts, C.J. Burstone, E.P. Harvold, described in detail in previous studies [8, 9, 11].

In the course of the study, all the indicators of the above methods, we were divided into three groups. *The first group* included metric characteristics of the skull, which usually do not change during surgical and orthodontic treatment. Most of these indicators are basic in modern cephalometric analyzes. In relation to them, lateral teleroentgenograms determine the inclination, anterior-posterior or vertical position of the bone structures (upper and lower jaw, occlusal plane, individual teeth). *The second group* includes indicators of the tooth-jaw system, the definitions of which most often need to be guided by the orthodontic treatment of growing patients and orthodontic surgery, which allows people with already formed bone skeleton to change the width, length, angles and position of the bones of the upper and lower jaws. *The third group* includes indicators that actually characterize the position of each individual tooth relative to each other, to the bony cranial structures and face profile.

According to the cephalometric method of E.P. Harvold [15], we carried out the simulation of the following indicators included in the second group, depending on the indicators of the first group (Fig. 1):

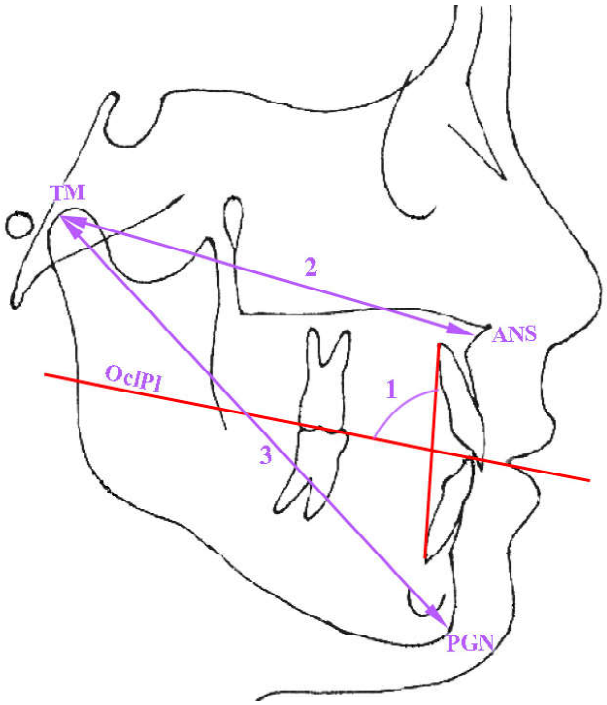

Fig. 1. Teleroentgenographic indicators used in the method of E.P. Harvold. 1 - angle Ap1uAp1l-DOP; 2 - distance ANS-Cond (TM-ANS); 3 - distance Pog-Cond (TM-PGN).

ANS-Cond (maxillary length, in the method E.P. Harvold is marked as **TM-ANS**) - distance from point TM to point ANS (anterior nasal spine), determining the maxillary length (mm);

Pog-Cond (mandibular length, in the method E.P. Harvold is marked as TM-PGN) - distance from point TM to point PGN, determining the mandibular length (mm);

Max-Mand - (Difference in Jaw Lengths) - difference of the lengths of the lines TM-ANS and TM- PGN (mm).

The modeling of E.P. Harvold, which was included in the third group, depending on the indicators of the first and second groups (see Fig. 1), was also conducted:

Ap1uAp1l-DOP - (angle Ap1uAp1l-DOP) - angle between Occlusal Plane and the connecting line between the root tips of the central upper and lower incisor (°).

The construction of regression models of individual teleroentgenographic indicators used in the method of E.P. Harvold was carried out in the licensed package "Statistica 6.0". In the direct stepwise regression analysis, we determined the following conditions: 1 - the final version of the regression equation should have a determination coefficient of not less than 0.50; 2 - the value of the F-criterion is not less than 3.0; 3 - the number of free members included in the regression equation should be as low as possible.

Results

The results of modeling of teleroentgenographic indices by the method of E.P. Harvold, which belonged to the second group, depending on the indicators of the first group, have the form of the following linear equations.

For young men:

ANS-Cond = 7.934 + 0.988 x Pt-N - 0.716 x P-PTV (R^2=0.931; $F_{(2.35)}$=236.0; p<0.001; Error of estimate=3.515),

Pog-Cond = -1.318 + 1.088 x Pt-N - 1.450 x P-PTV (R^2=0.940; $F_{(2.35)}$=272.1; p<0.001; Error of estimate=4.617),

Max-Mand = -19.55 - 0.869 x P-PTV + 0.396 x POR-NBA (R^2=0.616; $F_{(2.35)}$=28.12; p<0.001; Error of estimate=4.354),

where here and in the future, R^2 - coefficient of determination; $F_{(!,!!)}$=!!,!! - critical $_{(!,!!)}$ and got (!!,!!) value of Fisher's criterion; St. Error of estimate - standard error of the standardized regression coefficient; POr-NBa - the angle of the cranial tilt (deflection), the angle formed by the lines Po-Or and Ba-N (°); P-PTV - distance from the point Po to the point Pt, parallel to the Frankfurt plane (mm); Pt-N - the front part of the base of the skull, the distance from the point Pt to the point N, determines the length of the front of the skull base (mm).

For young women:

ANS-Cond = -5.672 - 1.060 x P-PTV + 0.812 x Pt-N + 0.290 x POr-NBa (R^2=0.857; $F_{(3.51)}$=102.2; p<0.001; Error of estimate=2.801),

Pog-Cond = -0.847 + 1.209 x N-CC - 1.095 x P-PTV (R^2=0.792; $F_{(2.52)}$=98.73; p<0.001; Error of estimate=4.656),

where here and in the future, N-CC - front length of the skull base, distance from the point N to the point CC (mm).

The determination coefficient of the regression equation of the difference in jaw lengths (Max-Mand) in young women with orthognathic bite is 0.328 and therefore has no practical significance for orthodontists.

The results of simulation of teleroentgenographic indices by the method of E.P. Harvold included in the third group, depending on the indicators of the first and second groups, have the form of the following linear equations.

For young men:

AP1UAP1L = 96.28 - 1.131 x A-B + 0.140 x P-PTV (R^2=0.626; $F_{(2.35)}$=29.24; p<0.001; Error of estimate=2.550),

where here and in the future, A-B - distance from the point A to the point B on the occlusal plane (apOcP-ppOcP) (mm).

For young women:

AP1UAP1L = 110.0 - 1.062 x A-B - 0.297 x MeGo-NPog - 0.320 x ANS-Xi-PM + 0.180 x Max-Mand + 0.193 x N-CF-A (R^2=0.584; $F_{(5.49)}$=13.74; p<0.001; Error of estimate=2.849),

where, ANS-Xi-PM - angle of the lower height of the face, the angle is formed by lines ANS-Xi and Xi-Pm (°); Max-Mand - difference in jaw lengths, difference between length TM-ANS and TM-PGN (mm); MeGo-NPog - facial cone, angle formed by lines Me-Go and N-Pog (°); N-CF-A - angle of the upper jaw, angle formed by lines N-CF and CF-A (°).

Discussion

In a number of studies, the study of ethnic, regional, age and sexual characteristics of the Harvold method has been studied. Alam M. K. and co-authors [3] identified features of cephalometric indices for Bangladesh. In the analysis of 100 lateral teleroentgenograms from ethnic Bangladesh, 50 men and women aged 18-24 years old, it has been found that practically all indicators, except position of the incisors, are in accordance with the Harvold methodology. Also, signs of sexual dimorphism were revealed.

Daer A.A. and Abuaffan A.H. [10] in 2016 set normative indicators for the population of Yemen. For this purpose, a group of volunteers from 105 women and 89 men aged 18-25 who had a symmetrical face and no dental or orthodontic interventions in history were formed. After statistical analysis, there were significant differences for such skeletal indices as SNB, ANB, SNPg and SNBa angles, and distances ML-NL, NL-NSL, ML-NSL and Gn-tgo-Ar.

However, the work of domestic scientists in the study of

the method of E.P. Harvold remains small [8], which has negative consequences for the full use of this technique in order to provide orthodontic care to the Ukrainian people.

In young men with orthognathic bite and harmonious face we have constructed all three possible reliable models (length of the upper and lower jaw and difference in jaw lengths) of teleroentgenographic indices using the E.P. Harvold method with a determination coefficient of greater than 0.5 which are included in *the second group* depending on the indicators of *the first group*, and in young women - only the length of the upper and lower jaws. It is established that in similar models in young men, the determination coefficient in models is higher than in young women (in young men R^2=0.931 and 0.940, and in young women - 0.857 and 0.792). In both young men and women, all models of *the second group* of models built according to the indicators of *the first group* included the distance P-PTV. Two models for young men and one model for young women included the distance Pt-N, which defines the length of the anterior part of the base of the skull. Also, entered one model for young men and women - angle of the cranial tilt (POr-NBa). Only in young women the models of teleroentgenographic indices by the method of E.P. Harvold which entered *the second group*, depending on the indicators of *the first group* includes the front length of the base of the skull (N-CC).

In both young men and women also constructed a reliable model of the angle Ap1uAp1l-DOP (*the third group* indicator, depending on the indicators of *the first* and *second groups*) (respectively, R^2=0.626 and R^2=0.584). And in young men and women, the size of the distance A-B included in the constructed regression equations. In addition, in young men, the regression equation includes the value of the distance P-PTV; while in young women - angles of the ANS-Xi-PM, MeGo-NPog and N-CF-A, as well as the difference in jaw lengths Max-Mand.

The above-mentioned perspectives on the possibilities of full (taking into account age, gender, ethnicity, etc.) use of the method of E.P. Harvold encourages further study of this topic and the development of regression models of individual teleroentgenographic indicators used in this method in other regions of Ukraine.

Conclusions

1. In the young men, with normal occlusion close to the orthognathic bite, all three reliable valid models of teleroentgenographic indices according to E.P. Harvold method, included the second group depending on the indicators of the first group (R^2= from 0.616 to 0.940), and in young women only 2 models (R^2=0.857 and 0.792); both in young men and women, a reliable model of the angle Ap1uAp1l-DOP (the third group indicator, depending on the indicators of the first and second groups) was constructed (respectively, R^2=0.626 and R^2=0.584).

2. In both young men and women, for all models of second-group teleroentgenographic models constructed by E.P. Harvold method, depending on the indicators of the first group, the distance P-PTV was entered. In addition, up to two models in young men and one model in young women entered the distance Pt-N.

3. In both young men and women, among the teleroentgenographic indices of the first and second groups that are included in the models of the third group by the method of E.P. Harvold, the distance A-B entered.

References

[1] Al Sabbagh, R. (2014). Syrian norms of McNamara cephalometric analysis. *International Arab Journal of Dentistry*, 3(5), 95-101.

[2] Al Taki, A., Yaqoub, S., & Hassan, M. (2018). Legan-Burstone soft tissue profile values in a Circassian adult sample. *Journal of orthodontic science*, 7, 18.

[3] Alam, M. K., Basri, R., Purmal, K., Sikder, M. A., Saifuddin, M., & Iida, J. (2013). Cephalometric norms in Bangladeshi adults using Harvold's analysis. I*nternational Medical Journal*, 20(1), 92-94.

[4] Argancev, A. P., & Ahmedova, Z. R. (2014). Features of X-ray examination with endodontic treatment. *Endodontics today*, 3, 13-19.

[5] Atit, M. B., Deshmukh, S. V., Rahalkar, J., Subramanian, V., Naik, C., & Darda, M. (2013). Mean values of Steiner, Tweed, Ricketts and McNamara analysis in Maratha ethnic population: A cephalometric study. *APOS Trends in Orthodontics*, 3(5), 137-151.

[6] Bae, E. J., Kwon, H. J., & Kwon, O. W. (2014). Changes in longitudinal craniofacial growth in subjects with normal occlusions using the Ricketts analysis. *The Korean Journal of Orthodontics,* 44(2), 77-87.

[7] Bagwan, A. A., AL-Shennawy, M. I., & Alskhawy, M. M. (2015). Evaluation of soft tissue parameters for adults with accepted occlusion using Legan and Burstone analysis. *Tanta Dental Journal,* 12(1), 1-6.

[8] Chernysh, A. V. (2018). Cephalometric studies of Ukrainian young men and women with orthognathic bite by the method of E.P. Harvold. *Reports of Morphology,* 23(2), 38-43. https://doi.org/10.31393/morphology-jornal-2018-24(2)-06

[9] Chernysh, A. V., Gunas, I. V., Gavryluk, A. O., Dmytrenko, S. V., Serebrennikova, O. A., Kyrychenko, Y. V., & Balynska, M. V. (2018). Cephalometric studies of ukrainian boys and girls with orthognathic bite by the method of R. M. Ricketts. *World of Medicine and Biology,* 14(64), 88-93. doi: https://doi.org/10.26724/2079-8334-2018-2-64-88-93

[10] Daer, A. A., & Abuaffan, A. H. (2016). Cephalometric norms among a sample of Yamani adults. *Orthodontic Waves,* 75(2), 35-40. https://doi.org/10.1016/j.odw.2016.03.001

[11] Dmitriev, M., Chernysh, A., & Chugu, T. (2018). Cephalometric studies of Ukrainian boys and girls with physiological bite by the method of Charles J. Burstone. *Biomedical and Biosocial Anthropology,* 30, 62-67. doi: https://doi.org/10.31393/bba30-2018-09

[12] Dmitriev, M. O. (2016). Determination of normative cephalometric parameters by the method of Stainer for Ukrainian boys and girls. *World of Medicine and Biology,* 3, 28-32.

[13] Dmitriev, M. O., Chugu, T. V., Gerasimchuk, V. V., & Cherkasova, O. V. (2017). Determination of craniometric and gnatometric indices by A. M. Schwartz's method for Ukrainian boys and

girls. *Biomedical and biosocial anthropology,* 29, 53-58.
[14] Fadeev, R. A., & Yakovishina, Ye. A. (2013). Studying the diagnostic value of the Harvold EP lateral teleroentgenograms analysis method for determining the age parameters of the upper and lower jaws in growing patients. *Institute of Dentistry,* 4, 40-41.
[15] Harvold, E. P. (1974). *The activator in orthodontics.* St. Louis, Mo., Mosby.
[16] Khan, S. A., Mohammad, P. A., Tariq, J., Khursheed, T., Jehan, S., Alam, M. K., & Qamruddin, I. (2017). Cephalometric Study of Pakistani Population Using McNamara Analysis. *International Medical Journal*, 24(1), 144-146.
[17] Korobeinikova, Yu. L. (2013). Comparative characteristic of modern X-ray methods of diagnostics in dentistry. *Actual problems of modern medicine: Bulletin of the Ukrainian Medical Stomatological Academy,* 13(3), 44-46.
[18] Kuramae, M., de Araujo Magnani, M. B. B., Nouer, D. F., Ambrosano, G. M. B., & Inoue, R. C. (2016). Analysis of Tweed's Facial Triangle in Black Brazilian youngsters with normal occlusion. *Brazilian Journal of Oral Sciences*, 3(8), 401-403.
[19] Mahroof, V. (2017). A Cephalometric Analysis for Pakistani Adults Using Jarabak Bjork's Analysis.*International medical journal,* 24(1), 128-131.
[20] Sahoo, N., Mohanty, R., Mohanty, P., Nayak, T., Nanda, S. B., & Garabadu, A. (2016). Cephalometric Norms for East Indian Population using Burstone Legan Analysis. *Journal of International Oral Health,* 8(12), 1076-1081.
[21] Singh, A. K., Ganeshkar, S. V., Mehrotra, P., & Bhagchandani, J. (2013). Comparison of different parameters for recording sagittal maxillo mandibular relation using natural head posture: A cephalometric study. *Journal of orthodontic science,* 2(1), 16-22. doi: 10.4103/2278-0203.110328
[22] Soni, A., Alladwar, N., Goel, S., Chopra, R., & Sharma, S. (2015). Evaluation of lateral Cephalometric Norms for Burstone's Analysis in Chhattisgarh by using Nemoceph Software with Lateral Cephalograms Taken in Natural Head Position'. *International Journal of Oral Health Dentistry,* 1(3), 114-119.
[23] Wu, B. W., Kaban, L. B., & Peacock, Z. S. (2018). Do Steiner or Harvold Cephalometric Analyses Better Correlate with Clinical Impression in Orthognathic Surgery Patients? *Journal of Oral and Maxillofacial Surgery,* 76(10), 15-16. DOI: https://doi.org/10.1016/j.joms.2018.06.055

РЕГРЕСІЙНІ МОДЕЛІ ІНДИВІДУАЛЬНИХ ЦЕФАЛОМЕТРИЧНИХ ПОКАЗНИКІВ, ЩО ВИКОРИСТОВУЮТЬСЯ В МЕТОДИЦІ E.P. HARVOLD

Черниш А.В., Гасюк П.А., Яcько В.В., Смолко Д.Г.

У багатьох наукових дослідженнях при проведенні лінійних вимірювань як для верхньої, так і для нижньої щелеп, доведено перевагу методики Harvold. Мета роботи - побудувати та провести аналіз регресійних моделей телерентгенографічних показників, що використовуються у методиці E.P. Harvold, в юнаків і дівчат з нормальною оклюзією, наближеною до ортогнатичного прикусу, та гармонійним обличчям. Аналіз бокових телерентгенограм 38 юнаків (віком від 17 до 21 року) та 55 дівчат (віком від 16 до 20 років) з нормальною оклюзією, наближеною до ортогнатичного прикусу та гармонійним обличчям, отримані за допомогою пристрою Veraviewepocs 3D, Morita (Япония), проводили за методиками R.M. Ricketts, C.J. Burstone, E.P. Harvold. При проведенні дослідження усі показники вищевказаних методик були розділені на три групи: 1 - метричні характеристики черепа, які, зазвичай, не змінюються під час хірургічного та ортодонтичного лікування; 2 - показники зубощелепної системи, котрі дозволяють в осіб зі вже сформованим кістковим скелетом змінювати ширину, довжину, кути та положення кісток верхньої та нижньої щелеп; 3 - показники, котрі власне характеризують положення кожного окремого зуба по відношенню один до одного, до кісткових черепних структур та профілю обличчя. В ліцензійному пакеті "Statistica 6.0" будували регресійні моделі наступних показників, що увійшли до другої групи в залежності від показників першої групи: ANS-Cond (довжина верхньої щелепи, у методиці E.P. Harvold зазначається як TM-ANS), Pog-Cond (довжина нижньої щелепи, в методиці E.P. Harvold зазначається як TM-PGN), Max-Mand - (міжщелепна різниця); а також показника, що увійшов до третьої групи в залежності від показників першої та другої груп - Ap1uAp1l-DOP (кут Ap1uAp1l-DOP). В юнаків побудовані усі 3 можливі достовірні моделі телерентгенографічних показників за методикою E.P. Harvold, які увійшли до другої групи в залежності від показників першої групи (R^2 = від 0,616 до 0,940), а у дівчат - лише довжина верхньої та нижньої щелеп (R^2 = 0,857 і 0,792). Як в юнаків, так і у дівчат до усіх побудованих моделей показників другої групи в залежності від показників першої групи увійшла відстань P-PTV. До двох моделей в юнаків і до одної моделі у дівчат увійшла відстань Pt-N. Також до однієї моделі в юнаків і дівчат увійшов кут краніального нахилу (POr-NBa). Лише у дівчат до моделей входить передня довжина основи черепа (N-CC). Як в юнаків, так і у дівчат нами також побудована можлива достовірна модель показника третьої групи в залежності від показників першої та другої груп (кута Ap1uAp1l-DOP) (відповідно R^2=0,626 та R^2=0,584). І в юнаків, і у дівчат до побудованих регресійних рівнянь входить величина відстані A-B. Крім того, в юнаків до регресійного рівняння входить величина відстані P-PTV; а у дівчат - величина кутів ANS-Xi-PM, MeGo-NPog і N-CF-A, а також міжщелепна різниця Max-Mand.

Ключові слова: *регресійний аналіз, цефалометрія, аналіз Harvold, юнакі та дівчата, ортогнатичний прикус.*

РЕГРЕССИОННЫЕ МОДЕЛИ ИНДИВИДУАЛЬНЫХ ЦЕФАЛОМЕТРИЧЕСКИХ ПОКАЗАТЕЛЕЙ, ИСПОЛЬЗУЕМЫХ В МЕТОДИКЕ E.P. HARVOLD

Черниш А.В., Гасюк П.А., Яcько В.В., Смолко Д.Г.

Во многих научных исследованиях доказано преимущество методики Harvold при проведении линейных измерений, как для верхней, так и для нижней челюстей. Цель работы - построить и провести анализ регрессионных моделей телерентгенографических показателей, используемых в методике E.P. Harvold, у юношей и девушек с нормальной окклюзией, приближенной к ортогнатическому прикусу, и гармоничным лицом. Анализ боковых телерентгенограмм 38 юношей (в возрасте от 17 до 21 года) и 55 девочек (в возрасте от 16 до 20 лет) с нормальной окклюзией, приближенной к ортогнатическому прикусу и гармоничным лицом, полученные с помощью устройства Veraviewepocs 3D, Morita (Япония), проводили по методикам R.M. Ricketts, C.J. Burstone, E.P. Harvold. При проведении исследования все показатели вышеуказанных

методик, были разделены на три группы: 1 - метрические характеристики черепа, которые обычно не меняются в ходе хирургического и ортодонтического лечения; 2 - показатели зубочелюстной системы, позволяющие у лиц с уже сформированным костным скелетом изменять ширину, длину, углы и положения костей верхней и нижней челюстей 3 - показатели, которые собственно характеризируют положение каждого отдельного зуба по отношению друг к другу, к костным черепным структурам и профилю лица. В лицензионном пакете "Statistica 6.0" построены регрессионные модели следующих показателей, вошедших во вторую группу в зависимости от показателей первой группы: ANS-Cond (длина верхней челюсти, в методике E.P. Harvold отмечается как TM-ANS), Pog-Cond (длина нижней челюсти, в методике E.P. Harvold отмечается как TM-PGN), Max-Mand - (межчелюстная разница); а также показателя, вошедшего в третью группу в зависимости от показателей первой и второй групп - Ap1uAp1l-DOP (угол Ap1uAp1l-DOP). У юношей построены все 3 возможные достоверные модели телерентгенографических показателей по методике E.P. Harvold, которые вошли во вторую группу в зависимости от показателей первой группы (R^2 = от 0,616 до 0,940), а у девушек - только длина верхней и нижней челюстей (R^2=0,857 и 0,792). Как у юношей, так и у девушек ко всем построенным моделям показателей второй группы, в зависимости от показателей первой группы, вошло расстояние P-PTV. К двум моделям у юношей и в одной модели у девушек вошло расстояние Pt-N. Также к одной модели у юношей и девушек вошел угол краниального наклона (POr-NBa). Только у девушек к моделям входит передняя длина основания черепа (N-CC). Как у юношей, так и у девушек нами также построена возможная достоверная модель показателя третьей группы в зависимости от показателей первой и второй групп (угла Ap1uAp1l-DOP) (соответственно R^2=0,626 и R^2=0,584). И у юношей, и у девушек к построенным регрессионным уравнениям входит величина расстояния A-B. Кроме того, у юношей к регрессионному уравнению входит величина расстояния P-PTV; а у девушек - величина углов ANS-Xi-PM, MeGo-NPog и N-CF-A, а также межчелюстная разница Max-Mand.

Ключевые слова: *регрессионный анализ, цефалометрия, анализ Harvold, юноши и девушки, ортогнатический прикус.*

DOI: 10.31393/morphology-journal-2018-24(4)-05 Reports of Morphology, Vol. 24, №4, Pages 35-40

ISSN 1818-1295 eISSN 2616-6194

REPORTS OF MORPHOLOGY

Official Journal of the Scientific Society of Anatomists, Histologists, Embryologists and Topographic Anatomists of Ukraine

journal homepage: https://morphology-journal.com

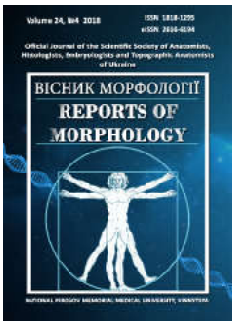

Organometric parameters of the remaining kidney after removal of the contralateral in immature rats

Monastyrskyi V.M.
National Pirogov Memorial Medical University, Vinnytsya, Ukraine

ARTICLE INFO
Received: 5 October, 2018
Accepted: 6 November, 2018

UDC: 611.611:611.061:611.068:616.61-089.87

CORRESPONDING AUTHOR
e-mail: vova.monastirskiy@gmail.com
Monastyrskyi V.M.

The processes of compensatory hypertrophy of the kidney to the period of puberty are insufficiently studied. Changes in renal parameters after contralateral removal are of scientific interest. The purpose of the study was to establish and compare changes in organometric parameters of the kidney that remained after nephrectomy in non-sexually adult male rats and in sexually mature male rats. Experimental study was performed on 84 non-adult white male rats weighing 53-71 grams, which were kept on a standard vivarium diet. All animals were divided into two groups (42 in each): the first - control, the second - the experimental group. In the control group, the abdominal cavity was opened under ketamine anesthesia, after which the abdominal wall was sutured in layers. All animals of the experimental group performed removal of the left kidney. Animals were withdrawn from the trial by intra-pleural administration of thiopental-sodium 50 mg/kg after 7, 14, 21, 30, 90 days after nephrectomy. Macroscopic evaluation and description of the kidneys of animals was performed after their removal. The statistical analysis of the obtained results was carried out using the "STATISTICA 5.5" program, using parametric and non-parametric methods for evaluating the obtained results. It was found that in the immature rats, the weight of animals in the experimental group (after nephrectomy) was statistically significantly lower in all terms of the observation compared to the control group, and the weight of the kidney of animals in the experimental group, on the contrary, was statistically significantly higher in all terms of observation. The length, width, thickness, volume of kidneys of animals of the experimental group, as well as the magnitude of increment of these parameters with each term of observation are determined. The greatest increase in organometric parameters of the kidney was observed after 30 days of the postoperative period ($p<0.05$). Subsequently, on the 60th and 90th day, the magnitude of the increase in organometric parameters of the kidney significantly decreased. The index of hypertrophy of the kidney remained unpaired by nephrectomy, which varied from 52.24% to 63.21%. The highest rates of hypertrophy were observed between the 21st and 30th days.
Keywords: *kidney, nephrectomy, organometry, immature rats.*

Introduction

The remaining kidney after nephrectomy cannot be considered an absolutely healthy organ [25]. This is evidenced by various pathological processes that develop in it over time [5]. Studies have shown that to ensure the release of nitrogen metabolism products and the balance of the internal environment of the body, the remaining kidney works at the limit of its capabilities [8].

The remaining functioning kidney, since childhood, has compensatory hyperfiltration, which leads to kidney damage for the period of adolescence in more than 50% of patients [23]. Experimental studies have shown that male animals show a higher degree of hyperfiltration [6], elevated blood pressure [14], and higher glomerular pressure and hypertrophy of renal corpses.

The controversial statement of clinicians that the growing child's body is characterized by expressed compensatory mechanisms that are not always kept in adults [21]. Several epidemiological clinical studies have shown that one kidney birth increases the risk of developing hypertension, proteinuria and renal failure in childhood [27] and in adulthood [26]. Recent studies have shown that kidney donors are at increased risk (up to 8 times) for renal failure [16].

Many authors emphasize that the younger organism has more intensive and more advanced processes of hypertrophy [3]. The majority of patients who have been admitted to nephrectomy in the short term become disabled in connection with the development of chronic renal failure and nephrogenic hypertension, whereas in children, including when they become adults, the percentage of disability is minimal [1, 2]. However, the functional state of a single kidney in children is often significantly disturbed, and chronic renal failure can occur already in childhood or adolescence [13]. In the kidney, left after nephrectomy in children, established with the help of renosonography, the unevenness of proliferative and fibrotic-sclerotic processes, the presence of dysmetabolic disorders, prolonged violations of the natural passage of urine [15]. With age, glomerular hyperfiltration may worsen existing glomerulosclerosis and lead to renal insufficiency [22].

Compensatory mechanisms that underlie hypertrophy of the kidneys are not yet fully understood, mechanisms that provide stabilization of compensatory and adaptive processes are not sufficiently disclosed. Insufficiently studied issues on the preservation of compensatory and restorative mechanisms in the age aspect.

The *aim* of the study - to establish changes in organometric parameters of the kidney that remained after nephrectomy in immature male rats.

Materials and methods

An experimental study was performed on 84 immature white male rats weighing 53-71 grams, which were kept on a standard diet in vivarium of the National Pirogov Memorial Medical University, Vinnytsya, Ukraine.

According to the literature, experiments conducted on rats have shown that these animals can be used as a model for studying the course of recovery of the body after nephrectomy and resection of the kidney and the selection of corrective therapy, aimed at the earliest adaptation of the organism to existence in the new conditions [10, 11]. Male rats were more sensitive and less adapted to renal excretion [24].

Animal retention and manipulation were conducted in accordance with the "General Ethical Principles of Animal Experiments" adopted by the First National Congress on Bioethics (Kyiv, 2001), and also guided by the recommendations of the "European Convention for the Protection of Vertebrate Animals used for Experimental and Other Scientific Purposes" (Strasbourg, 1985) and the provisions of the "Rules for Preclinical Safety Assessment of Pharmacological Products (GLP)".

All animals were divided into two groups (42 in each): the first - control, the second - the experimental group.

In the control group, the abdominal cavity was opened under ketamine anesthesia, after which the abdominal wall was sutured in layers.

All animals of the experimental group performed surgical intervention - nephrectomy of the left kidney. Rats under general intra-muscle anesthesia (aminazine 10 mg/kg and ketamine 20 mg/kg) were given left-sided nephrectomy by crossing the renal leg between two ligatures and then removing the organ. The operation was carried out as follows. The animal was inserted and fixed with soft straps for the limbs in the position on the back to the operating table. With pararectal incision in the length up to 3-5 cm, layer open the abdominal cavity. The small intestine with a gauze napkin was pulled down and medially. The livers of the kidney and its vessels were isolated from the surrounding tissues. The kidney was molded into the wound and isolated from the fatty tissue of the upper third of the ureter. A clamping device was applied to the ureter, under which they were tied with a catgut lighthouse and then crossed under a clamp. In a droop way, they isolated the renal artery and vein and imposed two clips, between which they were crossed. The kidney was removed, and the stump of the blood vessels were catgut ligatures. The layer of the wound was tightly sewn. Isolated by blunt renal artery and vein and imposed two terminals between which they crossed. The kidney was removed and the stump of blood vessels catgut tied ligatures. The layer of the wound was tightly sewn.

Animals were withdrawn from the trial by intra-pleural administration of thiopental-sodium 50 mg/kg after 7, 14, 21, 30, 90 days after nephrectomy. Macroscopic evaluation and description of the kidneys of animals was performed after their removal. Their mass was determined on the laboratory scale of HLR-200 to 0.1mg, and the length, width and thickness of the organ were measured with the help of a caliper to an accuracy of 0.05 mm. The volume of the kidney was calculated according to the formula: **V = 0,523** x **a** x **b** x **c**, where a - is length, b - is width, c - is the thickness of the kidney.

The kidney mass index was calculated by obtaining a percentage correlation between the weight of the kidney and the weight of the body of the rat being examined. In the case of animals of the second group, the index of kidney hypertrophy was calculated. It was calculated by obtaining a percentage correlation between the mass of the single kidney and the weight of the two kidneys of the rats of the first control group at this time of the study.

The statistical analysis of the obtained results was carried out using the "STATISTICA 5.5" program, using parametric and non-parametric methods for evaluating the obtained results.

Results

The results of measuring the organometric parameters of the kidneys in the immature rats of the 1st group were as follows: with increasing body weight during the observation period, the organometric parameters of the kidneys were also increased. So the mass of the right kidney from the first to the 90th day of the observation period increased by 2.05 times (Table 1). The mass of the left kidney, in comparison with the right, on all terms of observation was slightly lower ($p>0.05$). At the same time, the index of kidney mass decreased by 1.22 times from the first to the 90th day of the observation period, indicating a predominance of growth

Table 1. Weight of the body and the right kidney of the immature rats of the control and experimental groups.

The term of the postoperative period	Control group (n=42)			Experimental groups (n=42)		
	Animal weight (g)	Weight of the kidney (g)	Kidney Weight Index (%)	Animal weight (g)	Kidney weight (g)	Kidney Weight Index (%)
1 day	61.33±4.03	0.372±0.012	0.603±0.022	62.55±4.09		
7 days	74.78±2.68*	0.385±0.015	0.510±0.007*	68.44±1.33#	0.440±0.027#	0.642±0.048#
14 days	86.07±2.61*	0.402±0.012	0.467±0.004*	80.67±2.49*#	0.475±0.012#	0.592±0.009#
21 days	97.35±2.63*	0.457±0.010*	0.459±0.003	91.83±2.32*#	0.558±0.012*#	0.597±0.007#
30 days	108.6±2.8*	0.477±0.007	0.442±0.006	102.8±2.4*#	0.597±0.010*#	0.585±0.007#
60 days	122.5±2.7*	0.540±0.023*	0.447±0.010	116.7±2.5*#	0.635±0.015*#	0.551±0.009*#
90 days	153.6±3.7*	0.760±0.040*	0.495±0.015*	132.7±2.3*#	0.788±0.015*	0.587±0.003*#

Note: * - statistically significant differences (p<0,05) according to the Mana-Whitney criterion between the corresponding indicators in comparison with the indicators of the previous term of research. # Are statistically significant differences (p<0.05) according to the Mana-Whitney criterion between the respective indices compared with the control animals.

rate of body weight of rats over the rate of weight gain of the kidneys. The volume of the right kidney thus increased during the course of observation from 75.24±4.65 mm^3 for the first day to 407.8±14.3 mm^3 for the 90th day. The length of the right kidney has increased from 7.950±0.150 mm to 14.40±0.07 mm, the width - from 4.733±0.100 mm to 7.883±0.089 mm, the thickness - from 3.817±0.089 mm to 6.867±0.156 mm.

In the immature animals of the second (experimental) group at day 7 after nephrectomy, the body weight of rats was less than that of the animals in the same group of animals in the same group at 8.47%, at 14 days - by 6.27%, at 21 days - 5, 67%, for 30 days - 5.34%, for 60 days - 4.76%, for 90 days - 13.63%. However, organometric parameters of the right kidney were statistically significantly more control values of animals of the first group at all times, especially on the 30th day of observation. Thus, for the 7th day after nephrectomy, the mass of the right kidney of rats was higher (p<0.05) values in the similar term of animals of the first group by 11.36%, for 14 days - by 16.67%, for 21 days - 17.86%, for 30 days - 20%, for 60 days - 15.62%. At 90 days no statistically significant difference was noted.

The index of kidney weight in non-immature animals in the second (experimental) group was statistically significantly higher throughout the post-operation observation period compared to the similar terms of animals in the first control group.

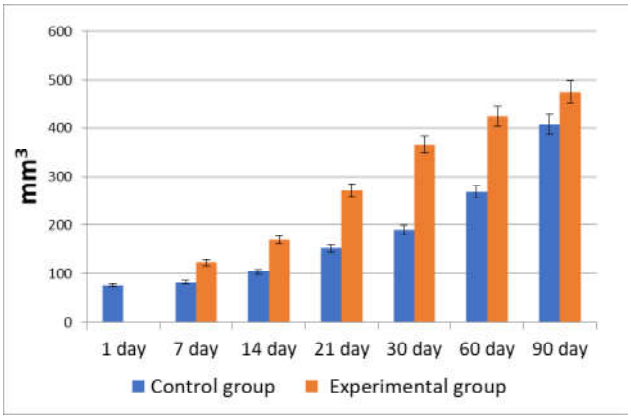

Fig. 1. Volume of the right kidney of immature rats in different terms after the operation of the control and experimental groups.

Parameters of other organometric indices of the right kidney of animals of the second (experimental) group also had significant differences. The length of the right kidney compared with the similar indicator of animals in the first control group was greater after 7 days after nephrectomy by 12.27%, after 14 days - by 15.02%, in 21 days - by 17.49%, after 30 days - by 19.73%, after 60 days - by 15.03%, after 90 days - by 4.00%. The width of the right kidney was greater after 7 days after nephrectomy by 12.50%, after 14 days - by 14.94%, in 21 days - by 17.62%, 30 days later - by 19.62%, after 60 days - by 12.22%, after 90 days - by 6.52%. The thickness of the right kidney was greater after 7 days after nephrectomy by 12.30%, after 14 days - by 15.26%, in 21 days - by 17.53%, after 30 days - by 19.45%, after 60 days - by 14.74%, after 90 days - by 4.18%.

The statistically significant decrease in the growth rates of all organometric indices in 90 days draws attention.

It is very important to know how the volume of the kidney has changed, since it is believed that the volume of kidneys is the optimal parameter for prediction of renal function [12]. The volume of the right kidney, after 7 days after nephrectomy, was 32.71% higher, compared with the same indicator of animals in the first control group (fig. 1). The largest increase in volume was observed after 30 days of postoperative period (48.05%). Subsequently, on the 60th and 90th day, the increase in renal volume decreased to 36.38% and 14.02% respectively.

It should be noted that the index of hypertrophy of the kidney after the removal of the contralateral ranged from 52.24% to 63.21%. The highest rates of hypertrophy were observed between the 21st and 30th days.

Discussion

The data we obtained are in agreement with the results of other authors [4], when the absolute dry kidney weight

was increased in rats 7 days after unilateral nephrectomy (hypertrophy of the kidneys), and the mean value was 29.9% higher than the values removed from the contralateral kidney.

A progressive increase in the weight of kidney of rats was also established after removal of the left kidney, which reached its peak after 30 days [9].

According to research [28, 29], renal compensatory hypertrophy restores normal renal function after nephrectomy due to an increase in organ size due to cell growth, and not their proliferation [17].

In the compensatory reaction of the kidney remaining after nephrectomy in immature rats, a significant increase in the indexes of all structural components of the nephron of the cortical substance was established [19]. The highest rate of growth occurs in a seven-day period after the removal of the kidney. Ultrastructure of the cortical substance of the kidneys of unborn animals after the performed nephrectomy is changing already in the early stages of the experiment, when significant reactive changes occur in all components of the nephron. Although the kidney compensatory reaction develops as a reaction to restore normal renal function, in the cortical substance, in addition to hypertrophied, the number of atrophied, diminished kidney cells increases [18]. Enlarged capsules are enlarged and uneven. In the late stages of the experiment, after nephrectomy, the presence of both compensatory and destructive changes in the components of the nephron was established.

The use of flow cytometry with simultaneous histological studies showed that the response of adults and young rats to the removal of one of the kidneys is the same, but in immature animals, the growth of cells in the phase S cell cycle after 7-14 days is statistically significantly more than that of the mature [20]. According to recent studies, with loss of renal tissue in the renal epithelial cells MDCK (Madin-Darby cells), a protein with a zona occludens 2 (ZO-2) compound causes cellular hypertrophy by two mechanisms: prolonging the time that cells are carried out in the phase G1 cell cycle due to the increase in the cyclone D1 level and increasing the rate of protein synthesis [7].

In the future, it is planned to compare changes in organometric parameters of the kidney, remaining after nephrectomy, in immature and mature animals.

Conclusions

1. In the immature rats, the weight of animals in the experimental group (after nephrectomy) was statistically significantly lower in all observation periods compared to the control group.

2. The weight of the kidney of the animals of the experimental group, as compared with the control group, was, conversely, statistically significantly higher in all terms of observation.

3. The length, width, thickness and volume of the kidneys of animals in the experimental group were also larger with each observation period ($p<0.05$).

4. The largest increase in organometric parameters of the kidney was observed after 30 days of postoperative period. Subsequently, on the 60th and 90th day, the magnitude of the increase in organometric parameters of the kidney significantly decreased.

References

[1] Abdihalikov, T. Zh. (2016). Functional condition of the single kidney in patients after surgical intervention due to urinary stone disease. *Bulletin of KRSU,* 16(7), 3-6.

[2] Abdihalikov, T. Zh., Chernetsova, G. S., & Kolesnichenko, I. V. (2013). Rehabilitation of patients with a single kidney after undergoing nephrectomy. *Bulletin of KRSU*, 13(11), 3-5.

[3] Alaygut, D., Soylu A., Kasap, B., Turkmen, M., Cakmakci, H., & Kavukcu, S. (2013). The Relationships Between Renal Compensatory Hypertrophy Etiologic Factors and Anthropometric Development in the Pediatric Age Group. *Urology,* 82(2), 442-447. doi:10,1016 / j.urology.2013.03.024

[4] Babić, N., Huskić, J., & Nakać-Išindić, E. (2007) Angiotensin Converting Enzyme Activity in Compensatory Renal Hypertrophy. *Bosn. J. Basic Med. Sci.,* 7(1), 79-83. doi: 10.17305 / bjbms.2007.3098

[6] Celebi, Z. K., Peker, A., Kutlay, S., Kocak, S., Tuzuner, A., Erturk, S., Keven, K. & Sengul, S. (2017) Effect of unilateral nephrectomy on urinary angiotensinogen levels in living kidney donors: 1 year follow-up study. *Journal of the Renin-Angiotensin Aldosterone System,* 18(4), 1-6. Doi: 10.1177/ 1470320317734082

[7] Delgadillo, D., Barbier, O., Sierra, G., & Reyes, J. L. (2014). Retinoic acid improves recovery after nephrectomy and decreases renal TGFbeta1 expression. Gender-related effects. *Fundam Clin Pharmacol.,* 28, 170-179. doi.org/ 10.1111/fcp.12013

[8] Domínguez-Calderóna, A., Ávila-Floresb, A., Poncea, A., López-Bayghenc, E., Calderón-Salinasd, J. V., Reyesa, J. L. … González-Mariscala, L. (2016). ZO-2 silencing induces renal hypertrophy through a cell cycle mechanism and the activation of YAP and the mTOR pathway. *Mol. Biol. Sel.,* 27(10), 1581-1595. doi: 10.1091/mbc.E15-08-0598

[9] Dvorak, V. S., Boiko, A. I., Shcherbak, O. Iu., & Sosnin, M. D. (2010). The only kidney: the problem of relapse or disease of nephrolithiasis. *Urology,* 14(addition), 248-250.

[10] Eladl, M. A., Elsaed, W. M., Atef, H., & El-Sherbiny, M. (2017). Ultrastructural changes and nestin expression accompanying compensatory renal growth after unilateral nephrectomy in adult rats. *Int. J. Nephrol. Renovasc. Dis.,* 10, 61-76. doi: 10.2147/IJNRD.S121473

[11] Ivanov, A. P., & Fateev, D. M. (2011). Effect of nephrectomy and kidney resection on catecholamine metabolism in rats. *Yaroslavl Pedagogical Bulletin.* (Natural Sciences), 3(1), 104-108.

[12] Ivanov, A. P., & Tyuzikov, I. A. (2011). The effect of experimental operational stress (nephrectomy and kidney resection) on mediator-hormonal homeostasis in rats. *Modern problems of science and education*, 3. Doi: http://www.science-education.ru/ru/article/view?id=4657

[13] Jeon, H. G., Gong, I. H., Hwang, J. H., Choi, D. K., Lee, S. R., & Park, D. S. (2012). Prognostic significance of preoperative kidney volume for predicting renal function in renal cell carcinoma patients receiving a radical or partial nephrectomy. *BJU Int.,* 109(10), 1468-1473. doi: 10,1111/j.1464-

410X.2011.10531.x
[14] Kundin, V. Iu. (2014). Complex radionuclide evaluation of structural and functional state of the single kidney in children. *Ukrainian Journal of Nephrology and Dialysis,* 42(2), 19-24.
[15] Lankadeva, Y. R., Singh, R. R., Tare, M., Moritz, K. M., & Denton, K. M. (2014). Loss of a kidney during fetal life: long term consequences and lessons learnt. Am. J. Physiol. Renal Physiol., 306, F791-F800. doi.org/10.1152/ajprenal.00666.2013
[16] Makieieva, N. I., & Pidvalna, N. A. (2015). Ultrasonic characteristics of structural and tissue changes of solitary kidney in children. *Pediatrics,* 2, 40-42.
[17] Muzaale, A. D., Massie, A. B., Wang, M. C., Montgomery, R. A., McBride, M. A., Wainright, J. L., & Segev, D. L. (2014). Risk of End-Stage Renal Disease Following Live Kidney Donation. *JAMA,* 311(6), 579-586. doi:10,1001/jama.2013.285141
[18] Oliveria, C. S., Joshee, L., Zalups, R. K., & Bridges Ch.C. (2016). Compensatory Renal Hypertrophy and the Handling of an Acute Nephrotoxicant in a Model of Aging. *Exp. Gerontol.,* 75, 16-23. doi: 10.1016/j.exger.2016.01.001
[19] Pivtorak, V. I., & Monastyrskyi, V. M. (2015). Electron Microscopic Changes Only Kidney, Remaining after the Contralateral Nephrectomy, in Immature Rats. *Bulletin of problems in Biology and Medicine*, 2(121), 250-254.
[20] Pivtorak, V. I., & Monastyrskyi, V. M. (2015). Features of Structural Components of the Nephron of Renal Cortex of the Solitary Kidney in Immature Rats. *Galician Medicinal Herald,* 22(3), 43-46.
[21] Pivtorak, V. I., & Monastyrskyi, V. M. (2016). Changes cell cycle kidney cells cortex contralateral after nephrectomy in immature rats. *Bulletin of problems in Biology and Medicine,* 2(129), 253-257.
[22] Pugachev, A. G., Chernetsova, G. S., Usupbaev, A. Ch., & Moskalev, I. N. (2005). *The results of the treatment of obstructive uropathy (in children, adults operated on in children, and in adult patients.* Bishkek, 225.
[23] Saxena, A. B., Myers, B. D., Derby, G., Blouch, K. L., Yan, J., Ho, B., & Tan, J. C. (2006). Adaptive hyperfiltration in the aging kidney after contralateral nephrectomy. *Am. J. Physiol. Renal Physiol.,* 291(3), 629-634. doi:10,1152/ajprenal.00329.2005
[24] Schreuder, M. F. (2018). Life with one kidney. Pediatr Nephrol. 33(4), 595-604. doi: 10.1007/s00467-017-3686-4
[25] Shapiro, J. I., & Dial, L. D. (2012). How Safe Is Unilateral Nephrectomy? *Hypertension,* 60(6), 1383-1384. doi:[10.1161/HYPERTENSIONAHA.112.200550]
[26] Stus, V. P., & Barannik K. S. (2016). Functional state and compensatory adaptive powers of the paired organ - the kidneys under conditions of one-sided defeat or a single kidney remaining after nephrectomy. *Urology,* 20(1), 5-16.
[27] Westland, R., Kurvers, R. A. J., van Wijk, J. A. E., &Schreuder, M. F. (2013). Risk Factors for Renal Injury in Children with a Solitary Functioning Kidney. *Pediatrics,* 131(2): e478-e485. doi: 10,1542/peds.2012-2088
[28] Westland, R., Schreuder, M. F., Bökenkamp, A., Spreeuwenberg, M. D., & van Wijk, J. A. E. (2011). Renal injury in children with a solitary functioning kidney - the KIMONO study. *Nephrol. Dial. Transplant.*, 26(5), 1533-1541. doi.org/10.1093/ndt/gfq844
[29] Williams, Cl. R., Wynne, B. M., Walker, M., Hoover, R. S., & Gooch, J. L. (2014). Compensatory renal hypertrophy following uninephrectomy is calcineurin-independent. *J. Cell Mol. Med.,* 18(12), 2361-2366. doi: 10.1111/jcmm.12438
[30] Xu, J., Chen, J., Dong, Z., Meyuhas, O., & Chen, J.-K. (2015). Phosphorylation of ribosomal protein S6 mediates compensatory renal hypertrophy. *Kidney Int.,* 87(3), 543-556. doi: 10.1038/ki.2014.302

ОРГАНОМЕТРИЧНІ ПАРАМЕТРИ НИРКИ, ЩО ЗАЛИШИЛАСЯ ПІСЛЯ ВИДАЛЕННЯ КОНТРАЛАТЕРАЛЬНОЇ, У СТАТЕВОНЕЗРІЛИХ ЩУРІВ

Монастирський В.М.

Процеси компенсаторної гіпертрофії нирки до періоду статевої зрілості вивчені недостатньо. Зміни параметрів нирки після видалення контралатеральної представляють науковий інтерес. Мета дослідження - встановити зміни органометричних показників нирки, що залишилась після нефректомії, у статевонезрілих щурів-самців. Експериментальне дослідження виконано на 84 статевонезрілих білих щурах-самцях масою 53-71 грамів, котрих утримували на стандартному раціоні віварію. Всіх тварин розподілили на дві групи (по 42 у кожній): перша - контрольна, друга - дослідна група. У контрольній групі під кетаміновим знеболенням розкривали черевну порожнину, після чого пошарово ушивали черевну стінку. Усім тваринам дослідної групи виконували видалення лівої нирки. Тварин виводили з досліду шляхом внутрішньоплеврального введення Тіопенталу натрію 50 мг/кг через 7, 14, 21, 30, 90 діб після нефректомії. Макроскопічну оцінку та описання нирок тварин проводили після їх вилучення. Статистичний аналіз отриманих результатів проведений із застосуванням програми "STATISTICA 5.5" з використанням параметричних і непараметричних методів оцінки отриманих результатів. Встановлено, що у статевонезрілих щурів маса тварин дослідної групи (після нефректомії), порівняно з контрольною групою, була статистично значуще меншою, а маса нирки тварин дослідної групи, навпаки, була статистично значуще більшою на всіх термінах спостереження. Визначені довжина, ширина, товщина, об'єм нирки тварин дослідної групи, а також величини приросту цих параметрів у кожний термін експерименту. Таким чином, максимальну величину приросту органометричних показників нирки спостерігали через 30 діб післяопераційного періоду ($p<0,05$). У подальшому, на 60 та 90 добу експерименту, величина приросту органометричних показників нирки суттєво зменшувалася. Визначено індекс гіпертрофії нирки, що залишилася після нефректомії, котрий коливався від 52,24% до 63,21%. Найбільші показники гіпертрофії встановлені між 21 та 30 добою.

Ключові слова: *нирка, нефректомія, органометрія, статевонезрілі щури.*

ОРГАНОМЕТРИЧЕСКИЕ ПАРАМЕТРЫ ПОЧКИ, ОСТАВШЕЙСЯ ПОСЛЕ УДАЛЕНИЯ КОНТРАЛАТЕРАЛЬНОЙ, У НЕПОЛОВОЗРЕЛЫХ КРЫС

Монастырский В.Н.

Процессы компенсаторной гипертрофии почки до периода половой зрелости изучены недостаточно. Изменения параметров почки после удаления контралатеральной представляют научный интерес. Цель исследования - установить изменения органометрических показателей почки, оставшейся после нефрэктомии, у неполовозрелых крыс-самцов. Экспериментальное исследование выполнено на 84 неполовозрелых белых крысах-самцах массой 53-71 граммов, которых

содержали на стандартном рационе вивария. Всех животных разделили на две группы (по 42 в каждой): первая - контрольная, вторая - опытная группа. В контрольной группе под кетаминовым обезболиванием вскрывали брюшную полость, после чего брюшную стенку послойно ушивали. Всем животным опытной группы выполняли удаление левой почки. Животных выводили из опыта путем внутриплеврального введения Тиопентала натрия 50 мг/кг через 7, 14, 21, 30, 90 суток после нефрэктомии. Макроскопическую оценку и описание почек животных проводили после их удаления. Статистический анализ полученных результатов проведен с применением программы "STATISTICA 5.5" с использованием параметрических и непараметрических методов оценки полученных результатов. Установлено, что у неполовозрелых крыс масса животных опытной группы (после нефрэктомии) по сравнению с контрольной группой, была статистически значимо меньше, а масса почки животных опытной группы, наоборот, была статистически значимо больше на всех сроках наблюдения. Определены длина, ширина, толщина, объем почки животных опытной группы, а также величины прироста этих параметров в каждый срок эксперимента. Таким образом, максимальную величину прироста органометрических показателей почки наблюдали через 30 суток послеоперационного периода ($p<0,05$). В дальнейшем, на 60 и 90 сутки эксперимента величина прироста органометрических показателей почки существенно уменьшалась. Определен индекс гипертрофии почки, оставшейся после нефрэктомии контралатеральной, который колебался от 52,24% до 63,21%. Наибольшие показатели гипертрофии установлены между 21 и 30 сутками.

Ключевые слова: *почка, нефрэктомия, органометрия, неполовозрелые крысы.*

DOI: 10.31393/morphology-journal-2018-24(4)-06 Reports of Morphology, Vol. 24, №4, Pages 41-46

ISSN 1818-1295 eISSN 2616-6194

REPORTS OF MORPHOLOGY

Official Journal of the Scientific Society of Anatomists, Histologists, Embryologists and Topographic Anatomists of Ukraine

journal homepage: https://morphology-journal.com

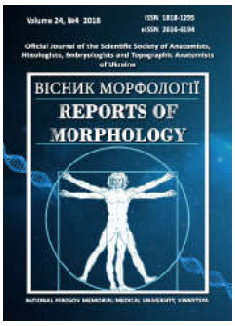

General phenotypological picture of the finger dermatoglyphics of Ukrainian men: the contribution of individual regions

Gunas V.I.[1], Mishalov V.D.[2], Serebrennikova O.A.[1], Klimas L.A.[1]

[1]National Pirogov Memorial Medical University, Vinnytsya, Ukraine
[2]National Medical Academy of Postgraduate Education named after P.L. Shupyk, Kyiv, Ukraine

ARTICLE INFO

Received: 2 October, 2018
Accepted: 1 November, 2018

UDC: 340.6:572.524.12:616.-055.1(477)

CORRESPONDING AUTHOR

e-mail: freekozak1@gmail.com
Gunas V.I.

The formation of regional gene pools and the contribution of each of them to the formation of the population of Ukraine remains an actual topic of the present. The purpose of the study is to assess the contribution of each of the 5 territorial-administrative regions of Ukraine to the overall phenotypological picture of the finger dermatoglyphics of the male population of Ukraine. By the method of H. Cummins and Ch. Midlo conducted a dermatological study of 400 practically healthy men from 5 administrative-territorial regions of Ukraine. Statistical processing of the obtained results was carried out in the package "Statistica 6.1" using nonparametric methods. It was established that among practically healthy men of Ukraine without administrative-territorial distribution and representatives of various administrative-territorial regions 37.96% of reliable or tendencies of differences of information indicators of finger dermatoglyphics were revealed out of 108 analyzed parameters. The best information ability of quantitative (47.83%) indicators of finger dermatoglyphics was proved in comparison with qualitative (35.29%) indicators. The greatest number of differences in the signs of finger dermatoglyphics is established between men without division into administrative-territorial regions and men, residents of the southern (11.11%), eastern (10.19%) and western (8.33%) regions of Ukraine. Less number of differences from the overall picture of the country are found in men in the northern region, its rates significantly differed almost at the level of error and amounted to 5.56%. Indicators of finger dermatoglyphics of men in the central region in general do not differ significantly from those in general in Ukraine. Thus, the dominant component in the general phenotypological picture of finger dermatoglyphics of the male population of Ukraine has a central region whose rates were not significantly different from the country's total, and to a lesser extent, the dermatoglyphics of the northern region. The obtained results indicate that the main genetic landscape of the gene pool of Ukraine, according to finger dermatoglyphics, forms the central and northern regions of the country.

Keywords: *finger dermatoglyphics, males, administrative-territorial regions of Ukraine, contribution of separate regions.*

Introduction

Since its inception as a separate section of morphology, dermatoglyphics is of considerable interest to scientists from various fields of science. It found her application not only in forensics but also in practical medicine, allowing to detect or predict the risk of certain diseases [7].

Today, one of the promising areas of dermatoglyphics is its possible application for the purpose of identifying a person's regional and ethnic belongings. Particularly relevant this method of investigation may be to determine the place of origin of illegal migrants, identify victims of armed conflicts, and so on.

It is worth noted that the special interest for practical application will be full bases, which will include a database of the characteristics of dermatological indicators of the population of all ethnic groups and regions of the country. Therefore, scientists around the world are actively conducting research of this type, with the ultimate goal - the formation of a complete database [1, 3, 12, 13, 15, 19, 20, 23].

Thus, Abue A.D., Rose C. and Courage N. in their work in 2018 revealed the features of dermatological attributes in the tribe of Ntamante, living in southern Nigeria. 200 people aged from 18 to 68 were involved, which in the third

generation are representatives of this ethnic group. The statistical analysis revealed the following distribution of the frequency of patterns among men: ulnar loops 12.6±9.2, arches 4.7±2.8, whorls 3.3±3.0 and radial loops 0.1±0.4; in women - ulnar loops 9.1±9.7, whorls 6.4±4.4, arcs 4.9±3.8 and radial loops 1.0±1.6 [2].

S. Biswas [5] studied palmar and finger dermatoglyphic indices among the ethnic group of Dhimals living in northern Bengal (India). The patterns of patterns were: whorls 55.1%, 50.2%, loops 42.16%, 48.24% and arches 2.75%, 1.57% for men and women, respectively. The density of patterns was 15.24 for men and 14.86 for women. Total ridges count was 162.18±3.38.

The features of dermatoglyphic indices and their manifestations of sexual dimorphism among the population of Sardinia [8] were determined. The higher values of ridge count b-c, c-d on the right hand and a-b, a-d indicators on the left hand were revealed. Men showed higher rates of a-b, c-d on their right hand than in women.

Studies conducted in 2011 by Jaja B.N.R., Olabiyi O. and Noronha C.C. [11] found that the rates of whorl detection, the total ridge count, and the palmar ridge count A-B indicate a close affinity of the Nigerian tribe Ogoni to the tribes of southern Ghana, indicating possible historical migration of this ethnic group.

Features of the indexes of finger and palm prints were found for the Muzeina Bedouin living in the south of the Sinai Peninsula [14]. The highest index of whorl frequency on the fourth finger, ulnar loop on the third finger of both hands for both sexes was revealed.

However, in Ukraine, these studies are few, have a regional character and do not allow creating one, integral image of the dermatoglyphic population [16, 17].

The study of the gene pool of the population of Ukraine is important not only for the country itself, but, as Otevska O.M. [25] notes, due to his position, for the study of the European gene pool too.

The general structure of the gene pool of Ukraine historically consisted of the genetic features of the population in different parts of the ethnic range, caused by different conditions of the intensity of international contacts and migration processes, the level of urbanization and the nature of the natural reproduction of the population, the share of the presence of impurities of other nationalities. In population-genetic studies, various markers are used: physiological, immuno-biochemical, DNA markers, quasi-genetic (distribution of surnames) [10, 21, 24]. Among them, a simple and powerful analytical tool - a method of dermatoglyphics - takes a special place, which allows determining the contribution to the formation of the ethnic community of the indigenous and inborn population that was involved in marital ties with the indigenous population. It should be noted that the fragmentation of the literary data [22] does not allow to make a complete picture of the gene pool of Ukrainians in general and the contribution of each of the five territorial administrative regions of Ukraine to the general phenotypological picture of the finger dermatoglyphics of the male population of Ukraine, which became the *goal* of our work.

Materials and methods

Researched fingerprints of 400 practically healthy men aged from 19 to 35 years in the third generation residents of the relevant regions of Ukraine: 72 - from the north (Zhytomyr, Kyiv, Chernihiv, Sumy regions), 47 - from the south (Odessa, Mykolaiv, Kherson, Zaporizhzhya region and AR Crimea), 165 - from the central (Vinnytsia, Cherkasy, Kirovohrad, Poltava and Dnipropetrovsk regions), 71 - from the west (Volyn, Rivne, Lviv, Chernivtsi, Ternopil, Khmelnytsky, Transcarpathian and Ivano-Frankivsk regions), 45 residents from the eastern (Kharkiv, Lugansk, Donetsk regions) regions. The dermatological study was performed according to H. Cummins and Ch. Midlo [6].

Fingerprints obtained by using ink on a sheet of paper [9]. Analysis subject 108 indicators of digital dermatoglyphics, of which 85 related to quality indicators and 23 indicators related to quantitative traits. Bioethics Committee of National Pirogov Memorial Medical University, Vinnytsya found that the studies are not contrary to the fundamental bioethical standards of the Helsinki Declaration, the European Convention on Human Rights and Biomedicine (1977), the relevant provisions of the WHO and the laws of Ukraine (protocol number 8 from 10.09.2013).

Statistical processing of the obtained results was carried out in the package "Statistica 6.1" using nonparametric methods.

Results

Among the practically healthy men of the general group and representatives of the northern region of Ukraine, the following reliable or trends of the differences in the indicators of finger dermatoglyphics are established:

among the qualitative indicators, in men of the northern region, the percentage of central pockets on the I (36.1% versus 24.3%, $p<0.05$), III (19.4% vs. 10.5%, $p<0.05$) and IV (45.8% against 33.8%, $p=0.051$) fingers of the right hand and IV of the fingers of the left hand (33.3% vs. 21.0%, $p<0.05$) is higher than in total group, as well as a higher percentage of double loop on the IV finger of the left hand (26.4% vs. 16.3%, $p<0.05$);

among quantitative indicators - reliable or trends of differences are not established;

among asymmetries of qualitative and quantitative indices - in men of the northern region less than in the general group, the absolute value of the asymmetry of the ridge count of the III finger (0.278±4.514 versus 0.970±0.245 ridges, $p<0.05$), asymmetry, in contrast, right-handed.

Among the practically healthy men of the general group and representatives of the southern region of Ukraine, the following reliable or trends of the differences in the indicators of finger dermatoglyphics are established:

among the qualitative indicators - in men of the southern region, the percentage of the presence of whorl on the right IV finger (17.0% versus 8.3%, p=0.052) of the hand, and the arches on the III fingers as the right ones (31.9% vs. 18.8%, p<0.05) and left (25.5% vs. 14.8%, p=0.059) hands, as well as a lower percentage of ulnar loop on the II right finger (10.6% versus 26.3%, p<0.05), double loop on the I (4.3% against the 16.3%, p<0.05), central pocket on the II (6.4% vs. 19.5%, p<0.05) and random pattern on III (0% vs. 6.5%, p=0.072) fingers of the left hand higher than in total group;

among the quantitative indicators - in men of the southern region less than in the general group, the value of the ridge count of the III finger as the right (9.128±7.058 versus 11.37±6.62 ridges, p<0.05) and the left (10.36±6.82 versus 12.37±6.55 ridges, p<0.05), as well as ridge count of I finger (14.55±7.55 versus 16.61±7.53 ridges, p=0.078), total ridge count (60.09±23.97 versus 67.90±25.67 ridges, p<0.05) of left hand and total ridge count (122.6±46.4 versus 136.6±49.4 ridges, p=0.064);

among asymmetries of qualitative and quantitative indicators - reliable or trends of differences are not established.

Among the practically healthy men of the general group and representatives of the central region of Ukraine, the following reliable or trends of the differences in the indicators of finger dermatoglyphics are established:

among the qualitative indicators, the men in the central region had smaller than the general group, percentage of the presence of whorl on the IV fingers (4.2% vs. 8.3%, p=0.085) of the right hand and arches on the II left fingers (18.2% vs. 25.5%, p=0.063);

among quantitative indicators - reliable or trends of differences are not established;

among the asymmetries of qualitative and quantitative indicators - in men of the central region less than in the general group, the value of asymmetry by the type of pattern on the I finger (46.7% vs. 54.8%, p=0.080).

Among the practically healthy men of the general group and representatives of the western region of Ukraine, the following reliable or trends of the differences in the index of finger dermatoglyphics are established:

among the qualitative indicators, men in the western region had a greater percentage of the presence of ulnar loops on the I fingers (56.3% vs. 42.5%, p<0.05) and the arches on the V fingers (19.7% vs. 11.3%, p<0.05) of the right hand, as well as a higher percentage of the random pattern on the III finger (12.7% vs. 6.5%, p=0.067) and the double loop on the V finger (7.0% vs. 2.0%, p<0.05) of the left hand;

among the quantitative indicators - in men of the western region less than in the general group, the value of the ridge count of the IV right finger (13.35±6.87 versus 15.17±6.39 ridges, p<0.05) and the left (13.90±5.83 versus 15.27±6.03 ridges, p=0.078) hands, as well as V finger (10.94±6.94 versus 12.83±6.02 ridges, p<0.05) of the right hand;

among the asymmetry of qualitative and quantitative indicators - in men of the western region higher than in the general group, the value of the asymmetry of the ridge count of the II finger (1.493±5.712 versus 0.168±5.841 ridges, p=0.078) and less of the asymmetry value according to the type of the fingerprint pattern of V finger (54.9% against 66.0%, p=0.073).

Among the practically healthy men of the general group and representatives of the eastern region of Ukraine, the following reliable or trends of the differences in the indicators of finger dermatoglyphics are established:

among the qualitative indicators, the men of the eastern region had a higher percentage of arc on the right I finger (13.3% versus 6.0%, p=0.065) and the ulnar loop (82.2% versus 61.8%, p<0.01) and random the pattern on the III finger (0% vs. 6.5%, p=0.079), the radial loop on the IV finger (2.2% versus 0.3%, p=0.085), ulnar (84.4% versus 72.0%, p=0.076), and the radial (2.2% against the 0.3%, p=0.085) loops on the left V finger, as well as a lower percentage of the double loop on the right I finger (6.7% vs. 16.8%, p=0.079) and the central pocket of the right V finger (0% vs. 9.8 %, p<0.05) and on a I finger (4.4% vs. 13.8%, p=0.075), on the IV finger (8.9% vs. 21.0%, p=0.054) of the left hand then in the total group;

among the quantitative indicators - the men of the eastern region had less than in the general group, the value of the ridge count on the right I finger (15.78±7.35 versus 18.63±7.19 ridges, p<0.05);

among asymmetries of qualitative and quantitative indicators - reliable or trends of differences are not established.

Thus, the analysis of the differences in the indicators of finger dermatoglyphics between practically healthy men of Ukraine without administrative-territorial distribution and representatives of various administrative-territorial regions revealed that:

- the finger dermatoglyphics of the northern administrative-territorial region significantly differs from that in the country as a whole in terms of 4 indicators of qualitative characteristics and 1 indicator of asymmetry of the quantitative trait, and also shows a tendency for differences in 1 indicator of qualitative trait;

- the finger dermatoglyphics of the southern administrative-territorial region significantly differs from the country as a whole in terms of 4 indicators of qualitative and 3 indicators of quantitative characteristics, and also shows a tendency for differences in 3 indicators of qualitative and 2 indicators of quantitative attributes;

- the finger dermatoglyphics of the central administrative-territorial region is not significantly different from that of the country as a whole, and also shows a tendency for differences in 2 indicators of qualitative characteristics and 1 indicator of asymmetry of a qualitative characteristic;

- finger dermatoglyphics of western administrative-territorial region significantly different from that in the whole country by three indicators of quality and 2 indices of quantitative traits, and shows a tendency difference by 1

indicator of quality, 1 indicator of quantitative trait, 1 indicator of the asymmetry of quality features and 1 indicator of the asymmetry quantity signs;

- finger dermatoglyphics of eastern administrative-territorial region significantly different from that in the whole country by 2 qualitative parameters and 1 indicator of quantitative characteristics and shows trend differences by 8 indicators of qualitative traits.

Discussion

An analysis of the differences between the indicators of finger dermatoglyphics among practically healthy men of Ukraine without administrative-territorial distribution and representatives of various administrative-territorial regions revealed 41 (37.96%), and without trends - 20 (18.52%) of the informative indicators out of 108 analyzed and demonstrated the best informative ability of quantitative ((11 (47.83%)), and without trends (7 (30.43%)), indexes of finger dermatoglyphics compare to qualitative ((30 (35.29%) and without trends - (13 (15.29%)) indicators.

The greatest number of differences in the signs of finger dermatoglyphics in terms of qualitative and quantitative indicators were established between men, inhabitants of Ukraine without division into administrative-territorial regions and men, residents of the southern ((12 (11.11%) indicators, 7 (6.48%) of which are reliable)), eastern ((11 (10.19%) indicators, 3 (2.78%) of which are reliable)) and western ((9 (8.33%) indicators, 5 (4.63%) of which are reliable)) regions of the country. Among the regions that show differences from the general picture of the country, the northern region is least diverse, its rates significantly differed almost at the level of error and amounted to 5.56%. At the same time, the indicators of finger dermatoglyphics of men in the central region do not significantly differ from such indicators in Ukraine (Fig. 1).

Thus, the core of the general phenotypological picture of the finger dermatoglyphics of the male population of Ukraine makes the central region. The expressed peculiarity of finger dermatoglyphics of Ukrainian men in the central region is confirmed by their differences from the southern, eastern and western regions, which is covered in our previous study [18]. The localization of the nucleus of peculiar values within the range of the ethnic group, and not at its borders, indicates that not the migration processes, but the peculiarities of their own self-development, form the basic genetic landscape of its gene pool [4]. The results obtained by us are confirmed by the data of the study of the distribution of Ukrainian surnames taking into account the administrative and geographical zoning of the territory of Ukraine according to the index of random isonomy (the frequency of marriages between individuals having the same surname) and calculated on its basis the indicator of random inbreeding

Fig. 1. Regional contribution of finger dermatoglyphics to the general phenotypological picture of dermatoglyphics of men in Ukraine.

(marriages between relatives) [10]. The authors proceeded from the fact that surnames are the most attractive among quasi-genetic markers, since in their most important manifestations - transmission in generations, distribution in populations - they resemble genes. In the given work it is shown that the minimum value of the index of random homonymity is characteristic for the southern region (2.2 x 10-4), eastern (2.7 x 10-4) and western (2.4 x 10-4), higher values in the central (3.2 x 10-4) and northern (3.4 x 10-4) regions. Similar data were obtained from the index of inbreeding: its highest value was observed in the northern (8.5 x 10-5) and central (7.9 x 10-5) regions, the lowest in the southern (5.6 x 10-5), the eastern (6.7 x 10-5) and the western (6.1 x 10-5) occupy an intermediate position.

Thus, the indicators of the genetic contribution of certain administrative-territorial regions in the overall picture of the country's finger dermatoglyphic are indirectly indicative of a significant coincidence with inbreeding indicators calculated on the basis of the names of the surnames, and therefore further research may be aimed at identifying correlations between them.

Conclusions

1. The dermatoglyphic populational typological picture of somatically healthy men of Ukraine is formed mainly due to the genetic contribution of people in the central region, since their indices do not significantly differ from such indicators in general in Ukraine.

2. Indicators of finger dermatoglyphics of men, residents of southern, eastern and western administrative-territorial regions differ from the indicators in general in Ukraine, the differences in the order of decrease make up 11.11%, 10.19%, 8.33% of indicators, respectively. The northern region is the least diverse, and the difference between its indicators and such in country in total is only 5.56%.

References

[1] Abue, A. D., Christopher, R., & Sunday, A. (2018). The Qualitative Dermatoglyphics Patterns in Both Hands for Males and Females in Ubang Clan Cross River State Nigeria. *Advances in Anthropology,* 8, 73-81. https://doi.org/10.4236/aa.2018.82004

[2] Abue, A. D., Rose, C., & Courage, N. (2018). Analyses of Dermatoglyphic Patterns in Ntamante, Boki Local Government Area (LGA) of Cross River State, Nigeria. *Advances in Anthropology,* 8(3), 83-90. doi: 10.4236/aa.2018.83005

[3] Abue, A. D., Ujaddughe, M., & Kpela, M. T. (2013). The arch pattern dermatoglyphics on the toes of Hausa ethnic group of Nigeria. *Advances in Anthropology,* 3(4), 237-239. http://dx.doi.org/10.4236/aa.2013.34033

[4] Balanovskiy, O. P., & Tehako, O. V. (2008). The gene pool of Belarusians according to data on three types of genetic markers - autosomal, mitochondrial, Y chromosomes. *Current issues of anthropology,* 2, 53-65.

[5] Biswas, S. (2011). Finger and palmar dermatoglyphic study among the Dhimals of North Bengal, India. *The Anthropologist,* 13(3), 235-238. https://doi.org/10.1080/09720073.2011.11891202

[6] Cummins, H., & Midlo, Ch. (1961). *Finger Prints, Palms and Soles.* An Introduction to Dermatoglyphics. Philadelphia.

[7] Dmytrenko, S. V., Klimas, L. A., Kushnir, V. A., Serebrennikova O. A., & Serheta, I. (2018). Features of quantitative indicators of finger and palmar dermatoglyphics in males and females with ichthyosis. *Biomedical and Biosocial Anthropology,* (32), 48-55. https://doi.org/https://doi.org/10.31393/bba32-2018-07

[8] Floris, G. (2015). Palmar Intertriradial Ridge Counts in Sardinians. *Advances in Anthropology,* 5(3), 137-143. http://dx.doi.org/10.4236/aa.2015.53012

[9] Gladkova, T. D. (1966). *Skin patterns of the hand and foot of monkeys and humans.* M.: Science. https://www.twirpx.com/file/1246327/

[10] Gorpinchenko, M., & Atramentova, L. (2015). Population-genetic characteristics of the population of Ukraine, obtained with the use of surnames. *Bulletin of the Taras Shevchenko National University of Kyiv. Biology,* 69, 68-72. ISSN 1728-3817.

[11] Jaja, B. N. R., Olabiyi, O., & Noronha, C. C. (2011). Dermatoglyphics of the Ogoni of Nigeria and its historiographic implications. *Anthropologischer Anzeiger,* 68(2), 175-183. https://doi.org/10.1127/0003-5548/2011/0057

[12] Jami, J., & Limbu, D. K. (2015). Digital and Palmar Dermatoglyphics of the Bhoi Khasis of Umden Village, Ri-Bhoi District, Meghalaya. *Journal of Life Sciences,* 7(1-2), 12-14. https://doi.org/10.1080/09751270.2015.11885231

[13] Kapoor, N., & Badiye, A. (2015). Digital dermatoglyphics: A study on Muslim population from India. *Egyptian Journal of Forensic Sciences,* 5(3), 90-95. http://dx.doi.org/10.1016/j.ejfs.2014.08.001

[14] Karmakar, B., & Kobyliansky, E. (2011). Finger and palmar dermatoglyphics in Muzeina Bedouins from South Sinai: qualitative traits. *Papers on Anthropology,* 20, 146-159. https://doi.org/10.12697/poa.2011.20.16

[15] Koneru, A., Hallikeri, K., Nellithady, G. S., Rekha, K., Prabhu, S., & Niranjan, K. C. (2014). Assessment and comparison of fingerprints between Kerala and Manipuri populations of India: A forensic study. *Journal of Advanced Clinical and Research Insights,* 1(2), 42-45. doi: 10.15713/ins.jcri.12

[16] Kozan, N. M., & Kotsyubynska, Y. Z. (2015). Sexual Dimorphism of Digital Dermatoglyphic Parameters among Population of Boyko Ethnic Group. *Galician Medical Journal,* 22(3), 161-163.

[17] Kozan, N. N. (2017). Forensic medical identification of an ethno-territorial affiliation of an unknown person with dermatoglyphic parameters of palms with discriminant analysis. *Reports of Vinnytsia National Medical University,* 21(1 (2)), 252-255.

[18] Mishalov, V. D., Serebrennikova, O. A., Klimas, L. A., & Gunas, V. I. (2018). Regional trends indicators finger dermatoglyphics among modern Ukrainians. *Biomedical and biosocial anthropology,* 30, 5-12. doi: 10.31393/bba30-2018-01

[19] Namouchi, I. (2011). Anthropological significance of dermatoglyphic trait variation: an intra-Tunisian population analysis. *International Journal of Modern Anthropology,* 1(4), 12-27. doi: 10.4314/ijma.v1i4.1

[20] Paul, C. W., & Paul, J. N. (2017). Gender Variation Studies at Level 2 Dermatoglyphic Details of the Kalabari Ethnic Group in Rivers State, Nigeria. *Sch. J. App. Med. Sci.,* 5(11A), 4297-4301. doi: 10.21276/sjams.2017.5.11.3.

[21] Pshenichnikov, A. S. (2007). *The structure of the gene pool of Ukrainians according to the data on polymorphism of mitochondrial DNA and Y chromosome* (PhD thesis). http://earthpapers.net/

[22] Segeda, S. P. (2001). *Anthropological composition of the Ukrainian people: ethnogenetic aspect.* Publishing house named after Olena Teliha.

[23] Sen, J., Kanchan, T., & Mondal, N. (2011). A comparison of palmar dermatoglyphics in two ethnic Indian populations of north Bengal, India. *Journal of forensic sciences,* 56(1), 109-117. https://doi.org/10.1111/j.1556-4029.2010.01554.x

[24] Sorokina, I. N. (2005). *The study of population-demographic structure of the population of the Belgorod region* (PhD thesis). http://www.dslib.net/

[25] Utaevska, O. M. (2017). *Genetic fund of Ukrainians under various systems of genetic markers: origin and place on the European genetic space* (Doctoral dissertation). http://nrcrm.gov.ua/

ЗАГАЛЬНА ФЕНОТИПОЛОГІЧНА КАРТИНА ПАЛЬЦЕВОЇ ДЕРМАТОГЛІФІКИ ЧОЛОВІКІВ УКРАЇНИ: ВНЕСОК ОКРЕМИХ РЕГІОНІВ

Гунас В.І., Мішалов В.Д., Серебреннікова О.А., Клімас Л.А.

Становлення регіональних генофондів і внесок кожного з них у формування народонаселення України залишається актуальною темою сьогодення. Мета дослідження - оцінити внесок кожного з 5 територіально-адміністративних регіонів України до загальної фенотипологічної картини пальцевої дерматогліфіки чоловічого населення України. За методикою H. Cummins і Ch. Midlo проведено дерматогліфічне дослідження 400 практично здорових чоловіків із 5 адміністративно-територіальних регіонів України. Статистична обробка отриманих результатів проведена в пакеті "Statistica 6.1" з використанням непараметричних методів. Встановлено, що між практично здоровими чоловіками України без адміністративно-територіального розподілу та представниками різних адміністративно-територіальних регіонів виявлено 37,96 % достовірних, або тенденцій відмінностей інформаційно здатних показників пальцевої дерматогліфіки зі 108 проаналізованих показників. Доведено кращу інформаційну здатність кількісних (47,83 %) показників пальцевої дерматогліфіки порівняно з якісними (35,29 %) показниками. Найбільшу кількість відмінностей ознак пальцевої дерматогліфіки встановлено між чоловіками без поділу на адміністративно-територіальні регіони і чоловіками, мешканцями південного (11,11 %), східного (10,19 %) та західного (8,33 %) регіонів України. Меншу кількість відмінностей від загальної картини по країні встановлено у чоловіків північного регіону, його показники достовірно відрізнялись практично на рівні похибки і становили 5,56%. Показники пальцевої дерматогліфіки чоловіків центрального регіону взагалі достовірно не відрізняються від таких показників загалом

по Україні. Таким чином, домінуючою складовою в загальній фенотипологічній картині пальцевої дерматогліфіки чоловічого населення України є така центрального регіону, показники якого достовірно не відрізнялися від загальних по країні, а також, в дещо меншій мірі, - дерматогліфіка північного регіону. Отримані результати вказують на те, що основний генетичний ландшафт генофонду України, за даними пальцевої дерматогліфіки, формують центральний та північний регіони країни.
Ключові слова: *пальцева дерматогліфіка, чоловіки, адміністративно-територіальні регіони України, внесок окремих регіонів.*

ОБЩАЯ ФЕНОТИПОЛОГИЧЕСКАЯ КАРТИНА ПАЛЬЦЕВОЙ ДЕРМАТОГЛИФИКИ МУЖЧИН УКРАИНЫ: ВКЛАД ОТДЕЛЬНЫХ РЕГИОНОВ

Гунас В.И., Мишалов В.Д., Серебренникова О.А., Климас Л.А.

Становление региональных генофондов и вклад каждого из них в формирование народонаселения Украины остается актуальной темой сегодняшнего дня. Цель исследования - оценить вклад каждого из 5 территориально-административных регионов Украины в общую фенотипологическую картину пальцевой дерматоглифики мужского населения Украины. По методике H. Cummins и Ch. Midlo проведено дерматоглифическое исследования 400 практически здоровых мужчин из 5 административно-территориальных регионов Украины. Статистическая обработка полученных результатов проведена в пакете "Statistica 6.1" с использованием непараметрических методов. Установлено, что между практически здоровыми мужчинами Украины без административно-территориального деления и представителями различных административно-территориальных регионов обнаружено 37,96% достоверных или тенденций различий информационно способных показателей пальцевой дерматоглифики из 108 проанализированных показателей. Доказано лучшую информационную способность количественных (47,83%) показателей пальцевой дерматоглифики по сравнению с качественными (35,29%) показателям. Наибольшее количество различий признаков пальцевой дерматоглифики установлено между мужчинами без разделения на административно-территориальные регионы и мужчинами, жителями южного (11,11%), восточного (10,19%) и западного (8,33%) регионов Украины. Меньшее количество отличий от общей картины по стране установлено у мужчин северного региона, его показатели достоверно отличались практически на уровне погрешности и составили 5,56%. Показатели пальцевой дерматоглифики мужчин центрального региона вообще достоверно не отличаются от таких показателей в целом по Украине. Таким образом, доминирующей составляющей в общей фенотипологической картине пальцевой дерматоглифики мужского населения Украины есть такая центрального региона, показатели которого достоверно не отличались от общих по стране, а также, в несколько меньшей степени - дерматоглифика северного региона. Полученные результаты указывают на то, что основной генетический ландшафт генофонда Украины, по данным пальцевой дерматоглифики, формируют центральный и северный регионы страны.
Ключевые слова: *пальцевая дерматоглифика, мужчины, административно-территориальные регионы Украины, вклад отдельных регионов.*

DOI: 10.31393/morphology-journal-2018-24(4)-07 Reports of Morphology, Vol. 24, №4, Pages 47-52

ISSN 1818-1295 eISSN 2616-6194

REPORTS OF MORPHOLOGY

Official Journal of the Scientific Society of Anatomists, Histologists, Embryologists and Topographic Anatomists of Ukraine

journal homepage: https://morphology-journal.com

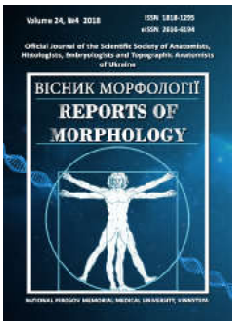

Comparative anatomy of the uterine tube of human and laboratory white rat females

Podolyuk M.V.
Danylo Halytskyy National Medical University of Lviv, Lviv, Ukraine

ARTICLE INFO
Received: 4 October, 2018
Accepted: 6 November, 2018

UDC: 611. 656 - 019

CORRESPONDING AUTHOR
e-mail: lvatseba@gmail.com
Podolyuk M.V.

The world literature has accumulated a considerable amount of data to characterize the main components of the female genital system, functional relationships between them, as well as the links between this system and other systems of the organism. The relevance of the study is also due to the fact that in the structure of female infertility 60-70% is occupied by a tubo-peritoneal factor. The problems associated with this pathology have been studied for more than half a century. Until now, information about the microanatomy of the fallopian tube of a human and, especially, of the female white laboratory rat is contradictory. The aim of the study was to conduct a comparative analysis of the structural organization of the uterine tube of a human and female laboratory white rat. The article and analyzes the data of research conducted on 10 sexually mature white rats in females of reproductive age. The method of preparation was used, for the study of macroanatomy of the uterine tube of females, and also standard histological methods (cuts of the wall of the fallopian tube in the thickness of 5-7 microns, stained with hematoxylin and eosin). The external structure of the fallopian tube of the female rat and man has some differences. Unlike humans, the fallopian tube of a white laboratory rat has the appearance of a thin and short tubule, spirally twisted into a compact lump. In the fallopian tube of the female white rat, it is advisable to distinguish 2 parts: the funnel and the fallopian part. The uterine part connects to the uterine horn cavity of the uterine opening of the fallopian tube, and the fallopian tube opens into the cavity of the peritoneum to the surface of the ovary by the abdominal opening of the fallopian tube. Around the funnel of the fallopian tube, its mucous membrane is gathered in folds - the fringe of the fallopian tube and the ovarian fringe (in humans - one ovarian fringe), which are attached to the ovary. The diameter of the fallopian tube of the female white rat decreases in the direction from the funnel to the uterine part. In particular, in the area of the funnel, the diameter of the fallopian tube is 0.90±0.10 mm, and the diameter of the fallopian part is 0.70±0.09 mm. The uterine tube of a laboratory white rat, like a human, has a mesentery of the fallopian tube. Both in human and in female white rat, the wall of the fallopian tube consists of three layers: the inner lining is mucous, the middle lining is muscular, the outer lining is serous. It was established that the female uterine tube of a white rat in its macroscopic structure differs from the uterine tube of a person. The microscopic structure of human and the white rat female uterine tube is rather similar and, therefore, may serve as an object of the experimental modeling of certain pathological conditions of the reproductive system.
Keywords: *reproductive system, uterine tube, white rat.*

Introduction

The female sexual system is an integral part of a complex biological system - the body as a whole [11, 21]. In world literature, a significant amount of data has been accumulated to characterize the main components of the female genital system, functional relationships between them, and the relationships between this system and other systems of the body [2]. The female reproductive system is a complex biological phenomenon, through which nature implements a program of preservation and extension of the genus. The fallopian tube is considered a sterile organ, in which the final maturation of the gametes, fertilization and early development of the embryo occurs [23].

One of the most urgent problems of gynecology is female infertility in the structure of which 60-70% occupies tube-peritoneal factor. Despite significant advances in reproductive medicine, the problems of diagnosis and treatment of tubal peritoneal infertility remain relevant. Acute and chronic inflammatory diseases of the fallopian tubes, operative interference on the pelvic organs, infection of the genital tract, autoimmune, and tumor processes have the leading place among the factors of the formation of the tube-peritoneal factor. In addition, there are reports in the literature that the secretory cells of the uterine mucosa are the source of ovarian carcinoma [13]. Pathological processes in the fallopian tube can be the cause of ectopic pregnancy. Problems associated with this pathology have been studied for more than half a century [18, 20, 24]. The evaluation of macro- and microanatomy of the fallopian tubes remains an important test in the examination of infertile couples, as well as in the definition of treatment approaches. Despite the many published scientific papers on the mechanisms of development of the tubal-peritoneal factor, numerous etiological factors and clinical aspects remain open. An analysis of the current trends in the study of the structure and function of the fallopian tube shows that the issue of a comprehensive approach to the morphofunctional justification for assessing the state of a given organ under conditions of physiological norm and pathology remains inadequately studied.

The *purpose* of our study was to conduct a comparative analysis of the structural organization of the uterine tube of a human and laboratory white rat.

Materials and methods

The study was performed on 10 sexually mature white rats of reproductive age (10 females) weighing 180-200 g. As a research material, wet macroscopic preparations of human uterine tube from the Fund of the Department of Normal Anatomy of the Danylo Halytskyy National Medical University of Lviv were also used. The method of preparation for the study of macroanatomy of the uterine tube of female white rats, as well as standard histological methods (sections of the wall of the fallopian tube in the thickness of 5-7 microns, stained with hematoxylin and eosin) were used to study the microanatomy of the wall of the uterine tube of a white rat and a human. Images from the histologic preparations of the uterine wall on the computer monitor were taken from a microscope MICROmed SEO SCAN and with a Vision CCD Camera.

All experimental animals were kept under the vivarium of the Danylo Halytskyy National Medical University of Lviv. The research was conducted in accordance with the provisions of the "European Convention for the Protection of Vertebrate Animals used for Experimental and Other Scientific Purposes" (Strasbourg, 1986), Council of Europe Directives 86/609/EEC (1986), Law of Ukraine No. 3447-IV "On the Protection of Animals from ill-treatment", the general ethical principles of experiments on animals adopted by the First National Congress of Ukraine on Bioethics (2001). Euthanasia of animals was performed by overdose of intraperitoneal anesthesia using sodium thiopental (at a rate of 25 mg/kg body weight of the animal).

Results

The fallopian tube of a laboratory white rat, like the human's fallopian tube, is a paired hollow organ. Located in the cavity of a small pelvis, almost horizontally, near the upper edge of a broad ligament of the uterus. The outer structure of the rats and humans fallopian tube has some differences. The female tube has a cylindrical shape, 4 parts: the interstitial (pars uterina), which passes through the wall of the uterus and opens into the uterus cavity as uterine tube (ostium uterinum tubae uterinae); isthmus of uterine tube (isthmus tubae uterinae), which is closest to the uterus; ampulla of uterine tube (ampulla tubae uterinae) - the largest part of the fallopian tubes; fimbria of fallopian tubes (infundibulum tubae uterinae) - an enlarged part that opens as the abdominal hole of the fallopian tube (ostium abdominale tubae uterinae) into the abdominal cavity and is surrounded by fimbriae (fimbria tubaria), one of which is the fimbria ovarica, longer than the other, while its diameter decreases from the fimbria (2-4 mm) to the uterine part (1 mm).

The fallopian tube of a laboratory white rat has the form of a thin and short tube, twisted spirally into a compact glomeruli (Fig. 1A, 1B). In our opinion, it is advisable to distinguish 3 parts in the uterine tube of rats: fimbria, middle (spiral) and uterine part. The uterine part is connected to the uterine horn cavity by the uterine hole of uterine tube (ostium uterinum tubae uterinae), and the fimbria (infundibulum tubae uterinae) is opened in the peritoneal cavity to the ovary surface by the abdominal hole of tube (ostium abdominale tubae uterinae).

Around the fimbria of the uterine tube, its mucosa is collected in folds - the fimbriae of the uterine tube and the ovary fimbriae (in humans, as already mentioned above, one ovary fimbriae), which are attached to the ovary. In this case, the diameter of the uterine tube of the white rat also decreases in the direction from the fimbria to the uterine part. In particular, in the area of the fimbria, the diameter of the uterine tube is 0.90±0.10 mm, and the diameter of the uterine part is 0.70±0.09 mm. The fallopian tube, in laboratory white rat, like in human, has mesosalpinx. As in human, uterus tube wall in rats consists of three layers: the inner - mucosa, the middle - subserosa, and the outer membrane - serosa (Fig. 2).

The mucosa of the fallopian tubes of white rat forms branched longitudinal and transverse folds that thicken towards the abdomen part of the fallopian tube. The mucosa is covered by a simple columnar epithelium consisting of ciliated cells and peg cells. The epithelium is located on a thin basal membrane, under which lies amina propria, formed by a loose connective tissue. The muscular plate of the mucous membrane and the submucosal base in

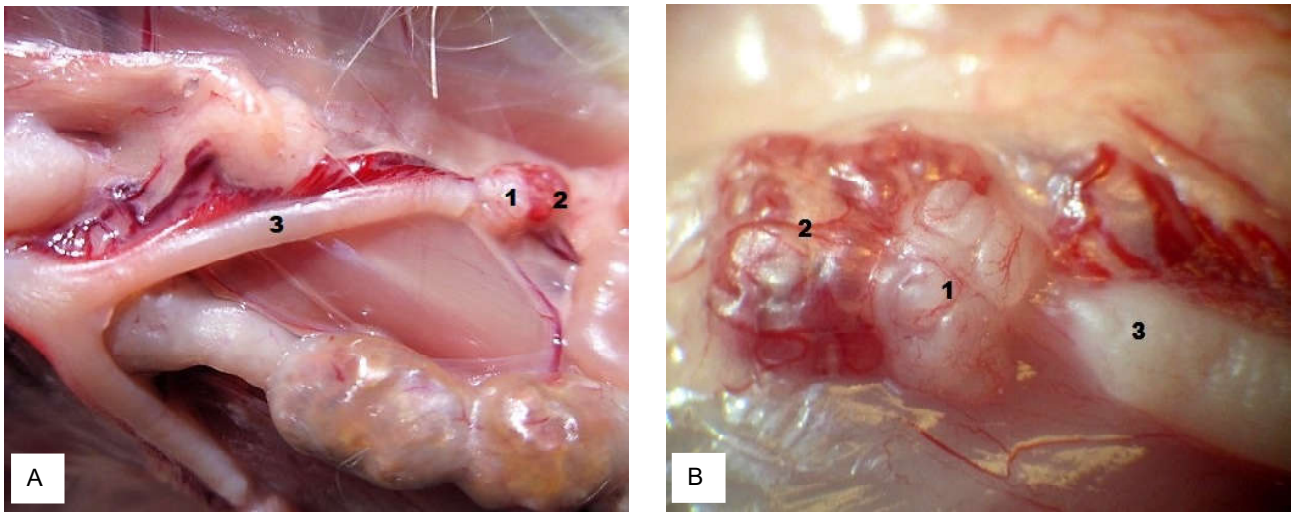

Fig. 1. A - Uterine tube of white rat in norm. Photomacrograph. 1 - uterine tube, 2 - ovary, 3 - uterine horn; B - Uterine tube of white rat in norm. Photomacrograph (binocular enlargement). 1 - uterine tube, 2 - ovary, 3 - uterine horn.

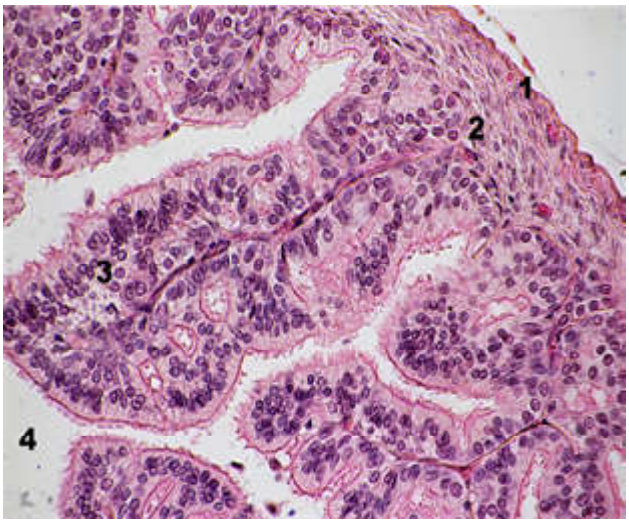

Fig. 2. Uterine tube wall of white rat in norm. Hematoxylin-eosin. Photomicrograph. x400. 1 - serosa, 2 - subserosa, 3 - mucosa, 4 - fallopian tube lumen.

the uterine tube are absent, so the connective tissue of the own plate directly passes into the muscle skeleton. It should be noted that the mucous membrane of the uterine tube along with the endometrium undergoes cyclic changes during the menstrual cycle, during pregnancy, and during puberty. In addition, the mucosa of the uterine tube does not contain glands, and this function is performed by the peg cells, functioning of which is regulated by the endocrine system. In laboratory white rats, subserosa consists of an internal circular and outer longitudinal layers, which passes into the myometrium of the uterine horn. Due to the peristaltic contraction of smooth myocytes and the movement of cilia, the egg cell moves along the fallopian tube towards the uterus. In humans, subserosa also consists of the inner circular and outer longitudinal layers. Externally, the uterine tube is covered with a serosa.

Discussion

The blood supply to the fallopian tubes is carried out from two sources: tubal branches of ovarian artery and tubal branch of uterine artery. Venous blood from the uterine tube flows out on the veins of the same name. Lymphatic vessels of the tube enter the lumbar lymph nodes. However, in literary sources, there are data on the autonomic blood supply ampulla and isthmus of the uterine tube [3, 12]. In the literature on the structure of the human uterine tube, there are data that in the ampule and the fimbria of the uterine tube on the longitudinal folds of the mucosa there are secondary, which, in turn, may appear tertiary folds [1, 14]. However, in the mucosa of the white rats uterine tube we did not detect of secondary and tertiary folds. The role of cilia is most pronounced in the ampulla of the uterine tube, where the thickness of the subserosa is up to five times smaller than the isthmus [6, 13]. According to many authors, the contraction of the subserosa help to captures the egg by fimbriae [2, 4, 19]. Other authors believe that the frequency of cilia movement influences the speed of movement of the egg and the embryo [8, 16, 22]. In addition, we have investigated that the number of epithelial cells of the mucosa of the uterine tube (secretory, basal, ciliated) is not the same throughout the length of the uterine tube of both human and white rats. The largest number of cilia in the fimbriae and ampulla gradually decreases in the direction of the uterus, and the secretory cells are the smallest in the fimbriae and ampulla, and most in the uterine part, which is consistent with the literature [2, 25]. As for the structure of the subserosa, there are also several thoughts. Some authors believe that there are outer longitudinal and inner circular smooth muscle coats [5], while others - distinguish three layers: the weakly developed outer longitudinal layer, the middle - circular, and internal longitudinal, which is particularly well developed in the uterine part of the tube [16, 17]. In addition, there are data

that in the area of the isthmus of the fallopian tube, the subserosa has an additional inner longitudinal layer in which smooth myocytes are located obliquely spirally [1, 7]. There is no clear boundary between the longitudinal and circular layers. Thus, the muscular stratum is less pronounced in the fimbria of the uterine tube than in the isthmus, in which the inner layers of smooth myocytes have the greatest development and form the muscle of the uterine tube [9, 15].

The serosa of the fallopian tubes, both human and white rat, consists of six layers: mesothelium, basement membrane, surface fibrous collagen layer, surface elastic mesh, deep elastic mesh, lattice collagen layer. It is precisely this structure that allows one body parts to lengthen, while others reduce and this allows the lumen of the uterine tube to increase, without simultaneously increasing its length. The results of our histological studies of the fallopian tubes of white rats allowed us to establish the following patterns: on the outside, the uterine tube is covered with a thin serosa, consisting of a single layer of mesothelial cells lying on a thin connective tissue basement membrane. Under the serous membrane is located an outer circular layer of the muscular membrane, under it - the inner longitudinal. Between the subserosa and the mucosa of the fallopian tubes there is lamina propria. The mucosa of the uterine tube is structurally similar to the endometrium, the epithelium of the mucous membrane is cylindrical, represented predominantly by cilia.

The obtained results of the study may be useful in the modeling of diseases of the reproductive system, because it is necessary to take into account the features of the macro- and microstructure of the experimental animal in order to extrapolate experimental data to medical practice.

Conclusions

1. Uterine tube of white rats in their macroscopic structure different from human uterine tube.

2. The microscopic structure of the uterine tube of a human and white rat is quite similar, which allows it to be used as an object in the experimental modeling of the determination of pathological states of the reproductive system.

References

[1] Adamyan, L. V., Kharchenko, E. I., Bragina, E. E., Murvatov, K. D., Stepanyan A. A., & Zobova A. V. (2015). Epithelium structure of the fimbrial branch of the fallopian tubes in women of reproductive age. *Reproduction Problems,* 21(4), 8-16.

[2] Aketayeva A. (2016). Modern view on the anatomy and function of the fallopian tubes. *Clinical medicine of Kazakhstan*, 40(2), 14-21. doi:10.23950/1812-2892-2016-2-14-21.

[3] Akhmedova, M. I., Khozhanazarova, S. Zh., Ashurova, F. K., & Mardonov, B. R. (2016). Morphological characteristics of intraorgan tubal vessels in experimental diabetes mellitus. *Journal of Theoretical and Clinical Medicine,* 1, 9-11.

[4] Asaturova. A. V, Ezhova, L. S, Fayzullina, N. M., Adamyan, L. V, Habas, G. N., & Sannikova, M. V. (2017). Expansion of secretory cells of the uterine tube epithelium in the early stages of pathogenesis serous carcinoma of the ovary. *Archive of pathology,* 79(3), 10-18.

[5] Bakhmet, A. A., Kuznetsova, M. A., Miroshkin, D. V., & Kupriyanov, I. E. (2015). Morphological structure of the mucous membrane of the ureter and fallopian tubes. *Academic Journal of Western Siberia,* 11(2), 141-142.

[6] Chen, H., Klein, R., Arnold, S., Chambers, S., & Zheng, W. (2016). Cytologic studies of the fallopian tube in patients undergoing salpingo-oophorectomy. *Cancer Cell. Int.,* 16, 78. DOI: 10.1186/s12935-016-0354-x.

[7] Col?n, E., & Carlson, J. W. (2014). Evaluation of chemotherapy after persistence of the tube after neoadjuvant chemotherapy: persistence of serous tubal intraepithelial carcinoma. *Int. J. Gynecol. Pathol.* 33(5), 463-469. doi: 10.1097/PGP.0b013e3182 a142 c.2.

[8] Deel, C. D., Allen, R. A., Holman, L. L., & Zuna, R. E. (2016). Adenocarcinoma of the cervix involving the fallopian tube mucosa: report of a case. *Diagn Pathol.,* 11, 77. doi: 10.1186/s13000-016-0529-8.

[9] Dixon, D., Alison, R., Bach, U., Colman, K., Foley, G. L., Harleman, J. H. … Yoshida M. (2014). Nonproliferative and Proliferative Lesions of the Rat and Mouse Female Reproductive System. *J. Toxicol. Pathol.* 27(3-4). 1S-107S. doi: 10.1293/tox.27.1S.

[10] Dzhadranov, E. S., Ibadullaeva, G. S., Yergazina, M. Zh., Krasnoshtanov, A. V., Krasnoshtanov, V. K., Kemelbekova, A. K., & Zhusip, B. P. (2016). Structural features of some internal organs of the laboratory mice of reproductive age. *Bulletin of KazNMU*, 4, 266-269.

[11] Dzis, N. P. (2014). Before feeding on the reproductive function of women from a gynecologic pathology of the pilot and non-spontaneous genesis. *Bulletin of Vinnitsa National Medical University,* 18(1), 2, 302-306.

[12] Foti, P. V., Ognibene, N., Spadola, S., Caltabiano, R., Farina, R., Palmucci, S. ... Ettorre, G. C. (2016). Non-neoplastic diseases of the fallopian tube: MR imaging with emphasis on diffusion-weighted imaging. *Insights Imaging*, 7(3), 311-327. doi: 10.1007/s13244-016-0484-7.

[13] Hua, G., Lv, X., He, C., Remmenga, S. W., Rodabough, K. J., Dong, J., & Wang, C. (2016). YAP induces high-grade serous carcinoma in fallopian tube secretory epithelial cells. *Oncogene,* 35(17), 2247-2265. doi: 10.1038/onc.2015.288.

[14] Kessler, M., Fotopoulou, C., & Meyer, T. (2013). The Molecular Fingerprint of High Grade Serous Ovarian Cancer Reflects Its Fallopian Tube Origin. *International Journal of Molecular Sciences,* 14(4), 6571-6596. doi: 10.3390 / ijms14046571.

[15] Kessler, M., Hoffmann, K., Brinkmann, V., Thieck, O., Jackisch, S., Toelle, B. … Meyer, T. F. (2015). The Notch and Wnt pathways regulate stemness and differentiation in human fallopian tube organoids. *Nat. Commun.,* 6, 8989. doi: 10.1038/ncomms9989.

[16] Kharchenko, E. I., Adamyan, L. V., Bragina, E. E., Murvatov, K. D., Stepanyan, A. A., & Arslanian, K. N. (2012). Ultrastructural study of tubal epithelium in women of reproductive age with benign tumors and ovarian cysts. *Obstetrics and gynecology,* 7, 50-53.

[17] Klyuchko, S. S., Yevtushenko, V., Sokolovskiy, D. M., & Shilan, K. V. (2016). Morphological features of the lymphoid component of the sheath of the uterine tubes of the domestic market. *Actual problems of medicine,* 16-4 (56-2), 14-17.

[18] Lee, N. K., Choi, K. U., Han, G. J., Kwon, B. S., Song, Y. J., Suh,

D. S., & Kim K. H. (2016). Pseudocarcinomatous hyperplasia of the fallopian tube mimicking tubal cancer: a radiological and pathological diagnostic challenge. *J. Ovarian Res.,* 9, 79. doi: 10.1186/s13048-016-0288-x.

[19] Matsumoto, H. (2017). Molecular and cellular events during blastocyst implantation in the receptive uterus: clues from mouse models. *J. Reprod. Dev.,* 63(5), 445-454. doi: 10.1262/jrd.2017-047.

[20] Niikura, R., Hayakawa, Y., Hirata, Y., Konishi, M., Suzuki, N., Ihara, S. … Koike, K. (2018). Distinct Chemopreventive Effects of Aspirin in Diffuse and Intestinal-Type Gastric Cancer. *Cancer Prev. Res.*, 11(4). doi: 10.1158/1940-6207.CAPR-17-0276.

[21] Sari, M. E., Ozdemir, O., Kadirogullari, P., Ertugrul, F. A., & Atalay, C. R. (2015). Mature Cystic Teratoma of the Fallopian Tube in a Postmenopausal Woman: A Case Report and Review of the Literature. *Case Rep. Obstet. Gynecol.,* 583021. doi: 10.1155/2015/583021.

[22] Teijeiro, J. M., & Marini, P. E. (2015). S100A7 in the Fallopian tube: a comparative study. *Zygote,* 23(2), 229-236. doi: 10.1017/S0967199413000464.

[23] Voznesenska, T. Yu., Koleinkova, O. M., Blashkiv, T. V., Brizgina, T. M., Sukhina, V. S., & Yanchiy, R. I. (2013). Functional organ of the reproductive system in the minds of the experimental ear-numbered stem from Misha. *Visnyk problems biologii i medicine,* 2(100), 125-128.

[24] Wang, C., Liu, Y., Chang, C., Wu, S., Gao, J., Zhang, Y. … Deng, G. (2016). Human fallopian tube proteome shows high coverage of mesenchymal stem cells associated proteins. *Biosci. Rep.*, 36(1). e00297. doi: 10.1042/BSR20150220.

[25] Yuan, J., Zhao, W., Yan, M., Zhu, Q., Qin, G., Qiu, J., Zhang, J. (2015). Ulipristal Acetate Antagonizes the Inhibitory Effect of Progesterone on Ciliary Beat Frequency and Upregulates Steroid Receptor Expression Levels in Human Fallopian Tubes. *Reprod. Sci.,* 22(12), 1516-1523. doi: 10.1177/1933719115589409.

ПОРІВНЯЛЬНА АНАТОМІЯ МАТКОВОЇ ТРУБИ ЛЮДИНИ ТА САМКИ ЛАБОРАТОРНОГО БІЛОГО ЩУРА

Подолюк М.В.

У світовій літературі накопичено значний обсяг даних для характеристики основних компонентів жіночої статевої системи, функціональних взаємозв'язків між ними, а також зв'язків між цією системою та іншими системами організму. Актуальність дослідження зумовлена також тим, що в структурі жіночого безпліддя 60-70% займає трубно-перитонеальний фактор. Проблеми, пов'язані з цією патологією, вивчають понад півстоліття. На сьогоднішній день дані про мікроанатомію маткової труби людини, а, тим паче, самки білого щура є суперечливими. Метою дослідження було провести порівняльний аналіз структурної організації маткової труби людини і самки лабораторного білого щура. Дослідження проводили на 10 статевозрілих білих щурах самках репродуктивного віку. Застосовано метод препарування (для дослідження макроанатомії маткової труби самки білого щура) та стандартні гістологічні методи (зрізи стінки маткової труби товщиною 5-7 мкм, забарвлені гематоксиліном та еозином). Зовнішня будова маткової труби самки щура і людини має деякі відмінності. На відміну від людини, маткова труба лабораторного білого щура має вигляд тонкої і короткої трубочки, скрученої спірально у компактний клубочок. У матковій трубі самки білого щура доцільно розрізняти 2 частини: лійку і маткову частину. Маткова частина з'єднується з порожниною рогу матки матковим отвором маткової труби, а лійка маткової труби відкривається в порожнину очеревини до поверхні яєчника черевним отвором маткової труби. Навколо лійки маткової труби її слизова оболонка зібрана в складки - торочки маткової труби та яєчникові торочки (у людини - одна яєчникова торочка), які кріпляться до яєчника. При цьому діаметр маткової труби самки білого щура зменшується в напрямку від лійки до маткової частини. Зокрема, в ділянці лійки діаметр маткової труби становить 0,90±0,10 мм, а діаметр маткової частини - 0,70±0,09 мм. Маткова труба лабораторного білого щура, як і людини, має брижу маткової труби. Як у людини, так і в самки білого щура стінка маткової труби складається з трьох шарів: внутрішня оболонка - слизова, середня оболонка - м'язова, зовнішня оболонка - серозна. Таким чином, маткова труба самки білого щура за своєю макроскопічною будовою відрізняється від маткової труби людини. Мікроскопічна будова маткової труби людини і самки білого щура досить подібні, що дозволяє використовувати її як об'єкт при експериментальному моделюванні певних патологічних станів репродуктивної системи.

Ключові слова: *репродуктивна система, маткова труба, білий щур.*

СРАВНИТЕЛЬНАЯ АНАТОМИЯ МАТОЧНОЙ ТРУБЫ ЧЕЛОВЕКА И САМКИ ЛАБОРАТОРНОЙ БЕЛОЙ КРЫСЫ

Подолюк М.В.

В мировой литературе накоплен значительный объем данных для характеристики основных компонентов женской половой системы, функциональных взаимосвязей между ними, а также связей между этой системой и другими системами организма. Актуальность исследования обусловлена тем, что в структуре женского бесплодия 60-70% занимает трубно-перитонеальный фактор. Проблемы, связанные с этой патологией, изучают более полувека. До сих пор сведения о микроанатомии маточной трубы человека и, тем более, самки лабораторного белой крысы противоречивы. Целью исследования было провести сравнительный анализ структурной организации маточной трубы человека и самки лабораторной белой крысы. В статье приведены и проанализированы данные исследования, которые проводили на 10 половозрелых белых крысах-самках репродуктивного возраста. Для исследования макроанатомии маточной трубы самки белой крысы применили метод препарирования, а также стандартные гистологические методы (срезы стенки маточной трубы толщиной 5-7 мкм, окрашенные гематоксилином и эозином). Внешнее строение маточной трубы самки крысы и человека имеет некоторые отличия. В отличие от человека, маточная труба лабораторной белой крысы имеет вид тонкой и короткой трубочки, скрученной спирально в компактный клубочек. В маточной трубе самки белой крысы целесообразно различать 2 части: воронку и маточную часть. Маточная часть соединяется с полостью рога матки маточным отверстием маточной трубы, а воронка маточной трубы открывается в полость брюшины к поверхности яичника брюшным отверстием маточной трубы. Вокруг воронки маточной трубы ее слизистая оболочка собрана в складки - бахромки маточной трубы и яичниковые бахромки (у человека - одна яичниковая бахромка), которые крепятся к яичнику.

При этом диаметр маточной трубы самки белой крысы уменьшается в направлении от воронки к маточной части. В частности, в области воронки диаметр маточной трубы составляет 0,90±0,10 мм, а диаметр маточной части - 0,70± 0,09 мм. Маточная труба лабораторной белой крысы, как и человека, имеет брыжейку маточной трубы. Как у человека, так и у самки белой крысы стенка маточной трубы состоит из трех слоев: внутренняя оболочка - слизистая, средняя оболочка - мышечная, внешняя оболочка - серозная. Таким образом, маточная труба самки белой крысы по своему макроскопическому строению отличается от маточной трубы человека. Микроскопическое строение маточной трубы человека и самки белой крысы достаточно похожи, что позволяет использовать ее как объект при экспериментальном моделировании определенных патологических состояний репродуктивной системы.
Ключевые слова: *репродуктивная система, маточная труба, белая крыса.*

DOI: 10.31393/morphology-journal-2018-24(4)-08 Reports of Morphology, Vol. 24, №4, Pages 53-57

ISSN 1818-1295 eISSN 2616-6194

REPORTS OF MORPHOLOGY

Official Journal of the Scientific Society of Anatomists, Histologists, Embryologists and Topographic Anatomists of Ukraine

journal homepage: https://morphology-journal.com

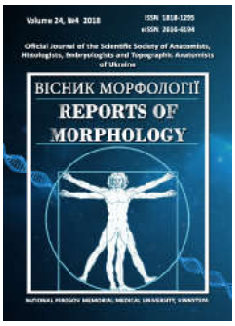

Electron microscopic changes of the testis germinal epithelium after an experimental thermal trauma in the application of cryo-lyophilized xenograft skin substrate

Volkov K.S., Muha S.Yu.

SHEI "I. Ya. Horbachevsky Ternopil State Medical University Ministry of Health of Ukraine", Ternopil, Ukraine

ARTICLE INFO

Received: 3 October, 2018

Accepted: 2 November, 2018

UDC: 611.631: 616 - 001.19: 612.08

CORRESPONDING AUTHOR

e-mail: KVolkov@gmail.com

Volkov K.S.

Deep, large area of thermal trauma of the skin leads to significant morphofunctional changes in organs in the composition of the burned organism. However, condition of the central organ of the male reproductive system - testicle after burns and, especially, in the treatment of thermally damaged areas of the skin remain poorly understood. The purpose of this study was to establish an ultrastructural re-organization of testis germinal epithelium cells in the stages of toxemia and septicotoxemia following an experimental thermal trauma when using xenograft skin substrate. The studies were carried out on 35 sexually mature white male rats, which were divided into three groups: 1 - intact animals (5 rats), 2 - animals with burn injury (15 rats), 3 - animals with burn injury, for which were used xenograft skin substrate (15 rats). The burn was applied under ketamine anesthesia with copper plates, heated in boiling water, on 18-20% shaved body surface of animals. Early necrectomy of the damaged areas of skin was carried out 1 day after the thermal burn. The formed wounds were covered with cryo-lyophilized xenograft skin substrate. Experimental animals were decapitated at 7, 14 and 21 days of the experiment (early, late toxemia and septicotoxemia). The material sampling for electron microscopy was carried out in accordance with a generally accepted methodology. It is established that in the stage of early toxemia (7 days of experiment) there are adaptive-compensatory changes and signs of destruction of spermatogenic cells of testis. In the stages of late toxemia and septicotoxemia (14 and 21 days of the trial), significant destructive changes occur in all components of the seminiferous tubules of the organ. Electron microscopically found that the closure of the burn wound after the early necrectomy of cryo-lyophilized xenograft skin substrate in severe experimental burn injury in the early stages of the experiment significantly reduces the damage of testis germinal epithelium of experimental animals and activates regenerative processes. This contributes to a significant improvement in the ultrastructure of the components of the convoluted tubules of the organ in the late stages of the experiment.

Keywords: *testicle, electron microscopic changes, experimental thermal trauma, cryo-lyophilized xenograft skin substrate.*

Introduction

An urgent medical problem is the establishment of a reorganization of organs of the reproductive system under the influence of external factors that are toxic in nature [18]. It is known that severe thermal trauma of the skin causes significant morphofunctional changes in the systems and organs of the organism, including the reproductive system [3, 5, 13]. The analysis of scientific literature has shown that still remain poorly understood condition of testis (the central organ of the male reproductive system) after burns of body.

According to modern ideas, one of the immediate causes of significant morphofunctional changes in organs and tissues in burns is exo- and endogenous intoxication [1, 14]. The products of decay of tissues, specific and nonspecific toxins are a trigger mechanism for burn infections, and, subsequently, the development of septicotoxemia [8, 9]. Therefore, from the theoretical and practical point of view, it is important to conduct studies to

study the changes of the testis germinal epithelium, the course of compensatory adjustment and regenerative processes in them at the closure of the burn wound after the early necrectomy of the affected skin sections with crushed cryo-lyophilized xenograft skin substrate [2, 10, 11].

The *purpose* of this work was to establish an ultrastructural reorganization of testis germinal epithelium cells in the stages of toxemia and septicotoxemia after an experimental thermal trauma when using xenograft skin substrate.

Materials and methods

Experiments were conducted on 35 sexually mature white male rats divided into three groups: 1 - intact animals (5 individuals), 2 - animals with burn injury (15 individuals), 3 - animals with burn injury, which were used as xenograft skin substrate (15 individuals). The burn was applied under ketamine anesthesia with copper plates heated in boiling water on 18-20% shaved body surface of animals. Early necrectomy of damaged areas of skin was carried out 1 day after the thermal burn. The formed wounds were covered with cryo-lyophilized xenograft skin substrate.

In conducting research, the international rules and principles of the "European Convention for the Protection of Vertebrate Animals used for Experiments and for Other Scientific Purposes" (Strasbourg, 1986) and "General Ethical Principles of Animal Experiments" (Kyiv, 2001) and the Law of Ukraine No. 3447 "On the Protection of Animals from Cruel Treatment - 2006" were followed. Histological examination of the skin testified to the development of the burn of the third degree.

Experimental animals were decapitated at 7, 14 and 21 days of the experiment, which met the terms of early, late toxemia and septicotoxemia. The material sampling for electron microscopic studies was carried out in accordance with the generally accepted method [16]. The small pieces of testis germinal epithelium were fixed in 2.5% glutaraldehyde solution with an active medium pH of 7.2-7.4 prepared on phosphate buffer. The postfixation of the material was carried out with a 1% solution of osmium tetrachloride, after which it was dehydrated in propylene oxide and poured into a mixture of epoxy resins with araldite. Ultra-thin sections made on ultramicrotome LKB-3 (Sweden) were contrasted with 1% aqueous uranyl acetate solution and lead citrate by Reynolds method and studied by electron microscope PEM-125K.

Results

Electron microscopic studies on day 7 after a thermal trauma found that the walls of the seminiferous tubules appear thickened due to the swelling of the fibrous layer and the sites of contraction of the myoid cells. In sustentacular cells there is enlightenment of the cytoplasm, hypertrophy of the mitochondria, damage to the integrity of the crist?. Part of the nuclei have uneven contours of the nuclear membrane, increased nuclear pore. Germinal epithelium cells are altered, spermatogonia is present with signs of mitosis, but less than in the testicles of the intact group of animals. Spermatocytes are not densely located due to enhanced intercellular spaces, in their cytoplasm vacuole-like structures are available in different sizes (Fig. 1).

Part of spermatocytes with elevated osmiophilic of karyoplasm and cytoplasm, deformed nuclei. In spermatids and spermatozoa, poorly contoured acrosome, high electron density of nuclei and damage to nuclear membrane (Fig. 2).

At 14 and especially 21 days after thermal trauma in the structural components of seminiferous tubules there is an increase in ultrastructural changes. There are heterogeneous changes in the myoid cells. In addition to cells with electronically bright, edematous cytoplasm, cells with osmophilic cytoplasm and picnotically altered nuclei are detected. Organelles in them are destructively altered.

Submicroscopically, in the late stages of the trial, a significant destruction is found in sustentacular cells. Incorrect form of their nuclei includes osmiophilic

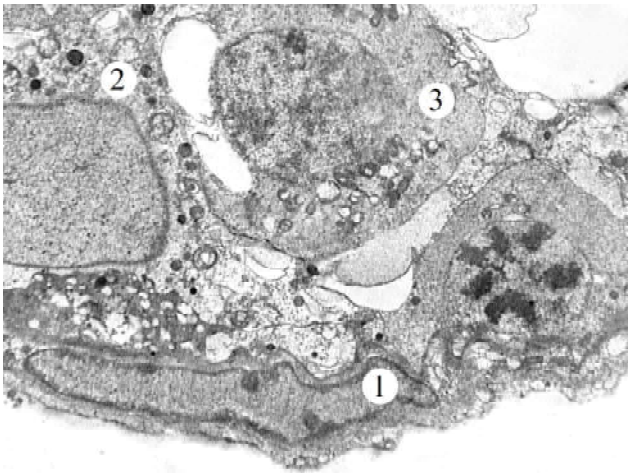

Fig. 1. Ultrastructural changes of the animal's seminiferous tubules on 7 day after a thermal trauma. Wall of tubules (1), Sertoli cell (2), primary spermatocyte (3). x13000.

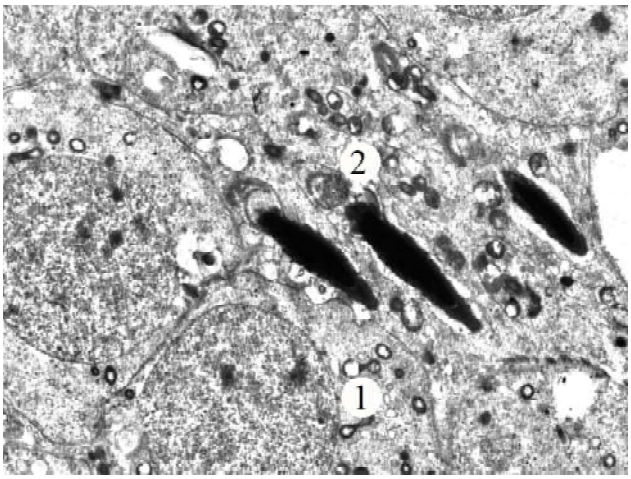

Fig. 2. Submicroscopic state of the spermatogenic cells of the testicle of the animal for 7 days after a thermal trauma. Primary spermatocyte (1), spermatids (2). x13000.

karyoplasm. In the cytoplasm of elevated electron density, organelles were poorly contoured, vacuole-like structures were present (Fig. 3).

In the spermatogenic cells, there were cells with signs of myotic division. In the part of spermatids and spermatozoa, poorly contoured acrosome, high electron density of nuclei and damage to nuclear membrane. A part of the cells was with increased osmiophilic of karyoplasm and cytoplasm, deformed nuclei. Expanded intercellular spaces, spermatocytes are not densely located, vacuole-shaped structures of varying sizes are available in their cytoplasm. Such a condition of the germinal epithelium characterizes significant violations of spermatogenesis.

Electron microscopic examination of the testicles of animals after 7 days of burning under the use of xenograft skin substrate revealed an improvement in their ultrastructure. Available spermatogonia with signs of mitosis, primary and secondary spermatocytes include round nucleus having euchromatin and small breasts of heterochromatin in the structure of the karyoplasm, and partly damaged organelles in the cytoplasm (Fig. 4). Spermates and spermatozoa are also less altered than in the group of animals with burns.

Sub-microscopic studies in the late terms of the experiment found that, especially at 21 day, there was a significant improvement in the state of the structural components of seminiferous tubules. The bodies of supporting cells are clearly contoured, they have a large cone-shaped body with sprouts located on the base of the basement membrane. A significant area of the cytoplasm of Sertoli cell includes the granulosa endoplasmic reticulum tubule and small vesicles of rough endoplasmic reticulum. Small mitochondria have a long or round shape depending on the plane of the cross-section. In the average electron density of the matrix and little crist?. Available dictyosomes of the Golgi complex, lysosomes, mainly primary, lipid inclusion, bubbles and vacuoles, mainly in adlucent compartment. Plasmalemma of sustentacular cells is in contact with the germinal epithelium.

In the germinal epithelium there are cells with signs of mitotic division. Primary spermatocytes have a large area of the cytoplasm that is electronically light, including many free ribosomes and small unevenly located mitochondria. In the nucleus of the cells, there are meiosis figures, varying degrees of regions of the condensed chromosomes are detected and, in particular, they are thickened in the stage of pachytene and diakinesis.

Secondary spermatocytes are smaller in size, include round eucharomatic nuclei, a small area of the cytoplasm and localized closer to the lumen of the seminiferous tubules. In spermatids and spermatozoa, the acrosome is well contoured, a high electron density of nuclei is present, and the mitochondrial vagina is formed (Fig. 5).

This condition of the germinal epithelium characterizes its normalization and the restoration of the phase nature of spermatogenesis.

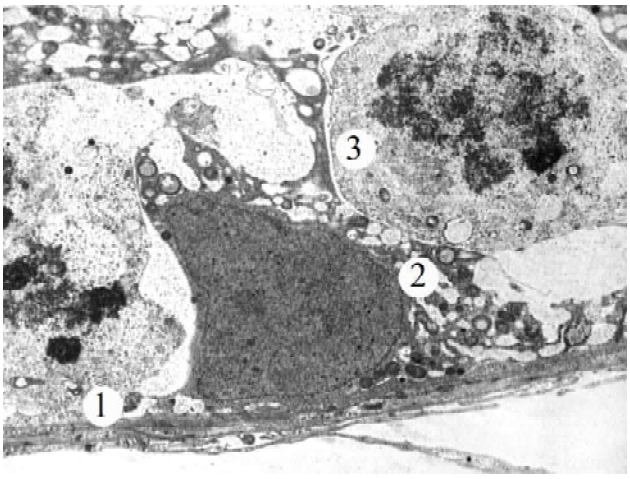

Fig. 3. Ultrastructural changes in the animal's seminiferous tubules on the 21st day after a thermal trauma. Wall of tubules (1), Sertoli cell (2), primary spermatocyte (3). x7000.

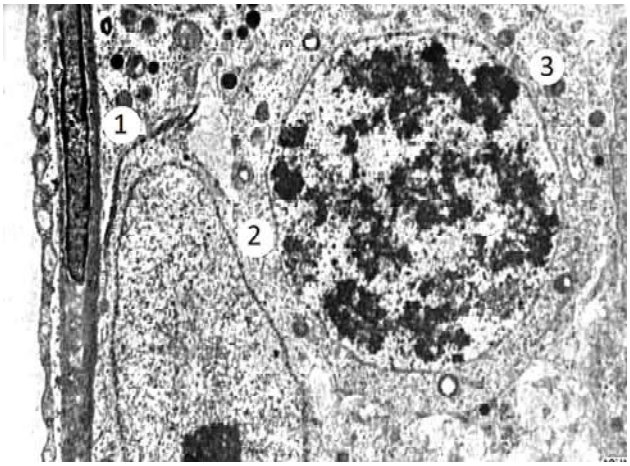

Fig. 4. Ultrastructural state of the seminiferous tubules of the animal for 7 days after the thermal trauma with the use of cryo-lyophilized xenograft skin substrate. Wall of tubules (1), Sertoli cell (2), primary spermatocyte (3). x12000.

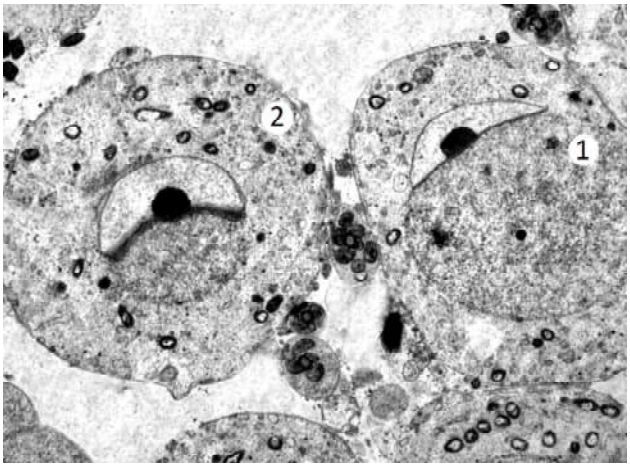

Fig. 5. Submicroscopic state of the spermatogenic cells of the seminiferous tubules animal for 21 days after the thermal injury of the animal with the use of cryo-lyophilized xenograft skin substrate. The nucleus (1) and the cytoplasm (2) of spermatids. x9000.

Discussion

The morphological state of the structural components of the testicles and their reproductive function greatly depend on the effect of the damaging factors [17]. Specific and non-specific toxins resulting from the decomposition of skin tissues after severe thermal trauma cause significant changes in the germinal epithelium ultrastructure and, in particular, in the stages of early and late toxemia. In the seminiferous tubules, the submicroscopic organization of Sertoli cells is affected, which affects the process of the formation of germ cells. Their destructive changes after a thermal trauma are established in all phases of spermatogenesis in the testes of the experimental group.

Significant changes in the area of burn of the skin and internal organs in the body systems are established in many studies [6, 12, 15, 19]. Therefore, it was advisable to conduct early necrectomy of wound-affected areas of the skin and use of cryo-lyophilized xenograft skin substrate on wounds. The electron microscopically positive effect of this xenograft skin substrate on the ultrastructure of all components of the testis germinal epithelium and, especially, in the late experiment (21 days) was proved.

The reduction of histological changes in the use of such a factor after skin burns in the experiment is established in studies of the structure of the myocardium, lungs, kidneys, liver and other internal organs of the experimental animals [10, 11].

Thus, severe, large-scale thermal lesions of the skin require the implementation of modern therapeutic measures to activate and accelerate regenerative processes not only for the healing of burn wounds, but also for the reduction of pathological changes and normalization of the morphofunctional state of the internal organs of the body [4, 7].

The obtained scientific results can be used for further investigations of the condition of the structural components of the testicles under the conditions of applying corrective factors in the experimental thermal trauma.

Conclusions

1. In the early term after the thermal trauma (7 day of the experiment), ultrastructural changes have signs of destruction of testis germinal epithelium cells and are adaptive-compensatory. In the long term after the thermal lesions (14 and 21 days of the trial), under conditions of endogenous intoxication, deep destructive changes of the germinal epithelium develop, and the inhibition of reparative regeneration is present.

2. Coating of the burn wound with crushed cryo-lyophilized xenograft skin substrate after excision of necrotizing tissues from the site of damage significantly reduces the destructive changes of cells of the germinal epithelium. The best preservation of the intracellular components of Sertoli cells and the activation of regeneration contributes to the relative normalization of the testis structure in the late stages of the experiment.

References

[1] Biguniak, V. V. & Folded, M. Yu. (2004). *Thermal defeats*. Ternopil: Ukrmedkbook.

[2] Eick, B. G., & Denke, N. J. (2018). Resuscitative Strategies in the Trauma Patient: The Past, the Present, and the Future. *J. Trauma Nurs.,* 25(4), 254-263. doi:10.1097/JTN.0000000000000383

[3] Evers, L. H. (2010). The biology of burn injury. *Exp. Dermatol.,* 19(2), 9, 777-783 doi:10.1111/j.1600-0625.2010.01105.x

[4] Gavryluk, A. O., Galunko, G. M., Chereshniuk, I. L., Tikholaz, V. O., Cherkasov, E. V., Dzevulska, I. V., & Kovalchuk O. I. (2018). Indicators cell cycle and DNA fragmentation in cells of small intestine mucosa 14, 21 and 30 days after skin burns on the background of preliminary infusion of solution lactoprotein with sorbitol or HAES-LX 5%. *World of Medicine and Biology,* 1(63), 104-108 doi:10.26724/2079-8334- 2017-4-62-104-108

[5] Gembitsky, E. V., Klyachkin, L. M., & Kirilov M. M. (1994). *Pathology of internal organs in trauma*. M.: Medicine.

[6] Gunas, I. V., Guminskiy, Yu. I., Ocheretna, N. P., Lysenko, D. A., Kovalchuk, O. I., Dzevulska, I. V., & Cherkasov, E. V. (2018). Indicators cell cycle and dna fragmentation of spleen cells in early terms after thermal burns of skin at the background of introduction 0.9% NaCl solution. *World of Medicine and Biology,* 1(63), 116-120. doi: 10.26.724/2079-8334-2018-1-63-116-120

[7] Janak, J. C., Clemens, M. S., Howard, J. T., Le T. D., Cancio, L. C., Chung, K. K., Gurney, J. M., Sosnov, J. A., Stewart, Ian J. (2018). Using the injury severity score to adjust for comorbid trauma may be double counting burns: implications for burn research. *Burns,* 44, 8, 1920-1929. doi: 10.1016/j.burns.2018.03.012

[8] Klimenko, M. O. & Netyukhailo, L. G. (2009). *Burn disease* (pathogenesis and treatment). Poltava 118 p.

[9] Kozinets, G. P., Kovalenko, G. P., & Slesarenko, S. V. (2006). Burn sickness. *Art of treatment*, 12, 9-15.

[10] Nagaychuk, V. I. (2010). Modern approaches to helping patients with burns. *Art of treatment,* 5, 24-27.

[11] Nebesna, Z. M. (2015). Morphological state of the heart, liver and lungs after experimental thermal trauma under conditions of application of crushed substrate of cryolophilized xenose. *World of Medicine and Biology,* 3(51), 99-103.

[12] Ocheretna, N. P., Guminskiy, Yu. I., & Gunas, I. V. (2018). Indicators of cell cycle and dna fragmentation of spleen cells in early terms after thermal burns of skin on the background of using "lactoprotein with sorbitol" or HAES-LX-5%. *Bulletin of scientific research,* 1, 141-146. doi:10.11603/2415-8798.2018.1.8627

[13] Osadchaya, O. I., Boyarskaya A. M. & Sheyman, B. S. (2008). Effect of enterosorption on the content of pro- and anti-inflammatory mediators in severe thermal trauma. *Internal Medicine,* 16(3), 76-78.

[14] Paramonov, B. A., Porembsky, Ya. O., & Yablonsky, V. G. (2000). *Burns: A Guide for Doctors.* SPb.: Spec. lit.

[15] Regas, F. C., & Ehrlich, H. P. (1992). Elucidating the vascular response to burns with a new rat model. *J. Trauma*, 32(5), 557-563. PMID:1588642

[16] Sarkisov, D. S., & Perova, Yu. L. (Ed.). (2002). *Microscopic technique.* M.: Medicine.

[17] Stravsky T. Y. (2015). Morphological and functional characteristics of the adjustment of parenchyma testis of

rats at metered stenosis of spermatic cord. *Bulletin of scientific research,* 4, 110-112. doi:10.11603/1681-276X.2015.4.5662

[18] Voloshina, I. S. (2011). Contemporary ideas about the morphogenesis of the internal organs of the male reproductive system under the influence of various factors. *Ukrainian morphological almanah*, 9(4): 155-160.

[19] Williams, F. N., Herndon, D. N., Suman, O. E., Lee, J. O., Norbury, W. B., Branski, L. K., … Jeschke, M. G. (2011). Changes in cardiac physiology after severe burn injury. *J. Burn Care Res.,* 32(2), 269-274. DOI: 10.1097/BCR.0b013e31820aafcf

ЕЛЕКТРОННО-МІКРОСКОПІЧНІ ЗМІНИ СПЕРМАТОГЕННОГО ЕПІТЕЛІЮ ЯЄЧОК ПІСЛЯ ЕКСПЕРИМЕНТАЛЬНОЇ ТЕРМІЧНОЇ ТРАВМИ ПРИ ЗАСТОСУВАННІ СУБСТРАТА КРІОЛІОФІЛІЗОВАНОЇ КСЕНОШКІРИ

Волков К.С., Муха С.Ю.

Глибока, велика за площею термічна травма шкіри призводить до значних морфофункціональних змін органів в складі систем обпеченого організму. Проте, маловивченим залишається при опіках центральний орган чоловічої статевої системи - яєчко і, особливо, при лікуванні термічно пошкоджених ділянок шкіри. Метою цього дослідження було встановлення ультраструктурної реорганізації клітин сперматогенного епітелію яєчок в стадіях токсемії та септикотоксемії після експериментальної термічної травми при застосуванні субстрата ксеношкіри. Дослідження проведені на 35 статевозрілих білих щурах-самцях, які були розподілені на три групи: 1 - інтактні тварини (5 особин), 2 - тварини з опіковою травмою (15 особин), 3 - тварини з опіковою травмою, яким застосовували субстрат ксеношкіри (15 особин). Опік наносили під кетаміновим наркозом мідними пластинами, нагрітими у киплячій воді, на 18-20% епільованої поверхні тіла тварин. Ранню некректомію пошкоджених ділянок шкіри проводили через 1 добу після нанесення термічного опіку. Рани, які утворились, покривали кріоліофілізованим ксенодермальним субстратом. Піддослідних тварин декапітували на 7, 14 та 21 доби експерименту, що відповідно темінам ранньої, пізньої токсемії та септикотоксемії. Забір матеріала для електронно-мікроскопічних досліджень проводили згідно із загальноприйнятою методикою. Встановлено, що в стадії ранньої токсемії (7 доба досліду) наявні пристосувально-компенсаторні зміни та ознаки деструкції клітин сперматогенного епітелію яєчок. У стадіях пізньої токсемії та септикотоксемії (14 і 21 доби досліду) відбуваються значні деструктивні зміни всіх компонентів звивистих канальців органу. Електронно-мікроскопічно встановлено, що закриття опікової рани після проведення ранньої некректомії субстратом кріоліофілізованої ксеношкіри за умов тяжкої експериментальної опікової травми вже в ранні терміни досліду суттєво зменшує пошкодження сперматогенного епітелію яєчок піддослідних тварин і активізує регенераторні процеси. Це сприяє суттєвому покращенню ультраструктури компонентів звивистих канальців органу в пізні терміни експерименту.

Ключові слова: *яєчко, електронно-мікроскопічні зміни, експериментальна термічна травма, субстрат кріоліофілізована ксеношкіра.*

ЭЛЕКТРОННО-МИКРОСКОПИЧЕСКИЕ ИЗМЕНЕНИЯ СПЕРМАТОГЕННОГО ЭПИТЕЛИЯ ЯИЧЕК ПОСЛЕ ЭКСПЕРИМЕНТАЛЬНОЙ ТЕРМИЧЕСКОЙ ТРАВМЫ ПРИ ПРИМЕНЕНИИ СУБСТРАТА КРИОЛИОФИЛИЗИРОВАННОЙ КСЕНОКОЖИ

Волков К.С., Муха С.Ю.

Глубокая, большая по площади термическая травма кожи приводит к значительным морфофункциональным изменениям органов в составе систем обожженного организма. Но малоизученным при ожогах остается центральный орган мужской половой системы - яичко и, особенно, при лечении термически поврежденных участков кожи. Целью этого исследования было установление ультраструктурной реорганизации клеток сперматогенного эпителия яичек в стадиях токсемии и септикотоксемии после экспериментальной термической травмы при использовании субстрата ксенокожи. Исследования проведены на 35 половозрелых белых крысах-самцах, которые были распределены на три группы: 1 - интактные животные (5 особей), 2 - животные с ожоговой травмой (15 особей), 3 - животные с ожоговой травмой, которым применяли субстрат ксенокожи (15 особей). Ожог наносили под кетаминовым наркозом медными пластинами, нагретыми в кипящей воде, на 18-20% эпилированой поверхности тела животных. Некрэктомию поврежденных участков кожи проводили через 1 день после нанесения термического ожога. Раны, которые образовались, покрывали криолиофилизированным ксенодермальным субстратом. Подопытных животных декапитировали на 7, 14 та 21 день эксперимента, что соответствует срокам ранней, поздней токсемии и септикотоксемии. Забор материала для электронно-микроскопических исследований проводили согласно общей существующей методики. Выявлено, что в стадии ранней токсемії (7 день опыта) присутствуют признаки деструкции клеток сперматогенного эпителия яичек и приспособительно-компенсаторные изменения. В стадиях поздней токсемии и септикотоксемии (14 и 21 день опыта) происходят значительные деструктивные изменения всех компонентов извитых канальцев органа. Электронно-микроскопически установлено, что закрытие ожоговой раны после проведения ранней некрэктомии субстратом криолиофилизированой ксенокожи при тяжелой экспериментальной ожоговой травме уже в ранние сроки опыта существенно уменьшает повреждение сперматогенного эпителия яичек экспериментальных животных, активизирует регенераторные процесы. Это способствует существенному улучшению ультраструктуры компонентов извитых канальцев органа в поздние сроки эксперимента.

Ключевые слова: *яичко, электронно-микроскопические изменения, экспериментальная термическая травма, субстрат криолиофилизированная ксенокожа.*

DOI: 10.31393/morphology-journal-2018-24(4)-09 Reports of Morphology, Vol. 24, №4, Pages 58-65

ISSN 1818-1295 eISSN 2616-6194

REPORTS OF MORPHOLOGY

Official Journal of the Scientific Society of Anatomists, Histologists, Embryologists and Topographic Anatomists of Ukraine

journal homepage: https://morphology-journal.com

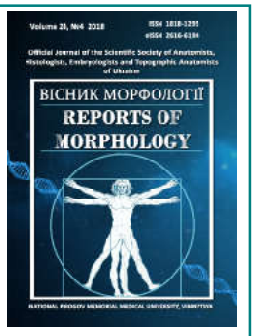

The role of the transcription factor Sox2 and cytokeratins in the formation and development of the gastroesophageal junction epithelial cell differon

Rekun T.O., Vernygorodskyi S.V., Kyselova T.M., Tataryna O.V., Cherepakha O.L.
Vinnytsya National Pirogov Memorial Medical University, Vinnytsya, Ukraine

ARTICLE INFO
Received: 10 October, 2018
Accepted: 12 November, 2018

UDC: 611.018.616.311:57.017.642

CORRESPONDING AUTHOR
e-mail: tatuana.rekun@gmail.com
Rekun T.O.

The source of the origin of the epithelium of the cardiac part stomach mucosa has been repeatedly discussed in the literature and different variants of the transformation of the epithelium as manifestation of normal anatomical peculiarities of a man and as a result of changing the program of stem cell differentiation, migration of bone marrow cells, transdifferentiation of simple columnar epithelium have been proposed. Probably it is related to difficulties of studying insignificant in size epithelium of the cardiac mucosa itself and establishment of connection of the duodenogastroesophageal reflux with the development of metaplasia in the epithelium of the terminal department of the esophagus mucosa, which resembles its structure in the cardiac part of the stomach. The purpose of the research was to study the expression of the transcription factor Sox2 and the distribution of cytokeratins in the epithelium of the gastroesophageal zone during the stages of the embryonic and fetal periods of ontogenesis. According to the purpose of the research, an immunohistochemical analysis of the epithelial differon of the esophageal-gastric junction (GEJ) was used. The current study was carried out on 169 human embryos and fetuses of gestational age from 4-5 till 38 weeks. It was established that the transcription factor Sox2 is expressed in basal epitheliocytes of GEJ in all terms of observation and plays a major role in the development, differentiation and formation of the epithelial cell lineage of GEJ. The peculiarity of expression of cytokeratin 7 was positive marking in the cytoplasm of spinosum epitheliocytes, despite the negative expression in the basal layer. It showed weak expression in the epitheliocytes of the esophageal part of the GEJ in the embryonic period with an increased reaction in the embryo-fetal period and with subsequent disappearance, starting at 14 weeks in the early fetal period. For the cardiac mucous membrane GEJ was characterized by its moderate expression on all terms of observation. Cytokeratin 8/18 is embryo-fetal for the esophageal part of the esophagus, as it is defined in early periods of embryogenesis and disappears in the late period (28-38 weeks). For the cardiac mucous membrane GEJ was characterized by its moderate expression on all terms of observation. Cytokeratin 14, unlike CK7 and CK8/18, was localized in the cytoplasm and membranes of basal epitheliocytes of the esophageal part of the mucosa from the 17 gestational weeks and was absent in the gastrointestinal part of the GEJ throughout the prenatal period. Thus, our data on the expression of the transcription factor Sox2 and cytokeratins in the GEJ epithelial differon in the prenatal period of ontogenesis will improve the diagnostic accuracy in determining tissue or organ belonging and can be widely used in various GEJ diseases.

Keywords: *gastroesophageal junction, immunohistochemical analysis, Sox2 transcription factor, cytokeratins, prenatal ontogenesis.*

Introduction

One of the major transcription factors involved in the induction and maintenance of pluripotent stem cells is Sox2. As for the definition of stem cells in the upper gastrointestinal tract, there are, at present, different, sometimes contradictory thoughts. Sox2 is proposed as one of the markers for the identification of stem cells in the esophagus and the

stomach, but its involvement in the differentiation and development of the gastroesophageal junction (GEJ) epithelial cell lineage remains poorly understood [6, 8, 13, 16].

Recognized immunohistochemical markers of the epithelium are cytokeratins - proteins of intermediate filaments (cytoskeleton) of epithelial cells. There are about 20 different cytokeratins that differ in amino acid composition, molecular weight, and isoelectric point. They are divided into two large groups: sour or type I (type A), which include cytokeratins 9-20 (CK9-CK20), and the main/neutral - 9 type II (type B), represented by CK1-CK8 [2, 9, 10, 17]. Cytokeratins are encoded by the genes of a large multigenic family (on chromosomes 11, 12 and 17). The different groups of epithelium are characterized by the corresponding groups of cytokeratins [3, 5].

In practical work for the immunocytochemical determination of the epithelial nature of atypical cells in the biopsies of tumors, antibodies against a specific cytokeratin or their wide spectrum (Pan-CK) are used. It is the cytokeratins responsible for the differentiation of the epithelium of various organs and the preservation of its cytoskeleton. Regarding the GEJ epithelial cell lineage, their distribution and role in the formation, ripening, cell migration and differentiation of the embryonic and epidermal epithelium of embryos and fetuses at present have not been sufficiently studied.

That is why the *purpose* of our study was to establish the expression of the transcription factor of Sox2 and the distribution of cytokeratins in the GEZ epithelium in the stages of embryonic and fetal periods of ontogenesis.

Materials and methods

The study was performed on embryos and fetuses of a person aged 4-5 up to 38 weeks of fetal development that developed in the uterus in the absence of explicit external and internal factors obtained from medical abortions or stillborn in relatively healthy women in the Vinnitsa Regional Anatomic Pathology Department (VRAPD) and maternity homes in the city of Vinnytsia and who died from causes not associated with GIT diseases.

Fetal preparations weighing more than 500.0 g were studied directly in VRAPD of Vinnitsa (Order of the Ministry of Health of Ukraine "On Approval of Instructions for Determining the Perinatal Period, Live Birth and Deadly Births, Procedure for Registration of Abandoned and Deadly Births" No. 179 dated 29.03.2006). The age of subjects was determined according to tables by T. Sadler (2001) on the basis of measuring the crown-rump length [4, 18, 19].

The total number of embryos and fruits was 169, which were distributed by age and crown-rump length (CRL) to the following groups (Table 1).

The objects under investigation were also distributed by age periodization by R.K. Danilov, T.G. Borova (2003), A.V. Mazurin, I.M. Vorontsov (2009), and included the following periods of prenatal development of a person [1, 4, 12, 21, 23]: embryonic period - from 5 to 6 weeks (35-42 days); embryo-fetal period - from 7 to 9 weeks (43-62 days); early fetal period - from 10 to 28 weeks (63-196 days); late fetal period - from 28 to 38 weeks (197-266 days by R.K. Danilov, T.G. Borova, 2003), [4].

Table 1. Distribution of human embryos and fetuses according to age groups (M±m).

Age (weeks)	Quantity	CRL (mm)
4-5	6	6.100±0.300
6-7	6	15.10±0.60
8-9	7	19.40±0.50
10-11	10	39.02±0.50
12-13	11	58.72±2.27
14-15	12	93.11±5.10
16-17	15	122.2±2.7
18-20	19	152.9±3.5
21-24	20	192.1±1.8
25-28	13	230.9±3.1
29-32	14	264.8±1.7
33-36	20	302.9±1.4
37-38	16	341.5±5.7
Total	169	-

The research has been carried out in accordance with the methodological recommendations "Compliance with ethical and legal norms and requirements in the course of scientific morphological research" and "Procedure for the seizure and use of biological objects from dead persons whose bodies are subject to forensic examination and pathological anatomical investigation for scientific purposes" [10, 13]. To determine morphological changes, general-histological (staining with hematoxylin-eosin) and immunohistochemical methods were used. For quantitative evaluation of the Sox2 transcription factor and expression of cytokeratins, a semi-quantitative method was used, according to which 4 categories were distinguished: 0 (-) - negative reaction (coloration <5% of cells), 1 (+) - weak coloration (positively colored 10-30% of cells), 2 (++) is a moderately pronounced reaction (most of the positively colored cells - 31-60%) and 3 (+++) - intense coloration (> 60% cells or almost all cells of the epithelium are positively colored). The coefficient of expression (CE) was calculated for each observation by the formula: $KE = \Sigma (i \times v)/100$, where i - the intensity of the color in points (from 0 to 3), v - the percentage of stained cells (from 0 to 100% of the most a pronounced reaction in 10 fields of view at x400) for each value of "i". Immunohistochemical research was carried out on the basis of the Vinnitsa Regional Anatomic Pathology Department.

Microscopy and photographing of histological preparations were performed using an optical microscope OLIMPUS BX 41 with magnifications of 40, 100, 200 and 400 times. Receive and process photos, perform

morphometry and statistical processing using the "Quick PHOTO MICRO 2.3" program. When performing morphometric studies were guided by the basic principles laid out in the G.G. Avtandilova (2002) guide [2]. The obtained digital results were processed by a variational statistical method using Student tables.

Results

At the immunohistochemical analysis of GEJ epithelial cell lineage, the Sox2 transcription factor already showed strong expression in the nuclei of epitheliocytes both in the gastric epithelium (Fig. 1) and in the esophageal part of the GEJ (Fig. 2) at the embryonic period of the study. The intensity of the expression of this marker is presented in Table 2.

Upon further study of this marker, we observed its positive conjugation with mainly basal nuclei of epitheliocytes, both on embryo-fetal, and in early fetal periods in both parts. The late fetal period was characterized by a positive strong, sometimes moderate, expression of the transcription factor of Sox2 in the nuclei of basal epitheliocytes, despite its weak marking in the nuclei of surface epitheliocytes of both the gastrointestinal and esophageal parts of GEJ. The most potent expression in the immunohistochemical analysis of the transcription factor of Sox2 was observed in basal epitheliocytes of the gastric part of GEJ in the late fetal period, despite its weak expression, and sometimes the lack of marking in surface epitheliocytes.

Table 2. Intensity of transcription factors Sox2 expression in cytoplasm of epitheliocytes of GEJ (M±m).

Age (weeks)	Sox2	
	Esophagus	Stomach
4-5	2.544±0.163	0.807±0.043
6-7	2.696±0.089	0.727±0.060
8-9	2.763±0.081	0.754±0.047
10-11	2.817±0.054	0.721±0.076
12-13	2.842±0.637	0.739±0.037
14-15	2.805±0.075	0.171±0.039
16-17	2.817±0.064	0.160±0.027
18-20	0.784±0.063	0.169±0.025
21-24	0.779±0.044	0.221±0.171
25-28	0.810±0.053	0.401±0.229
29-32	0.795±0.044	0.401±0.229
33-36	0.780±0.044	0.293±0.176
37-38	0.814±0.073	0.336±0.209

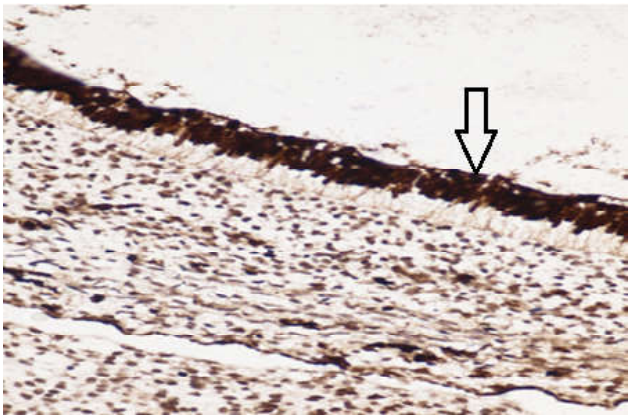

Fig. 1. A strong expression of Sox2 in the nuclei of the epithelial cells of GM is indicated by an arrow. Stomach of embryo 4-5 weeks with CRL 6.1±0.3 mm. Immunohistochemical labeling with Sox2, x400.

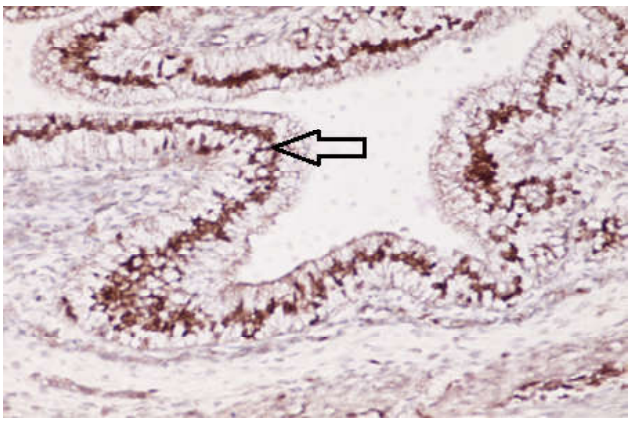

Fig. 2. The Sox2 strong expression in the epithelial cells of the esophageal part of the GEJ is marked with an arrow. Esophagus of embryo 6-7 weeks with CRL 15.1±0.6 mm. Immunohistochemical labeling. Sox2, x400.

The cytoplasmic marker of epithelial differentiation of high molecular weight cytokeratin 7 (CK7) during the embryonic period of the observation showed poor expression predominantly in the apical parts of the epithelial cell lineage of the esophagus and the stomach (Fig. 3). It intensively (+++) intensified during the formation of gastric pits, coinciding with the data of the next study [1, 21, 28], also in the gastral part of GEJ and at the beginning of the early fetal period in the esophageal part of the GEJ (Table 3).

The feature of its marking was the positive coloration of

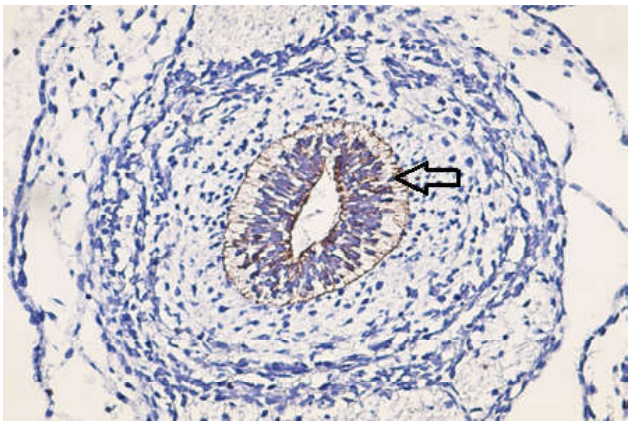

Fig. 3. Weak expression of CK7 in the apical part of the esophagus epithelium cytoplasm is marked with an arrow. Esophagus of embryo 4-5 weeks with CRL 6.1±0.3 mm. Immunohistochemical labeling with CK7. x200.

Table 3. Intensity of expression of cytokeratin 7 in cytoplasm of epitheliocytes of GEJ (M±m).

Age (weeks)	Cytokeratin 7	
	Esophagus	Stomach
4-5	0.230±0.080	0.149±0.027
6-7	0.264±0.081	0.232±0.148
8-9	0.885±0.200	0.334±0.168
10-11	2.549±0.170	0.345±0.168
12-13	0.252±0.173	0.736±0.099
14-15	-	0.794±0.006
16-17	-	0.753±0.116
18-20	-	0.781±0.098
21-24	-	0.817±0.106
25-28	-	0.809±0.132
29-32	-	0.810±0.065
33-36	-	0.848±0.065
37-38	-	0.821±0.622

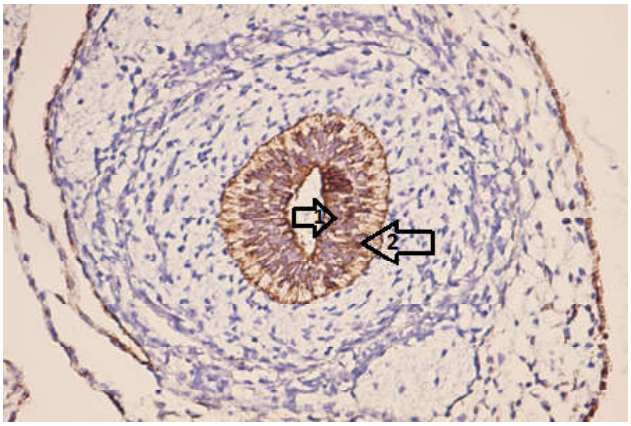

Fig. 4. Positive strong expression of CK8/18 in basal (arrow 1) and apical (arrow 2) cytoplasm epithelial cells and basal membrane of the esophagus. Esophagus of embryo 4-5 weeks with CRL 6.1±0.3 mm. Immunohistochemical labeling with CK8/18, x200.

this cytokeratin in undifferentiated epitheliocytes of gastric mucosa. Subsequently, the marking of CK7 increased from moderate at 9 week to a strong coloring at 11 week, which coincided with the acquisition of the properties of ciliated pseudostratified columnar epithelium. Cytokeratin 7 disappears already at the stratified squamous epithelium stage, cytokeratin 8 is enhanced in the stomach, and completely disappears in the esophageal epithelium at 37 week.

Immunohistochemical analysis of the cytokeratin 8 (CK8/18) in the GEJ epithelial cell lineage in the embryonic period (5-7 weeks) has established its moderate, sometimes vigorous expression, both in the apical and basal parts of the esophagus and stomach cytoplasm epitheliocytes. It should be noted that along with positive marking of cytoplasm, quite characteristic was fairly typical and strong expression of the marker in the basal membrane, which is stained in brown and well observed (Fig. 4).

Cytokeratin 8/18 was detected in the cytoplasm and plasmalemma of spinosum epitheliocytes of GEJ with perinuclear region localization of granules. In most cells, they were evenly distributed. Cytokeratins 8/18 coexpression observed in both esophageal and gastric epithelium of GEJ, while marking was intense in the early period of embryogenesis and insignificant at later dates (tab. 4).

Cytokeratin 8/18 is registered in plasmalemma in the esophagus up to 21 weeks and disappears from the 24 gestational weeks. At the end of the late fetal period, the epithelium of the esophageal part of the GEJ is negative in the esophagus, but with the appearance of a stratified squamous epithelium, it appears cytokeratin14 in basal epitheliocytes, which coincides with the subsequent study [15, 25, 26].

In the gastric part of the GEJ epithelial cell lineage, the expression of CK8/18 was moderate with a diffuse

Table 4. Intensity of expression of cytokeratin 8/18 in cytoplasm of epitheliocytes of GEJ (M±m).

Age (weeks)	Cytokeratin 8/18	
	Esophagus	Stomach
4-5	2.480±0.159	2.484±0.162
6-7	0.418±0.245	2.516±0.117
8-9	0.267±0.126	2.681±0.069
10-11	2.490±0.088	2.530±0.117
12-13	0.816±0.180	0.721±0.176
14-15	0.774±0.112	0.756±0.071
16-17	0.790±0.073	0.707±0.178
18-20	0.774±0.042	0.682±0.122
21-24	0.714±0.054	0.837±0.070
25-28	-	0.763±0.055
29-32	-	0.847±0.091
33-36	-	0.817±0.071
37-38	-	0.815±0.073

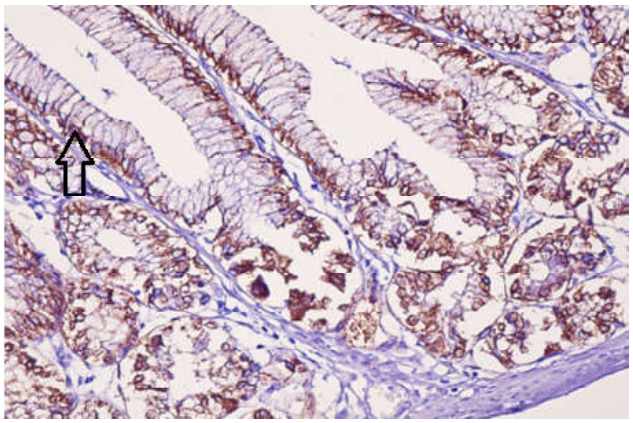

Fig. 5. Positive weak perinuclear expression of CK8/18 in the basal parts of the surface epithelium and glandular exocrinocytes is indicated by an arrow. Fetal stomach, 37-38 weeks with CRL 341.5±5.7 mm. Immunohistochemical labeling with CK8/18. x200.

distribution pattern of cytokeratins in the cytoplasm of epitheliocytes throughout the entire observation period. Marking prevailed in the gastric mucosa, where non-differentiated gastric epitheliocytes were localized (Fig. 5).

At immunohistochemical analysis of expression of cytokeratin 14 (CK14) it was found that it exhibited strong conjugation with basal epitheliocytes in the esophageal part of MM GEJ in the fetal period. From the 17th week, its appearance in the cytoplasm and plasmalemma basal epitheliocytes of the esophageal unit GEJ was recorded despite weak, sometimes moderate markings in the plasmalemma of suprabasal and superficial epitheliocytes. In this case, the positive marking remained in the data structural elements of MM GEJ throughout the fetal period to 38 weeks. The expression of this marker was absent in both the esophagus and the gastrointestinal part of the GEJ in the embryonic, embryo-fetal and early fetal periods. Also, its expression was negative in the epithelium of cardia part gastric mucosa in the late fetal period. It should be noted that in the fetal period, its expression in the cytoplasm coincided with the appearance in nuclei transcription factor p63 in the basal epitheliocytes of the esophageal part of the GEJ.

Thus, the data we obtained from the immuno-histochemical analysis of GEJ epithelial cell lineage allow us to estimate the biological potential of cells, to establish tissue and organ affinity, and can be widely used in the diagnosis of non-tumor nature and tumors of the gastrointestinal tract to facilitate the accurate classification of tumors and to obtain significant prognostic information when use of new molecular targeting therapy [22, 23, 24].

Discussion

The study of patterns of the implementation of mechanisms of histogenesis (a set of processes that lead to the formation and restoration of tissues in the course of individual development) is now impossible without determining the role of these processes of stem and progenitor cells, the peculiarities of the development and interaction of different cellular clones in the early stages of histogenesis [7, 17, 22]. Intensive study of stem cells significantly increased the level of our knowledge about the molecular genetic mechanisms of histogenesis and the development of methods for their regulation. Stem cells are a hierarchy of special undifferentiated pluripotent cells of living organisms that can asymmetrically divide with the formation of a similar parent (self-reproduction) and a new (progenitor) cell that is differentiated into a certain type of cell. Progenitor cells, in contrast to pluripotent stem cells, have stable biomarkers to distinguish between them and their offspring from cells of other cell lineages, the ability to proliferate is much lower than that of pluripotent stem cells. As for the epithelial cell lineage of both the esophagus and GEJ, the issue of identification of the stem cell precursor remains open today. Thus, their role is mainly offered by basal epitheliocytes of the epithelial cell lineage, but various authors find cells with various molecular genetic markers. Thus, basal epitheliocytes with positive expression of the transcription factor p63 were proposed by some researchers [13, 17], other authors - CD34 [17, 21], as well as cells with positive expression of the transcription factor of Sox2 [22]. In our opinion, this is due to the fact that the stem cell precursor of the epithelial cell lineage, due to heterogeneity, that is, the expression of several different transcription factors, can be differentiated in different directions. Further switching or shutdown of a particular transcription factor under the influence of factors not yet known to date leads to a change in the cellular phenotype. Thus, in our previous study, we recorded the disappearance of the expression of the transcription factor p63 at the end of the embryonic stage of embryogenesis (7 weeks), resulting in the appearance of a new epithelial cell lineage in the mucosa membrane of GEJ, in the esophagus part of the ciliated pseudostratified columnar epithelium, and in the cardia part - cuboidal and over time, the columnar epithelium, which remained negative for marking p63 until the end of the study. In the esophagus part with the appearance of a stratified squamous epithelium, the transcription factor p63 reappeared in basal epitheliocytes of stratified squamous epithelium [7, 16].

Unlike p63, the transcription factor of Sox2 was observed at all terms of the observation, which was detected predominantly in the nuclei of basal epitheliocytes of GEJ, consistent with the results of subsequent studies [25, 26, 27]. It should be noted that GEJ epithelial cell lineage cells had a strong positive expression for several molecular genetic markers, such as p63, Sox2, CK14, CK8/18, weak for CK7 for 4-6 weeks of the embryonic period. This confirms the presence in this epithelial cell lineage of pluripotency of the properties of stem cells. Over time, from 7-8 gestational weeks, these cells lost the ability to express one or another molecular genetic marker, indicating their transdifferentiation to the progenitor cell (stem cell precursor) of GEJ epithelial cell lineage.

The weak expression of CK7 in the apical sections of the esophagus epitheliocytes of the esophagus was observed by us from 5 week, which does not coincide with the data of the subsequent studies that recorded its appearance from 12 week of gestation with respect to cytokeratin 8/18, then its labeling is consistent with the results of foreign studies that also noted its expression at the early embryonic period. In the epithelial cell lineage of the gastric part of GEJ, the expression of CK8/18 was moderate and, unlike the esophagus, remained throughout the study period.

According to our data, cardia part of gastric mucosa is congenital rather than the result of meta-plastic transformations that coincided with the work of foreign authors [8, 16, 21, 26, 27]. From 5 to 7 weeks, the epithelial cell lineage remains heterogeneous with the properties of both the esophagus, gastric and intestinal phenotypes, differentiation begins with 8 weeks, determination and specialization in stratified squamous epithelium in the stomach from 10 weeks. Thus, based on our data on expression of transcription factors and cytokeratins, the GEJ

epithelial cell lineage can distinguish pluripotent stem cells with heterogeneous properties present at 4-6 weeks and have positive expression for p63, Sox2 CK7, CK8/18, and CK14, indicating their ability to differentiate into various cellular phenotypes.

Based on the data obtained in this and previous studies, the stem cell precursor stratified squamous epithelium in our opinion is those that had positive expression of p63, CK14 but lost the ability to express CK7, CK8/18 for stratified squamous epithelium. As for the columnar epithelium cardia part of GEJ, for its stem cell precursor, the positive expression of CK7 and CK8/18 was characteristic on all observation periods, with the advantage of marking CK8/18 and negative for p63 starting from 7-8 gestational weeks, despite weak expression Sox2 on all terms of the study.

The results of our study may be useful in developing methods for purposeful correction of key mechanisms of histo-, morpho-, organogenesis, as well as the formation of a new direction in science - regenerative biology and medicine. The most promising direction for this is the use of genetic, cellular, tissue and organ biotechnologies for the treatment of various diseases, as well as the cloning of cells and animals [15, 20].

Thus, the data we obtained from the immuno-histochemical analysis of GEJ epithelial cell lineage allow us to estimate the biological potential of cells, to establish tissue and organ affinity, and can be widely used in the diagnosis of non-tumor nature and tumors of the gastrointestinal tract to facilitate the accurate classification of tumors and to obtain significant prognostic information when use of new molecular targeting therapy [12, 23, 24].

Further studies and the establishment of the patterns of expression of the transcription factor of Sox2 and human cytokeratins in the GEJ epithelial cell lineage in the prenatal period of ontogenesis will complement current data on its morphology and increase the accuracy of the diagnosis and evaluation of pathological changes in the GEJ mucosa in various GEJ diseases.

Conclusions

1. The expression of the transcription factor of Sox2 was observed predominantly in basal epitheliocytes of GEJ and in all terms of observation, which may indicate its central role in the development, differentiation and formation of the GEJ epithelial cell lineage. The transcription factor p63 is involved in the formation of stratified squamous epithelium, its moderate expression was characteristic of the undifferentiated epithelium in the embryonic period and the already differentiated epithelium of the late fetal period. Its disappearance of the "exception" at the 8th gestational week in cardia mucous membrane of GEJ indicates transdifferentiation, a change in the cellular phenotype on the columnar epithelium.

2. The distribution of cytokeratins was characterized by heterogeneity, with the expression of cytokeratin 7 being positive in the cytoplasm of spinosum epitheliocytes, despite the negative expression in the basal layer. It showed weak expression in epitheliocytes of the esophageal part of the GEJ in the embryonic period with an increased reaction in the embryo-fetal period and subsequently disappeared from the 14th week in the early fetal period. For cardia mucous membrane of GEJ was characterized its moderate expression on all terms of observation

3. Cytokeratin 8/18 is an embryo-fetal for the esophagus part of the esophagus, as it was determined in the early periods of embryogenesis and disappears in the late period (28-38 weeks). Cardia of the mucous membrane of GEJ was characterized by its moderate expression on all terms of observation.

4. Cytokeratin 14, in contrast to CK7 and CK8/18, has been localized in the cytoplasm and membranes of basal epitheliocytes of the esophageal part of the GEJ mucosa membrane from the 17th gestational week and was absent in the gastral part of the GEJ throughout the prenatal period.

5. Based on the data of immunohistochemical analysis, it is possible to separate the major GEJ epithelial cell lineage in the prenatal period of ontogenesis: 4-6 gestational weeks - pluripotent stem cells with positive expression of p63, Sox2, CK8/18, CK7; 7-38 weeks - progenitor cell stratified squamous epithelium of the esophageal part of GEJ with positive expression of Sox2, p63, CK14; 14-38 weeks - progenitor cell of columnar epithelium cardia part of GEJ with positive expression of Sox2, CK8/18, CK7.

References

[1] Ahmed, Y. A., El-Hafez, A. A. E., & Zayed, A. E. (2016). *Histological and Histochemical Studies on the Esophagus, Stomach and Small Intestines of Vara-nus niloticus.* arXiv preprint arXiv: 1610.01717.

[2] Avtandilov, G. G. (2007). *Basics of pathoanatomical practice. Manual (third edition amended).* M.: Russian Medical Academy of Postgraduate Education.

[3] Chen, X., Qin, R., Liu, B., Ma, Y., Su, Y., Yang, C. S., ... & Shaheen, N. J. (2008). Multilayered epithelium in a rat model and human Barrett's esophagus: similar expression patterns of transcription factors and differentiation markers. *BMC gastroenterology,* 8(1), 1. doi: 10.1186/1471-230X-8-1.

[4] Danilov, R. K. & Borovaya, T. G. (2003). *General and medical embryology.* SPb.: SpecLit. ISBN: 5-299-00208-4

[5] De Hertogh, G., Van Eyken, P., Ectors, N., & Geboes, K. (2005). On the origin of cardiac mucosa: A histological and immunohistoc-hemical study of cytokeratin expression patterns in the developing esophagogastric junction region and stomach. *World journal of gastroenterology: WJG,* 11(29), 4490. doi: 10.3748/wjg.v11.i29.4490.

[6] DeWard, A. D., Cramer, J., & Lagasse, E. (2014). Cellular heterogeneity in the mouse esophagus implicates the presence of a nonquiescent epithelial stem cell population. *Cell reports*, 9(2), 701-711.

[7] Gunther, C., Neumann, H., & Vieth, M. (2014). Esophageal epithelial resistance. *Dig Dis,* 32, 6-10.

[8] Jacobs, I. J., Ku, W. Y., & Que, J. (2012). Genetic and cellular mechanisms regulating anterior foregut and esophageal

development. *Developmental biology,* 369(1), 54-64.
[9] Jazii, F. R. (ed.) (2012). Esophageal Cancer: Cell and Molecular Biology, Biomarkers, Nutrition and Treatment. *Intech. P.* ISBN: 978-953-51-0223-6
[10] Kalabis, J., Oyama, K., Okawa, T., Nakagawa, H., Michaylira, C. Z., Stairs, D. B., ... & Rustgi, A. K. (2008). A subpopulation of mouse esophageal basal cells has properties of stem cells with the capacity for self-renewal and lineage specification. *The Journal of clinical investigation,* 118(12), 3860-3869.
[11] Kulinichenko, V. L., Mishalov, V. D., Tchaikovsky, Yu. B., Pustovit, S. V., & Voichenko, V. V. (2007). Compliance with ethical and legislative norms and requirements in the course of scientific morphological research. *Morphology*, 1(4), 134-135.
[12] Mazurin, A. B. & Vorontsov, A. B. (2009). *Propedeutics of childhood diseases*. Foliant, Russia. ISBN: 978-5-93929-184-2
[13] McKeon, F. (2004). p63 and the epithelial stem cell: more than status quo? *Genes & development,* 18(5), 465-469.
[14] Mishalov, V. D., Voychenko, V. V., Malysheva, T. A., Dibrova, V. A., Kuzik, P. V., & Yurchenko, V. T. (2018). The procedure for the extraction and use of biological objects from dead persons whose bodies are subject to forensic examination and pathologoanatomical research, for scientific purposes. *Special edition of the newspaper "Osvita Ukrainy"*, 3-13.
[15] Namiot, Z., Sarosiek, J., Marcinkiewicz, M., Meade, C., & Edmunds Richard, W. (1994). McCallum Declined human esophageal mucin secretion in patients with severe reflux esophagiti. *Digestive Diseases and Sciences December,* 39(12), 2523-2529.
[16] Özefagus, ve Mide Gelişimi. (2017). Development of the esophagus and stomach. *Bezmialem Science,* 5, 175-82. DOI: 10.14235/bs.2017.811.
[17] Rishniw, M., Rodriguez, P., Que, J., Burke, Z. D., Tosh, D., Chen, H., & Chen, X. (2011). Molecular aspects of esophageal development. *Annals of the New York Academy of Sciences,* 1232(1), 309-315. doi: 10.1111/j.1749-6632.2011.06071.x.
[18] Sapin, M. R., Nikolenko, V. N., Chava, S. V., Alekseeva, T. N., & Nikityuk, D. B. (2013). Questions classification and morphogenesis of the glands of the walls of hollow internal organs. *Journal of Anatomy and Histopathology*, 1, 9-17.
[19] Sadler, T. V. (2001). *Medical Embryology by Langman* (textbook). Translation from English Edited by O.D. Lutsyk. Lviv: Nautilus. ISBN: 966-95745-3-6.
[20] Seery, J. P. (2002). Stem cells of the oesophageal epithelium. *Journal of cell science,* 115, 1783-1789.
[21] Ventura, A., do Nascimento, A. A., dos Santos, M. A. J., Vieira-Lopes, D. A., Sales, A., & Pinheiro, N. L. (2013). Histological Description of Morphogenesis of the Gastroesophageal Mucosa of Gallus gallus Domesticus (Linnaeus, 1758). *International Journal of Morphology,* 31(4), 1331-1339. DOI: 10.4067/S0717-95022013000400030
[22] Wang, D. H., Tiwari, A., Kim, M. E., Clemons, N. J., Regmi, N. L., Hodges, W. A., ... & Zhang, Q. (2014). Hedgehog signaling regulates FOXA2 in esophageal embryogenesis and Barrett's metaplasia. *The Journal of clinical investigation,* 124(9), 3767-3780. doi: 10.1172/JCI66603.
[23] Wang, X., Ouyang, H., Yamamoto, Y., Kumar, P. A., Wei, T. S., Dagher, R., ... & Crum, C. P. (2011). Residual embryonic cells as precursors of a Barrett's-like metaplasia. *Cell,* 145(7), 1023-1035. doi: 10.1016/j.
[24] Weaver, J. M., Ross-Innes, C. S., Shannon, N., Lynch, A. G., Forshew, T., Barbera, M. ... Fitzgerald, R. C. (2014). Ordering of mutations in preinvasive disease stages of esophageal carcinogenesis. *Nature genetics,* 46(8), 837-843. doi: 10.1038/ng.3013
[25] Willet, S. G., & Mills, J. C. (2016). Stomach organ and cell lineage differentiation: from embryogenesis to adult homeostasis. *Cellular and molecular gastroenterology and hepatology,* 2(5), 546-559. DOI: 10.1016/j.jcmgh.2016.05.006
[26] Zhang, Y., Jiang, M., Kim, E., Lin, S., Liu, K., Lan, X., & Que, J. (2017). Development and stem cells of the esophagus. In: *Seminars in cell & developmental biology,* 66, 25-35. Academic Press. doi: 10.1016/j.semcdb.2016.12.008
[27] Zhou, H., Greco, M. A., Daum, F., & Kahn, E. (2001). Origin of cardiac mucosa: ontogenic consideration. *Pediatric and developmental pathology,* 4(4), 358-363.

РОЛЬ ТРАНСКРИПЦІЙНОГО ФАКТОРА SOX2 ТА ЦИТОКЕРАТИНІВ У ФОРМУВАННІ ТА СТАНОВЛЕННІ ЕПІТЕЛІАЛЬНОГО ДИФЕРОНУ ГАСТРОЕЗОФАГЕАЛЬНОГО З'ЄДНАННЯ

Рекун Т.О., Вернигородський С.В., Кисельова Т.М., Татаріна О.В., Черепаха О.Л.

В літературі неодноразово обговорювали питання щодо джерела походження епітелію слизової оболонки кардіальної частини шлунка та пропонували різні варіанти трансформації епітелію як прояву нормальної анатомічної особливості людини, так і внаслідок зміни програми диференціювання стовбурової клітини, міграції клітин кісткового мозку, трансдиференціації одношарового циліндричного епітелію. Ймовірно, це пов'язано з труднощами вивчення незначного за розмірами епітелію слизової оболонки власне кардії й встановленням зв'язку дуоденогастроезофагеального рефлексу з розвитком метаплазії в епітелії слизової оболонки термінального відділу стравоходу, котрий нагадує його будову в кардіальному відділі шлунку. Мета дослідження - вивчити експресію транскрипційного фактора Sox2 та розподіл цитокератинів в епітелії гастроезофагеальної зони (ГЕЗ) на етапах ембріонального та фетального періодів онтогенезу. Згідно з метою дослідження використали імуногістохімічний аналіз епітеліального диферону стравохідно-шлункового переходу (СШП). Дослідження виконано на 169 ембріонах та плодах людини віком від 4-5 до 38 тижнів внутрішньоутробного розвитку. Встановлено, що транскрипційний фактор Sox2 експресується в базальних епітеліоцитах ГЕЗ на всіх термінах спостереження та виконує головну роль у розвитку, диференціації та становленні епітеліального диферону ГЕЗ. Особливістю експресії цитокератину 7 було позитивне маркування у цитоплазмі остистих епітеліоцитів попри негативну експресію в базальному шарі. Він проявив слабку експресію в епітеліоцитах стравохідної частини ГЕЗ в ембріональному періоді з посиленням реакції у ембріофетальному періоді та з подальшим зникненням, починаючи з 14 тижня у ранньому фетальному періоді. Для кардіальної слизової оболонки ГЕЗ була характерна його помірна експресія на всіх строках спостереження. Цитокератин 8/18 є ембріофетальним для стравохідної частини стравоходу, так як визначається на ранніх періодах ембріогенезу та зникає у пізньому періоді (28-38 тижнів). Для кардіальної слизової оболонки ГЕЗ була характерна його помірна експресія на всіх строках спостереження. Цитокератин 14, на відміну від СК7 та СК8/18, локалізувався в цитоплазмі та мембранах базальних епітеліоцитів стравохідної частини слизової оболонки ГЕЗ починаючи з 17 гестаційного тижня та був відсутнім у шлунковій частині СШП упродовж всього пренатального періоду. Таким чином, отримані нами дані щодо експресії

транскрипційного фактора Sox2 та цитокератинів в епітеліальному диферoні ГЕЗ у пренатальному періоді онтогенезу дозволять підвищити точність діагностики при визначенні тканинної або органної належності та можуть широко застосовуватися при різних захворюваннях СШП.
Ключові слова: *гастроезофагеальне з'єднання, імуногістохімічний аналіз, транскріпційний фактор Sox2, цитокератини, пренатальний онтогенез.*

РОЛЬ ТРАНСКРИПЦИОННОГО ФАКТОРА SOX2 И ЦИТОКЕРАТИНОВ В ФОРМИРОВАНИИ И СТАНОВЛЕНИИ ЭПИТЕЛИАЛЬНОГО ДИФФЕРОНА ГАСТРОЭЗОФАГЕАЛЬНОГО СОЕДИНЕНИЯ

Рекун Т.А., Вернигородский С.В., Киселёва Т.М., Татарина О.В., Черепаха Е.Л.

В литературе неоднократно обсуждали вопрос относительно источника происхождения эпителия слизистой оболочки кардиальной части желудка и предлагали различные варианты трансформации эпителия как проявление нормальной анатомической особенности человека, так и вследствие изменения программы дифференцировки стволовой клетки, миграции клеток костного мозга, трансдифференциации однослойного цилиндрического эпителия. Вероятно, это связано с трудностями изучения незначительного по размерам эпителия слизистой оболочки собственно кардии и установлением связи дуоденогастроэзофагеального рефлекса с развитием метаплазии в эпителии слизистой оболочки терминального отдела пищевода, который напоминает его строение в кардиальном отделе желудка. Цель исследования - изучить экспрессию транскрипционного фактора Sox2 и распределение цитокератинов в эпителии гастроэзофагеальной зоны (ГЭЗ) на этапах эмбрионального и фетального периодов онтогенеза. Согласно с целью исследования использовали иммуногистохимической анализ эпителиального дифферона пищеводно-желудочного перехода (ПЖП). Исследование выполнено на 169 эмбрионах и плодах человека в возрасте от 4-5 до 38 недель внутриутробного развития. Установлено, что транскрипционный фактор Sox2 экспрессируется в базальных эпителиоцитах ГЭЗ на всех сроках наблюдения и выполняет главную роль в развитии, диференциации и становлении эпителиальных диффероно в ГЭЗ. Особенностью экспрессии цитокератина 7 была положительная маркировка в цитоплазме остистых эпителиоцитов несмотря на негативную экспрессию в базальном слое. Он проявил слабую экспрессию в эпителиоцитах пищеводной части ГЭЗ в эмбриональном периоде с усилением реакции в эмбриофетальном периоде и с дальнейшим исчезновением, начиная с 14 недели в раннем фетальном периоде. Для кардиальной слизистой оболочки ГЭЗ была характерна его умеренная экспрессия во все сроки наблюдения. Цитокератин 8/18 является эмбриофетальной для пищеводной части ГЭЗ, так как определяется на ранних периодах эмбриогенеза и исчезает в позднем фетальном периоде (28-38 недель). Для кардиальной слизистой оболочки ГЭЗ была характерна его умеренная экспрессия на всех строках наблюдения. Цитокератин 14, в отличие от СК7 и СК8/18, локализовался в цитоплазме и мембранах базальных эпителиоцитов пищеводной части слизистой оболочки ГЭЗ, начиная с 17 гестационной недели, и был отсутствующим в желудочной части ГЭЗ в течение всего пренатального периода. Таким образом, полученные нами данные экспрессии транскрипционного фактора Sox2 и цитокератинов в эпителиальном дифферoне ГЭЗ в пренатальном периоде онтогенеза позволят повысить точность диагностики при определения тканевой или органной принадлежности и могут широко использоваться при различных заболеваниях ПЖП.
Ключевые слова: *гастроэзофагеальное соединение, иммуногистохимический анализ, транскрипционный фактор Sox2, цитокератины, пренатальный онтогенез.*

DOI: 10.31393/morphology-journal-2018-24(4)-10 Reports of Morphology, Vol. 24, №4, Pages 66-73

ISSN 1818-1295 eISSN 2616-6194

REPORTS OF MORPHOLOGY

Official Journal of the Scientific Society of Anatomists, Histologists, Embryologists and Topographic Anatomists of Ukraine

journal homepage: https://morphology-journal.com

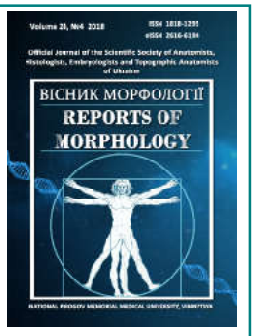

Pathological changes on basis of ischemia with associated virus infection in mice brain

Turchyna N.S.[1], Savosko S.I.[1], Ribalko S.L.[2], Starosila D.B.[2], Kolisnik D.I.[1]

[1]National Medical University named after O.O. Bohomolets, Kyiv, Ukraine;
[2]State Enterprise "Institute of Epidemiology and Infectious Diseases named after. L.V. Gromashevsky National Academy of Science of Ukraine", Kyiv, Ukraine

ARTICLE INFO
Received: 28 September, 2018
Accepted: 15 November, 2018

UDC: 616.832-005.4-092:616.9:578]

CORRESPONDING AUTHOR
e-mail: ntlturchina12@ukr.net
Turchyna N.S.

The global literature constantly receives new data showing the infectious pathogens as factors for development of atherosclerosis and acute cerebrovascular pathology, and the data showing the predictors of pathology of the heart-vessels as markers of inflammation. The results of research about the connection between the infectious agents and atherosclerosis are ambiguous, and the attempts to prove such connection have encouraged the experiments where the infectious agents with atherogenesis are modeled in animals. The connection of this data with ischemic lesion of brain is not properly explored, but certain experimental research show progressive degeneration in brain hemorrhage in mice with herpes virus 1 (HSV1) due to the post-stroke immunosuppression and reactivation of the infectious agent. The aim of this work is to explore experimentally the possible connection between the herpetic infection and the ischemic lesion to the cortex of mice. To achieve this goal we formed 5 groups of experimental animals (mice) for investigation into the possibility of connection between herpes infection and ischemiazaition of brain: 1st group (n=52) - with cholesterol diet; 2nd group (n=23) - with HSV1; 3d group (n=30) - with unilateral occlusion of the common carotid artery; 4th group (n=10) - with HSV1 and occlusion of the common carotid artery; 5th group (n=6) - with cholesterol diet, HSV1, occlusion of the common carotid artery. The microscopic slides evaluated changes morphometrically in the density of the neurons of the neocortex in the ocular of parietal temporal fields of the brain and the hippocampus. The results were processed statistically with Origin Lab 8.0. A probable increase in structural changes was identified in group 5 (with three pathological factors respectively) of the combined model compared to models without association and/or with several pathological signs from the groups 1-4 (1, 2, 3, 4). Comparison of the results between the 1-4th and 5th groups showed a significant increase in the relative number of neurons with cytopathological signs (hemochromatosis, deformation of the perikaryon, karyopyknosis), which may testify in favor of a sufficiently rapid lesion of the pyramidal neocortex neurons influenced by two or more pathological signs. The reduction in the density of pyramidal neurons in the temporal and/or temporal cortex in the combined model with ischemiazaition and viral association in was had greater probability compared to the models formed with only one risk factor. The revealed increase in the degree of neocortex induction during brain cerebral ischemia in mice with herpes infection is an evidence of possible connection between the two.

Keywords: *brain, mice, ischemia, viral infection.*

Introduction

In the world literature, there is a growing number of data indicating some infectious agents, as factors in the development of atherosclerosis (AS) and acute cerebrovascular pathology (ACP), and about the predictors of acute cardiovascular disease as markers of inflammation. The ambiguous results of the research on the relationship between infection and atherosclerosis and attempts to prove the existence of such an association have led to attempts to simulate infection-associated atherogenesis in animals [4, 10, 11, 21]. In the experimental work M.V. Avdeyev and colleagues in 2012 give data on the impact of various infectious agents on the development and progression of

atherosclerosis [3]. A study by R. Sorrentino et al. (2015) demonstrated the possibility of inducing AS by infection C. pneumoniae in the absence of hypercholesterolemia [25, 26].

One of the possible causes of damage to the arterial wall and, as a consequence, the development of atherogenesis, is herpesviruses [17, 30]. The role of herpes viruses, as etiologic factors of AS, has been thoroughly investigated in recent years and is now supported by numerous data. There is growing evidence of the involvement of viruses Herpes viridae (Herpes simplex virus (HSV) 1 and type 2, type 3 (VZV), Epstein-Barr virus (EBV), cytomegalovirus (CMV) in the processes of damage and maintenance of endothelium inflammation, accumulation cholesterol, changes in the coagulation properties of the endothelium, increased thrombogenesis [5, 18, 25]. HSV types 1 and 2 were found in the aorta and carotid artery of patients with AS of vessels [7, 20, 24]. In the in vitro study, it was found that HSV type 1 enhances absorption of low density lipoproteins by endothelial cells, and saturated cholesterol esters and triglycerides in unbranched cells [6, 16]. An experiments have shown that the Marek virus (herpes virus of birds) causes atherosclerotic changes in chickens [10]. D.G. Alber et al. (2000) demonstrated that infection with murine γ-herpesvirus-68 leads to AS in apoE-/-mice [1]. D.G. Alber et al. (2002) conducted another study that proves that the development of AS is the result of a specific manifestation of a specific viral infection rather than a systemic immune response to the presence of any HSV [2]. Thus, the literature describes the results of only a few studies devoted to the study of the relationship between the persistence of herpes viruses and the development of atherogenesis, but some contradictory data question the participation of the viral factor directly in its launch, emphasizing the complicity of infectious agents in the already initiated inflammation of the vascular wall, damage to the endothelium. The association of these changes with ischemic brain damage is even less researched, although some experimental studies have shown progressive degeneration in the brain of mice infected with HSV type 1, due to post-stroke immunosuppression and reactivation of the infectious agent [14, 22]. Understanding of the problem of herpes-associated atherosclerosis is facilitated by more recent experimental studies conducted.

The *purpose* of the work is to investigate in the experiment the possible connection between herpetic infection and ischemic damage to the cerebral cortex of mice.

Materials and methods

To investigate the possible relationship between the development of herpetic infection and cerebral ischemia, we have formed 5 groups of experimental animals (mice): 1 group (n=52), diet using cholesterol, group 2 (n=23) with HSV1 infection, group 3 (n=30) with unilateral occlusion of the common carotid artery (OCCA), group 4 (n=10) with HSV1 and OCCA infections, group 5 (n=6) with HSV1 infection, cholesterol diet and OCCA. Additionally, an additional control group (intact animals) is included.

For reproduction of dyslipidemia and structural changes in blood vessels of animals, 1 group was kept on a "cholesterol diet" [28] on the basis of granulated feed that additionally contained animal and vegetable fats, cholesterol (the quantitative composition of the atherogenic diet per 100 g of the finished product included: heat treated animal fats (pork fat, butter) - 30-45 g; heat-treated vegetable fats (margarine) - 15-20 g; cholesterol - 1.5-2 g; calcium carbonate (CaCO3) - 1 g; Mercazolil (1-methyl-2-mercapto-imidazole with the addition of potatoes starch, calcium stearate, refined sugar, talc) - 10 mg (equivalent to a daily dose animals - 10 mg/kg), which speeds up the metabolism and elimination of various hospital facilities; standard granulated feed - 32-52 g). Duration of the diet is 12 weeks.

Animals of the 2nd group infected HSV1 by the method described in the papers [14, 15, 22]. Manipulation with infected animals was carried out at the "Institute of Epidemiology and Infectious Diseases named after. L.V. Gromashevsky NAMS of Ukraine" (Head of the Laboratory of Experimental Chemotherapy of Viral Infections, MD, Prof. S.L. Rybalko). Animals of 1 and 2 groups were withdrawn from the experiment for 12 weeks by decapitation.

OCCA of animals from group 3 were done by imposing a ligature on the right common carotid artery (suture material 6/0, Ethilon, J & J) [19]. Surgical access to the artery was carried out under anesthesia (sodium thiopental, 40 mg/kg, intraperitoneally, 2% solution of lidocaine, 0.3 ml locally). The animals were withdrawn from the experiment on 1, 2, 3 and 4 days after OCCA by decapitation.

The brain of control and experimental animals was selected for histological examination. Brain samples were fixed in 10% neutral formalin solution. After dehydration in the rising concentrations of ethanol, dioxane and xylene, the material was poured into paraffin. Paraffin sections 4-6 microns thick colored with toluidine blue by Nissl, hematoxylin with eosin [23].

By micropreparations evaluated morphometrically changes in the density of the neurons of the neocortex of the parietal, temporal parts of the brain and the hippocampus. For this purpose, photographs of the same areas of the parietal, temporal, and hippocampal neocortex with the Olympus BX 51 microscope using the CarlZeiss software (AxioVision SE64 Rel.4.9.1) determined the total neuron density in the test area (microphotograph) and the number of damaged neurons (hyperchromatosis, deformation, neuronal edema).

Statistical processing of the results was carried out using the Origin Lab program, version 8.0. Normal distribution of results is estimated by the Kolmogorov-Smirnov criterion. Intergroup discrepancies between groups of samples were evaluated using nonparametric Kruskal-Wallis test (Kruskal-Wallis ANOVA). The results are presented as median (Me) and quartile intervals [Q1-Q3]. The difference was estimated to be significant at $p<0.05$.

Results

The analysis of micropreparations of experimental groups allowed to isolate the main zones and anatomical brain structures that were damaged under the set models of the experiment. Changes were mainly found in the neocortex of parietal, temporal and hippocampal regions. Morphological signs of neurodegeneration and inflammatory reaction were established in the studied brain

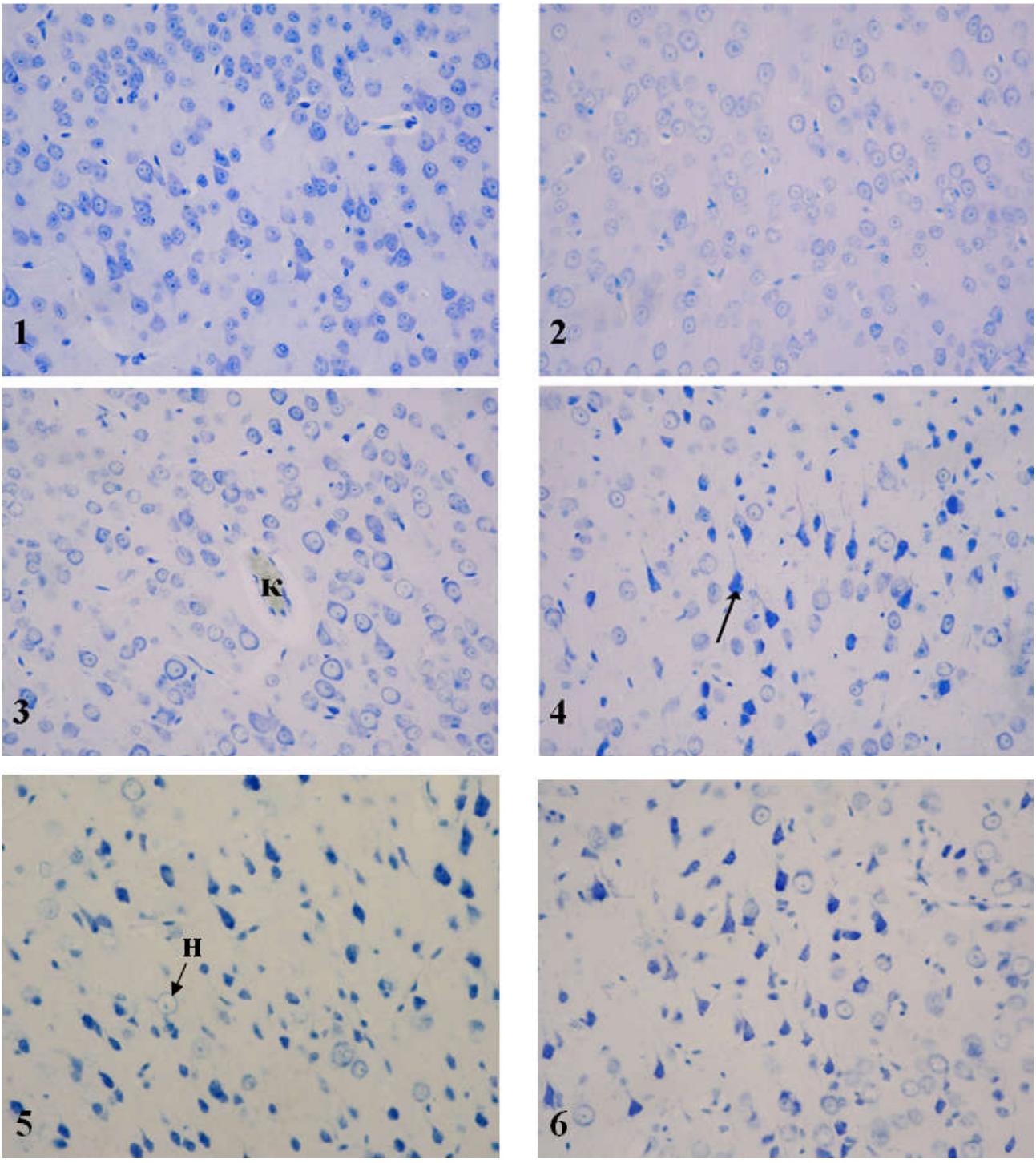

Fig. 1. Morphological manifestations of structural changes in the brain neurons in experimental group of mice. Degeneration of neurons in the parietal cortex of experimental groups. 1 - control; 2 - cholesterol diet, increasing the size of the nucleus of the neurons; 3 - OCCA for 1 day, intact the cerebral cortex; 4 - OCCA for 2 day, degenerative neurons (←); 5 - HSV1 + diet + OCCA for 1 day, degeneration and neuronal edema; 6 - HSV1 + diet + OCCA for 2 day, increase in the number of damaged neurons; к - capillary; н - swelling of the neuron. Toluidine blue. Lens 40, eyepiece 10.

specimens. The manifestation of heterogeneous neuronal damage was hyperchromatosis and deformation of perikaryon and neurites, karyopyknosis or karyolysis. Microphotographs of degenerative changes in the cerebral cortex of the studied groups are shown in Figure 1. In order to assess the type of brain damage of the neurons, the main changes were divided into focal and diffuse. Accordingly, in the first case, deformed neurons were located in separate groups in the parietal and temporal neocortex, in separate sectors of the hippocampus. In the second case, the total loss of neurons and gliocytes was detected by continuous layers of the neocortex or multiple zones, which did not allow estimation of such changes as separate tricks of degeneration (damage) (Fig. 1).

Between the comparison groups, a difference was found between the degree of structural changes:

1 group with cholesterol diet (n=52). In 22 (42.5%) animals of the 52 who took the diet, isolated degenerative neurons were found at the level of parietal and/or temporal neocortex. In 11 (50.0%) out of 22 samples, changes were assessed as diffuse, and in 10 (49.9%) out of 22 as focal. In 11 (21.1%) out of 52 animals, the morphological signs of the inflammatory reaction were observed: focal infiltration of monocytes and lymphocytes in 9 (17.3%) of 52 specimens in the peritoneal mucosa of the trunk, large sulcus, parietal and/or temporal cortex, hippocampus, cortex vessels, corpus callosum and subcortical structures (lateral and dorsomedial zones of the thalamic region), choroidal arteries of the third ventricle (from 2 to 6 foci in the projection of the frontal section of the brain). In 4 samples (7.6%) from 52 along the vessels, foci of infiltration of tissue basophils (from 3 to 16 cells), including degranulation, were recorded.

Group 2 with HSV1 infection (n=23). In 15 (69.5%) animals from 23 who successfully transmitted infection with HSV, degeneration of neurons in the cerebral cortex and hippocampus was established. In 11 (73.3%) of 15 samples, degeneration was assessed as diffuse, and in 4 (26.6%) of 15 as a local (focal). In 12 (52.1%) out of 23 animals, an inflammatory reaction was detected: focal infiltration of macrophages/microglyocytes around small caliber vessels (capillaries, arterioles, venules) in the cerebral cortex, corpus callosum, lateral areas of the thalamic zone.

3 group with OCCA (n=30). The structural changes in the neocortex depended on the time elapsed since the time of the OCCA and assessed as diffusive and focal in the following way: 1 day (n=15) - 40.0% and 13.3% (46.7% unchanged); 2 day (n=5) - 60% and 40.0%; 3 day (n=5) - 60% and 40%; 4 day (n=5) - 83.4% and 16.6%. That is, neurodegenerative changes (karyopyknosis and hyperchromatosis of neurons or hydropic dystrophy) have progressed from focal to diffuse over time after OCCA. Morphological signs of inflammatory reaction were found in only 1 (6.7%) of 15 specimens on 1 day.

Group 4 with HSV1 and OCCA (n=10). Like the OCCA group, diffuse and focal neocortex changes are estimated as follows: 1 day (n=5) - 60% and 20.0% (20.0% unchanged); 2 day (n=5) - 40% and 60.0%. If for 1 day only 1 infiltration focus was registered, then for 2 day from 3 to 14 separate centers. The term of 3 and 4 days was not evaluated due to the 100% mortality of the animals.

Group 5 with HSV1 infection, cholesterol diet and OCCA (n=6). In the neocortex, the focal changes dominated the diffuse ones: 1 day (n=3) - 33.3% and 66.7%; 2 day (n=3) - 100% focal degeneration around monocyte/lymphocyte infiltrates. For 2 day in all studied samples, 4 to 8 inflammation points were recorded. Experiment on days 3 and 4 also ended with 100% lethality, which showed the severity of the somatic state of experimental animals. Table 1 and 2 summarize the results of quantitative evaluation of neuronal density in the parietal region of the neocortex. The probable increase in structural changes in group 5 (with three pathological factors) of the combined model is established in comparison with the models without combination and/or combination of several pathological signs of groups 1, 2, 3 and 4. Comparison of results between 1-4 and 5 groups indicates a statistically significant increase in the relative number of neurons with cytopathological features (hyperchromatosis, deformation of perikaryon, karyopyknosis), which correlates with more pathological signs, and is likely to result in more rapid damage to neocortical pyramidal neurons.

Table 1. Changes in the density of the pyramidal neurons of the III-V layers of the neocortex of the experimental groups (Me [Q1-Q3]) in comparison with the control group.

Group	Neuronal density in the test zone, abs.	Relative number of neurons with signs of degeneration, %
Control	195 [185,7-205,7]	3,3 [1,9-3,9]
HSV-I	169 [157,5-179,5]*	8,98 [7,3-12,9]*
Diet	179 [171,5-186,5]#	11,4 [8,6-17,2] #
OCCA, 1 day	182 [170,2-192,7]	12,9 [7,3-17,1] #
OCCA, 2 day	169,5 [164,5-183]	9,2 [8,2-17,3]#
OCCA, 3 day	164 [154-179]#^	21,3 [20,1-48,5]#*^
OCCA, 4 day	140 [115,5-166,5]#*^	39,1 [22,7-59,2]#*^
HSV1+ OCCA, 1 day	167 [159,7-185,2]	19,4 [14,1-25,0]**
HSV1+ OCCA, 2 day	171,5 [164,5-180,7]	14,7 [9,0-28,0]
HSV1+ diet + OCCA, 1 day	157 [145,5-165] #*&	26,4 [24,8-31,5] #**&
HSV1+ diet + OCCA, 2 day	137 [129-163] #*&	43,0 [39,5-54,6]#*&"**

Notes (here and thereafter): OCCA - occlusion of the common carotid artery; # - p<0,05 compared to control; * - p<0,05 compared to 1 day; ^ - p<0,05 compared to 2 day; ** - p<0,05 compared to HSV-I; & - p<0,05 compared to OCCA; "- p<0,05 compared to HSV1 + OCCA; ! - p<0,05 compared with diffuse degeneration, the same observation period; according to Kruskal-Wallis criterion (Kruskal-Wallis ANOVA).

Table 2. Dependence of density of pyramidal neurons of III-V layers on the nature of changes and development of violations of experimental groups (Me [Q1-Q3]) in comparison with the control group.

Group	Neuronal density in the test zone, abs.	Relative number of neurons with signs of degeneration, %
Control	195 [185,7-205,7]	3,3 [1,9-3,9]
Diffuse degeneration of neuronal changes		
HSV1	169 [157,5-176,5]	10,9 [8,23-13,1]
Diet	184 [179-187]	10,7 [8,6-17,8]#
OCCA, 1 day	174 [162,5-179,5]	16,3 [11,2-20,9] #
OCCA, 2 day	176 [166,2-185]	9,2 [7,5-13,6] #
OCCA, 3 day	164 [148-176,5]	44,1 [19,1-49,2] #^
OCCA, 4 day	137,5 [112,7-170,2]	41,2 [24,8-64,3] #^
HSV1+ OCCA, 1 day	172 [159-185]	16,7 [6,3-30,8] #
HSV1+ OCCA, 2 day	178 [165-189]	13,4 [4,2-20,6] #
HSV1+ diet + OCCA, 1 day	165 [149-170]	26,4 [24,8-28,1] #&
HSV1+ diet + OCCA, 2 day	-	-
Focal degeneration of neurons		
HSV1	154,5 [139-199,2]	7,9 [3,3-12,5] #
Diet	176 [169-184]	13,6 [10,1-19,2] #
OCCA, 1 day	184 [182-196]!	13,1 [8,1-17,3] #
OCCA, 2 day	169 [163-186]	19,3 [8,5-24,2] #
OCCA, 3 day	179 [164-179]	20,1 [20,1-21,7] #
OCCA, 4 day	162 [158-165]	24,0 [19,7-27,2] #
HSV1+ OCCA, 1 day	162 [160-186]	21,4 [17,2-23,1] #
HSV1+ OCCA, 2 day	169 [163-174]	16,0 [10,6-50,3] #
HSV1+ diet + OCCA, 1 day	150 [142-157]	28,6 [25,3-34,5] #!&"
HSV1+ diet + OCCA, 2 day	137 [129-163]	43,0 [39,5-54,6] #!&"

Discussion

Thus, step-by-step experiments allow us to investigate the relationship between the presence of neuroinfection and the level of ischemic brain damage. An analysis of the mortality of animals and the results of histological studies allowed us to conclude that the fastest development of structural changes in the cerebral cortex of the 5th mice group, in which the conditions of the experiment immediately coincided 3 pathological factors: cholesterol diet, neuroinfection and ischemic lesion of the brain.

As indicated in the literature, cerebral ischemia in one-sided OCCA in mice and rats causes damage to the white matter of the brain, mild motor disorders and memory impairment [27, 31], which is a good model for the study of focal hypoxia [14], vascular dementia and neurodegeneration [29]. Changing the diet (cholesterol diet) increases the size of the area of brain damage of mice after a one-sided OCCA [18]. Bilateral OCCA initially causes ischemic tolerance, and later significant dystrophic and necrotic changes in the anatomical brain structures [28].

In our experiment, it has been shown that the addition of dietary fat in the diet of mice causes an increase in proteolytic enzymes in vessels, in particular, MMP-9, which worsens the state of both macro- and microvessels of the cerebral cortex. Ischemia of the brain increases the edema of the brain, the volume of ischemic damage worsens neurological functions in experimental animals [9].

The deterioration of the biochemical processes of the brain after the occlusion of the middle cerebral artery in animals with a fat diet is attributed to disorders of the metabolism carried out by the liver cells [20]. The views on these changes are controversial. Some authors believe that an increase in the level of ketone bodies (acetoacetate and β-hydroxybutyrate) has an effect on the restoration of the energy balance of cells, and may also have a neuroprotective effect [20]. According to another version, high levels of ketone bodies are toxic to the brain, and leads to ketoacidosis [12, 13]. Locomotor activity and changes in biochemical parameters, in particular, TBC-active products, deteriorate in the modeling of brain ischemia on the background of a fatty diet. Conducted clinical studies prove that there is a development of dysmetabolic processes with long-term use of fatty diet, which affects the increase of the area of diffuse changes in damaged brain in the case of ischemia. In his own studies, a fat diet was used to study vascular changes, and a deterioration was observed [3]. It was found that on the background of fatty diet, ultrastructural endothelial and non-stratified cell disorders develop, lipid deposits in vessels are accumulated, which may be considered as an initiatory stage of atherogenesis. OCCA in animals of the 3rd group was considered to a greater extent as a pathogenetically relevant model of brain ischemia. Therefore, the next stage of the experiments was the transfer of infected animals that successfully transmitted infections with neuroinfection, on a fat diet. The acute exacerbation of the inflammatory process and neurodegeneration after OCCA in animals fed fatty foods that successfully transmitted HSV1 contamination was confirmed by the fact that brain ischemia is probable under these conditions, which are factors in the weakening of the body. The increase in the area of the centers of the inflammatory process is due to the reactivation of HSV1, which was found in earlier experiments [8, 14, 15, 31]. The results of the conducted studies allow to broaden the idea of the influence of the viral association on the pathogenesis of ischemic stroke and to understand the role of the vascular wall in these changes.

Prospects for the continuation of experimental studies in the study of the association of viral infection and the development of ischemic stroke, as well as morphological changes in the heart and aorta in the development of the

infectious process and its correction is obvious. The prospect of further development is the study of morphological changes in the heart and aorta in the development of the infectious process and its correction.

Conclusions

1. OCCA caused a statistically significant decrease in the density of pyramidal neurons in the parietal and/or temporal cortex of the brain for 3-4 days, as opposed to the first 2 days, and is accompanied by morphological manifestations of neurodegeneration.

2. There is a tendency of increasing the damage to the cerebral cortex in up to 2 days after OCCA in infected animals with HSV1, and 100% mortality on the 3 day, indicating a relationship between the degree of ischemic damage to neuroinfection.

3. Reduction in the density of pyramidal neurons in the parietal and/or temporal cortex of the brain in a combined model with ischemia and viral association in the experiment was significantly greater than those in which only one risk factor was used.

4. The detected increase in the degree of damage to the neocortex in brain ischemia in mice with herpetic infection is evidence of a possible association between them, which is due to an increase in focal inflammation and progressive neurodegeneration.

References

[1] Alber, D. G., Powell, K. L., Vallance, P., Goodwin, D. A., & Grahame-Clarke, C. (2000). Herpesvirus infection accelerates atherosclerosis in the apolipoprotein E-deficient mouse. *Circulation,* 102(7), 779-785.

[2] Al-Ghamdi, A. (2012). Role of herpes simplex virus-1, cytomegalovirus and Epstein-Barr virus in atherosclerosis. *Pak. J. Pharm. Sci.,* 25(1), 89-97.

[3] Avdeeva, M. V., Samoylova, I. G., & Scheglov, D. S. (2012). Pathogenetics aspects of relationship mouth infectious diseases with development and progression atherosclerosis and possibility for their integrated prevention. *Journal Infectology,* 4(3), 30-34. https://doi.org/10.22625/2072-6732-2012-4-3-30-34

[4] Borisov, A. V., Semak, A. E., & Churakov, A. V. (2011). Role of infection in pathogenesis of cerebral atherosclerosis and infarct of brain. *Military Medicine,* 4, 99-105.

[5] Chirathaworn, C., Pongpanich, A., & Poovorawan, Y. (2004). Herpes simplex virus 1 induced LOX-1 expression in an endothelial cell line, ECV 304. *Viral Immunology,* 17(2), 308-314.

[6] Chiu, B., Viira, E., Tucker, W., & Fong, I. W. (1997). Chlamydia pneumoniae, cytomegalovirus, and herpes simplex virus in atherosclerosis of the carotid artery. *Circulation,* 96(7), 2144-2148.

[7] Deng, J., Zhang, J., Feng, C., Xiong, L., & Zuo, Z. (2014). Critical role of matrix metalloprotease-9 in chronic high fat diet-induced cerebral vascular remodelling and increase of ischaemic brain injury in mice†. *Cardiovascular research*, 103(4), 473-84.

[8] Edvinsson, M., Tallkvist, J., Nystram-Rosander, C., & Ilback N.G. (2017). Cholesterol uptake in the mouse aorta increases during Chlamydia pneumoniae infection. *Pathog. Dis,* 75(1), 1-8. doi: 10.1093/femspd/ftx004.

[9] Fabricant, C. G., Fabricant, J., Litrenta, M. M., & Minick, C. R. (1978). Virus-induced atherosclerosis. *J. Exp. Med,* 148(1), 335-340.

[10] Febbraio, M., & Silverstein, R. L. (2007). CD36: implications in cardiovascular disease. *The international journal of biochemistry & cell biology,* 39(11), 2012-2030. doi:10.1016/j.biocel.2007.03.012

[11] Fedorovich, S. V., Voronina, P. P., & Waseem, T. V. (2018). Ketogenic diet versus ketoacidosis: what determines the influence of ketone bodies on neurons?. *Neural regeneration research,* 13(12), 2060-2063. doi:10.4103/1673-5374.241442

[12] Flint, J.J., Blackband, S.J., & Thelwall, P.E. Unilateral common carotid artery occlusion: a transient ischemia model well suited to MR studies. *Proc. Intl. Soc. Mag. Reson. Med,* 14, 1457.

[13] Gumenyuk, A., Motorna, N., Rybalko, S., Savosko, S., Sokurenko, L., Starosyla, D. … Chaikovsky, Yu. (2017). Development of herpetic infection associated with stroke and its correction with acyclovir. *Curr Issues Pharm Med Sci,* 30(1), 20-23.

[14] Gumenyuk, A. V., Motorna, N. V., Rybalko, S. L., Savosko, S. I., Sokurenko, L. M., & Chaikovsky, Yu. B. (2016). Mutual influence of herpes virus infection activation and cerebral circulation impairment on the state of brain cells. *Biopolym. Cell,* 32, 2: 126-130.

[15] Hajjar, D. P., Pomerantz, K. B., Falcone, D. J., Weksler, B. B., & Grant, A. J. (1987). Herpes simplex virus infection in human arterial cells. Implications in arteriosclerosis. *The Journal of clinical investigation,* 80(5), 1317-1321. doi:10.1172/JCI113208

[16] Jalal, F. Y., Yang, Y., Thompson, J., Lopez, A. C., & Rosenberg, G. A. (2012). Myelin loss associated with neuroinflammation in hypertensive rats. *Stroke,* 43(4), 1115-1122. doi:10.1161/STROKEAHA.111.643080

[17] Key, N. S., Vercellotti, G. M., Winkelmann, J. C., Moldow, C. F., Goodman, J. L., Esmon, N. L., … Jacob, H. S. (1990). Infection of vascular endothelial cells with herpes simplex virus enhances tissue factor activity and reduces thrombomodulin expression. *Proceedings of the National Academy of Sciences of the United States of America*, 87(18), 7095-7099.

[18] Koch, K., Berressem, D., Konietzka, J., Thinnes, A., Eckert, G. P., & Klein, J. (2017). Hepatic Ketogenesis Induced by Middle Cerebral Artery Occlusion in Mice. *Journal of the American Heart Association,* 6(4), e005556.

[19] Kotronias, D., & Kapranos, N. (2005). Herpes simplex virus as a determinant risk factor for coronary artery atherosclerosis and myocardial infarction. *In Vivo,* 19(2), 351-358.

[20] Lucas, A., Dai, E., Liu, L. Y., & Nation, P. N. (1998). Atherosclerosis in Marek's disease virus infected hypercholesterolemic roosters is reduced by HMGCoA reductase and ACE inhibitor therapy. *Cardiovasc Res,* 38(1), 237-246.

[21] Motorna, N. V., Rybalko, S. L. Starosyla, D. B., Guzyk, M. M., Strokina, I. G., Kaminsky, R. F. … Chaikovsky, Y.B. (2018). The study of leukocyte phagocytic activity in the presence of herpetic infection and stroke. *Wiadomosci Lekarskie*, 71, 1, II, 155-159.

[22] Ooigawa, H., Nawashiro, H., Fukui, S., Otani, N., Osumi, A., Toyooka, T., & Shima, K. (2006). The fate of Nissl-stained dark neurons following traumatic brain injury in rats: difference between neocortex and hippocampus regarding survival rate.

Acta Neuropathol, 112(4), 471-481.
[23] Shi, Y., & Tokunaga, O. (2002). Herpesvirus (HSV-1, EBV and CMV) infections in atherosclerotic compared with non-atherosclerotic aortic tissue. Pathology International, 52(1), 31-39.
[24] Sorlie, P. D., Nieto, F. J., Adam, E., Folsom, A. R., Shahar, E., & Massing, M. (2000). A prospective study of cytomegalovirus, herpes simplex virus 1, and coronary heart disease: the atherosclerosis risk in communities (ARIC) study. *Arch. Intern. Med.*, 160(13), 2027-2032.
[25] Sorrentino, R., Yilmaz, A., Schubert, K., Crother, T. R., Pinto, A., Shimada, K. … Chen, S. (2015). A single infection with Chlamydia pneumoniae is sufficient to exacerbate atherosclerosis in ApoE deficient mice. *Cellular immunology,* 294(1), 25-32.
[26] Speetzen, L. J., Endres, M., & Kunz, A. (2013). Bilateral common carotid artery occlusion as an adequate preconditioning stimulus to induce early ischemic tolerance to focal cerebral ischemia. *Journal of visualized experiments: JoVE*, (75), e4387.
[27] Thong-asa, W., & Tilokskulchai, K. (2014). Neuronal damage of the dorsal hippocampus induced by long-term right common carotid artery occlusion in rats. *Iranian Journal of Basic Medical Sciences*, 17(3), 220-226.
[28] Turchyna, N. S., & Savosko, S. I. (2018). The study of the initial stages of atherogenesis against high-fat diet. *Physiological Journal,* 64(2), 54-64.
[29] Wu, Y. P., Sun, D. D., Wang, Y., Liu, W., & Yang, J. (2016). Herpes Simplex Virus Type 1 and Type 2 Infection Increases Atherosclerosis Risk: Evidence Based on a Meta-Analysis. *BioMed research international,* 2016, 2630865.
[30] Yao, H. W., Ling, P., Tung, Y. Y., Hsu, S. M., & Chen, S. H. (2014). In vivo reactivation of latent herpes simplex virus 1 in mice can occur in the brain before occurring in the trigeminal ganglion. *Journal of Virology,* 88(19), 11264-11270. DOI: 10.1128/JVI.01616-14.
[31] Yoshizaki K, Adachi K, Kataoka S, Watanabe A, Tabira T, Takahashi K, & Wakita H. (2008). Chronic cerebral hypoperfusion induced by right unilateral common carotid artery occlusion causes delayed white matter lesions and cognitive impairment in adult mice. *Exp. Neurol.*, 210(2), 585-591.

ПАТОЛОГІЧНІ ЗМІНИ ГОЛОВНОГО МОЗКУ МИШЕЙ НА ТЛІ МОДЕЛЮВАННЯ ІШЕМІЇ З АСОЦІЙОВАНОЮ ВІРУСНОЮ ІНФЕКЦІЄЮ

Турчина Н.С., Савосько С.І., Рибалко С.Л., Старосила Д.Б., Колісник Д.І.

У світовій літературі постійно зростає кількість даних, що свідчать про деякі інфекційні збудники, як чинників розвитку атеросклерозу та гострої цереброваскулярної патології, та про предиктори гострої серцево-судинної патології, як маркерів запалення. Неоднозначні результати досліджень взаємозв'язку між інфекцією і атеросклерозом та намагання довести існування такого взаємозв'язку обумовили спроби змоделювати інфекція-асоційованого атерогенезу на тваринах. Зв'язок цих даних з ішемічним пошкодженням мозку ще мало досліджений, хоча в окремих експериментальних роботах доведено прогресуючу дегенерацію при крововиливі у мозок мишей, заражених вірусом простого герпесу 1 типу (ВПГ1), що пояснюється пост-інсультною імуносупресією та реактивацією інфекційного агенту. Мета роботи - дослідити в експерименті можливий зв'язок між герпетичною інфекцією та ішемічним пошкодженням кори головного мозку мишей. Для досягнення поставленої мети нами було сформовано 5 груп експериментальних тварин (мишей): 1 група (n=52), в дієті використовували холестерин; 2 група (n=23), із зараженням ВПГ1; 3 група (n=30), з однобічною оклюзією загальної сонної артерії (ОЗСА); 4 група (n=10), із зараженням ВПГ1 та ОЗСА; 5 група (n=6), із зараженням ВПГ1, використанням холестеринової дієти та ОЗСА. Морфометрично на виготовлених мікропрепаратах оцінювали зміни щільності нейронів неокортексу тім'яної, скроневої ділянок мозку та гіпокампу. Статистичну обробку результатів проводили із застосуванням програми Origin Lab, версія 8.0. Встановлене вірогідне збільшення структурних змін у 5 групі (з трьома патологічними чинниками) комбінованої моделі порівняно з моделями без поєднання та/або з поєднанням декількох патологічних ознак 1, 2, 3 та 4 груп. Порівняння результатів між 1-4 та 5 групами, свідчить про статистично значуще збільшення відносної кількості нейронів з цитопатологічними ознаками (гіперхроматоз, деформація перикаріону, каріопікноз), яке корелює з більшою кількістю патологічних ознак, та вірогідно призводить до більш стрімкого пошкодження пірамідних нейронів неокортексу. Таким чином, редукція щільності пірамідних нейронів у тім'яній та/або скроневій корі мозку при комбінованій моделі з ішемізацією та вірусною асоціацією в експерименті була вірогідно більшою порівняно з моделями, у формуванні яких застосований лише один фактор ризику. Виявлене збільшення ступені пошкодження неокортексу при ішемізації головного мозку у мишей із герпетичною інфекцією є свідченням можливого зв'язку між ними.

Ключові слова: *головний мозок, миші, ішемія, вірусна інфекція.*

ПАТОЛОГИЧЕСКИЕ ИЗМЕНЕНИЯ ГОЛОВНОГО МОЗГА МЫШЕЙ НА ФОНЕ МОДЕЛИРОВАНИЯ ИШЕМИИ С АССОЦИИРОВАННОЙ ВИРУСНОЙ ИНФЕКЦИЕЙ

Турчина Н.С., Савосько С.И., Рыбалко С.Л., Старосила Д.Б., Колесник Д.И.

В мировой литературе постоянно растёт количество данных, которые свидетельствуют о некоторых инфекционных возбудителях, как факторах развития атеросклероза и острой цереброваскулярной патологии, и о предикторах острой сердечно-сосудистой патологии, как маркеров воспаления. Неоднозначны результаты исследований взаимосвязи между инфекцией и атеросклерозом, а намерения доказать существование такой взаимосвязи обусловили попытки смоделировать инфекция-ассоциированный атерогенез на животных. Связь этих данных с ишемическим поражением мозга ещё мало исследована, хотя в отдельных экспериментальных работах доказана прогрессирующая дегенерация при кровоизлиянии в мозг мышей, зараженных вирусом простого герпеса 1 типа (ВПГ1), что объясняется пост-инсультной иммуносупрессией и реактивацией инфекционного агента. Цель работы - исследовать в эксперименте возможную связь между герпетической инфекцией и ишемическим поражением коры головного мозга мышей. Для достижения поставленной цели нами было сформировано 5 групп экспериментальных животных (мышей): 1 группа (n=52), в диете которой использовали холестерин, 2 группа (n=23) с заражением ВПГ1, 3 группа (n=30) с односторонней окклюзией общей сонной артерии (ООСА), 4 группа

(n=10) с заражением ВПГ1 и ООСА, 5 группа (n=6) с заражением ВПГ1, использованием холестериновой диеты и ООСА. По микропрепаратам морфометрически оценивали изменения плотности нейронов неокортекса темянной, височной областей мозга и гиппокампа. Статистическую обработку результатов проводили с использованием программы Origin Lab, версия 8.0. Установлено достоверное увеличение структурных изменений в 5 группе (с тремя патологическими факторами) комбинированной модели по сравнению с моделями без объединения и/или с объединением нескольких патологических признаков 1, 2, 3 и 4 групп. Сравнение результатов между 1-4 и 5 группами свидетельствует о статистически значимом увеличении относительного количества нейронов с цитопатологическими признаками (гиперхроматоз, деформация перикариона, кариопикноз), которое коррелирует с большим количеством патологических признаков, и достоверно приводит к более стремительному поражению пирамидных нейронов неокортекса. Таким образом, редукция плотности пирамидных нейронов в теменной и/или височной коре мозга при комбинированной модели с ишемизацией и вирусной ассоциацией в эксперименте, была достоверно большей по сравнению с моделями, в формировании которых использован только один фактор риска. Выявленное увеличение степени поражения неокортекса при ишемизации головного мозга у мышей с герпетической инфекцией является свидетельством возможной связи между ними.

Ключевые слова: *головной мозг, мыши, ишемия, вирусная инфекция.*

REQUIREMENTS FOR ARTICLES

For publication, scientific articles are accepted only in English only with translation on Ukrainian or Russian, which contain the following necessary elements: UDC code; title of the article (in English, Ukrainian and Russian); surname, name and patronymic of the authors (in English, Ukrainian and Russian); the official name of the organization (institution) (in English, Ukrainian and Russian); city, country (in English, Ukrainian and Russian); structured annotations (in English, Ukrainian and Russian); keywords (in English, Ukrainian and Russian); introduction; purpose; materials and methods of research; research results; discussion; conclusions; bibliographic references.

The title of the article briefly reflects its contents and contains no more than 15 words.

Abstract. The volume of the annotation is 1800-2500 characters without spaces. The text of an annotation in one paragraph should not contain general phrases, display the main content of the article and be structured. The abstract should contain an introductory sentence reflecting the relevance of the study, the purpose of the study, a brief description of the methods of conducting research (2-3 sentences with the mandatory provision of the applied statistical methods), a description of the main results (50-70% of the volume of the abstract) and a concise conclusion (1 sentence). The abstract should be clear without familiarizing the main content of the article. Use the following expressions: "Detected ...", "Installed ...", "Fixed ...", "Impact assessed ...", "Characterized by regularities ...", etc. In an annotation, use an active rather than passive state.

Keywords: 4-6 words (or phrases).

"Introduction"

The introduction reflects the state of research and the relevance of the problem according to the world scientific literature (at least 15 references to English articles in international journals over the past 5 years). At the end of the entry, the purpose of the article is formulated (contains no more than 2-3 sentences, in which the problem or hypothesis is addressed, which is solved by the author).

"Materials and methods"

The section should allow other researchers to perform similar studies and check the results obtained by the author. If necessary, this section may be divided into subdivisions. Depending on the research objects, the ethical principles of the European Convention for the protection of vertebrate animals must be observed; Helsinki Declaration; informed consent of the surveyed, etc. (for more details, see "Public Ethics and its Conflict"). At the end of this section, a "statistical processing of results" section is required, which specifies the program and methods for processing the results obtained by the automobile.

"Results"

Requirements for writing this section are general, as well as for all international scientific publications. The data is presented clearly, in the form of short descriptions, and must be illustrated by color graphics (no more than 4) or drawings (no more than 8) and tables (no more than 4), the information is not duplicated.

"Discussion"

In the discussion, it is necessary to summarize and analyze the results, as possible, compare them with the data of other researchers. It is necessary to highlight the novelty and possible theoretical or practical significance of the results of the research. You should not repeat the information already listed in the "Introduction" section. At the end of the discussion, a separate paragraph should reflect the prospects for using the results obtained by the author.

"Conclusion"

5-10 sentences that summarize the work done (in the form of paragraphs or solid text).

"Acknowlegements"

Submitted after conclusion before bibliographic references.

"References"

References in the text are indicated by Arabic numerals in square brackets according to the numerology in the list of references. The list of references (made without abbreviations) sorted by alphabet, in accordance with the requirements of APA Style (American Psychological Association Style): with the obligatory referencing of all authors, work titles, journal names, or books (with obligatory publication by the publishing house, and editors when they are available), therefore, numbers or releases and pages. In the Cyrillic alphabets references, give the author's surnames and initials in English (Cyrillic alphabet in brackets), the title of the article or book, and the name of the magazine or the publisher first to be submitted in the original language of the article, and then in square brackets in English. If available, doi indexes must be provided on www.crossref.org (at least 80% of the bibliographic references must have their own doi indexes). Links to online publications, abstracts and dissertations are not welcome.

After the list of references, it is necessary to provide information about all authors (in English, Ukrainian and Russian): last name, first name and patronymic of the author, degree, place of work and position, **ORCID number** (each of the authors of the ORCID personal number if absence - free creation on the official website http://www.orcid.org) to facilitate the readers of this article to refer to your publications in other scientific publications.

The last page of the text should include the surname, name and patronymic of the author, degree, postal address, telephone number and e-mail of the author, with which the editors will maintain contact.

Concluding remarks

The manuscript should be executed in such a way that the number of refinements and revisions during the editorial of the article was minimal.

When submitting the article, please observe the following requirements. The volume of the article - not less than 15 and not more than 25 pages, Times New Roman, 14 pt, line spacing - one and a half, fields - 2 cm, sheet A4. Text materials should be prepared in the MS Word editor (* .docx), without indentations. Math formulas and equations to prepare in the embedded editor; graphics - in MS Excel. Use the units of the International Measurement System. Tables and drawings must contain the name, be numbered, and references to them in the text should be presented as follows: (fig. 1), or (table 1). The drawings should be in the format "jpg" or "tif"; when scanned, the resolution should be at least 800 dpi; when scanning half-tone and color images, the resolution should be at least 300 dpi. All figures must be represented in the CMYK palette. The statistical and other details are given below the table in the notes. Table materials and drawings place at the end of the text of the manuscript. All elements of the text in images (charts, diagrams, diagrams) must have the Times New Roman headset.

Articles are sent to the editorial board only in electronic form (one file) at the e-mail address nila@vnmu.edu.ua

Responsible editor - Gunas Igor Valeryovich (phone number: + 38-067-121-00-05; e-mail: gunas.red@gmail.com).

Signed for print 28.12.2018
Format 60x84/8. Printing offset. Order № 3110. Circulation 100.
Vinnytsia. Printing house “Tvory”, Keleckaya St., 51a
PO Box 8825, 600-Richchya Str., 21, Vinnytsya, 21007
Phone: +38 (0432) 603 000
+38 (096) 97-30-934, +38 (093) 89-13-852
e-mail: tvory2009@gmai.com
http://www.tvoru.com.ua